Past and future evolution of French Alpine glaciers in a changing climate : a deep learning glacio-hydrological modelling approach

Jordi Bolibar Navarro

Université Grenoble Alpes

THÈSE

Pour obtenir le grade de

DOCTEUR DE L'UNIVERSITE GRENOBLE ALPES

Spécialité : Sciences de la Terre et de l'Univers et de l'Environnement

Arrêté ministériel : 25 mai 2016

Présentée par

Jordi BOLIBAR

Thèse dirigée par **Antoine RABATEL**, Physicien-Adjoint, Univ. Grenoble Alpes, IGE
et codirigée par **Isabelle GOUTTEVIN**, IPEF, Météo-France
et **Eric SAUQUET**, Directeur de recherche, INRAE

préparée au sein de l'**Institut des Géosciences de l'Environnement** et **INRAE**
dans **l'École Doctorale Terre, Univers, Environnement**

Past and future evolution of French Alpine glaciers in a changing climate: a deep learning glacio-hydrological modelling approach

Thèse soutenue publiquement le **29 octobre 2020**,
devant le jury composé de :

M Ben MARZEION
Professeur, University of Bremen, Allemagne, Rapporteur
M Daniel FARINOTTI
Ass. Professeur, ETH Zurich, Suisse, Rapporteur
Mme Delphine SIX
Physicienne, Univ. Grenoble Alpes, France, Présidente du Jury
M Jocelyn CHANUSSOT
Professeur, Grenoble INP, France, Examinateur
M Matthieu LE LAY
Ingénieur docteur, EDF-DTG, France, Examinateur
M Antoine RABATEL
Physicien-Adjoint, Univ. Grenoble Alpes, France, Directeur de thèse

To my parents.

To Kadia.

Abstract

The European Alps are among the most affected regions in the world by climate change, displaying some of the strongest glacier retreat rates. Long-term interactions between society, mountain ecosystems and glaciers in the region raise important questions on the future evolution of glaciers and their derived environmental and socioeconomic impacts. In order to correctly assess the regional response of glaciers in the French Alps to climate change, there is a need for adequate modelling tools. In this work, we explore new ways to tackle both glacier evolution and glacio-hydrological modelling at a regional scale. Glacier evolution modelling has traditionally been performed using empirical or physical approaches, which are becoming increasingly challenging to optimize with the ever growing amount of available data. Here, we present, to our knowledge, the first effort ever to apply deep learning (i.e. deep artificial neural networks) to simulate the evolution of glaciers. Since both the climate and glacier systems are highly nonlinear, traditional linear mass balance models offer a limited representation of climate-glacier interactions. We show how important nonlinearities in glacier mass balance are captured by deep learning, substantially improving model performance over linear methods.

This novel method was first applied in a study to reconstruct annual mass balance changes for all glaciers in the French Alps for the 1967-2015 period. Using climate reanalyses, topographical data and glacier inventories, we demonstrate how such an approach can be successfully used to reconstruct large-scale mass balance changes from observations. This study also offered new insights on how glaciers evolved in the French Alps during the last half century, confirming the rather neutral observed mass balance rates in the 1980s and displaying a well-marked acceleration in mass loss from the 2000s onwards. Important differences between regions are found, with the Mont-Blanc massif presenting the lowest mass loss and the Chablais being the most affected one. Secondly, we applied this modelling framework to simulate the future evolution of all glaciers in the region under multiple (N=29) climate change scenarios. Our estimates indicate that most ice volume in the region will be lost by the end of the 21^{st} century independently from future climate scenarios. We predict average glacier volume losses of 75%, 80% and 88% under RCP 2.6 (n=3), RCP 4.5 (n=13) and RCP 8.5 (n=13), respectively. By the end of the 21^{st} century the French Alps will be largely ice-free, with glaciers only remaining in the Mont-Blanc and Pelvoux massifs. From this point, we used these results as a case study to investigate the effects of nonlinear glacier response to climatic forcing. We show that linear glacier MB models partially ignore nonlinearities in glacier MB compared to nonlinear deep learning, overestimating and underestimating extreme positive and negative MB rates respectively. Depending on future extreme climate scenarios, this behaviour can potentially introduce a significant cumulative bias in glacier MB projections in the last decades of the 21^{st} century. This could therefore have remarkable consequences on projections of future glacier evolution, suggesting that current global glacier models based on linear MB relationships might potentially be giving estimates of future sea-level rise that are too low for climate scenarios with the highest and lowest greenhouse gases emissions.

This marked glacier retreat in the French Alps will produce an array of consequences that will impact water resources during the warmest months of the year. Glaciers provide cold fresh water resources well after all snow has melted during summer, essential to inhabitants in the region that depend on it for agriculture, industry, ski resorts, hydropower generation and domestic use. Moreover, several aquatic and terrestrial ecosystems depend on these late summer water resources, that keep water temperature low and ecosystems humid throughout the year. Predicting these changes is of paramount importance in order to correctly anticipate the resulting impacts and to design adequate mitigation strategies. Hydrological models currently used in France generally suffer from a simplified representation of glaciers, modelling them as static ice reservoirs. This representation is highly prob-

lematic in the current context of rapid glacier retreat. Here, we introduce a dynamic representation of glaciers for the process-based J2K hydrological model, validated in a case study in the Arvan partially glacierized catchment. By taking into account the daily area evolution of glaciers, this updated glacio-hydrological model represents an excellent tool to assess the diverse hydrological consequences of glacier retreat at the scale of the French Alps.

Keywords: French Alps, glaciers, machine learning, deep learning, modelling, hydrology

Résumé

Les Alpes européennes sont parmi les régions du monde les plus touchées par le changement climatique, avec des taux de recul des glaciers parmi les plus élevés. Les interactions à long terme entre la société, les écosystèmes de montagne et les glaciers de la région soulèvent d'importantes questions sur l'évolution future des glaciers et les impacts environnementaux et socio-économiques qui en découlent. Afin d'évaluer correctement la réponse régionale des glaciers des Alpes françaises au changement climatique, il est nécessaire de disposer d'outils de modélisation adéquats. Dans ce travail, nous explorons de nouvelles façons d'aborder à la fois l'évolution des glaciers et la modélisation glacio-hydrologique à l'échelle régionale. La modélisation de l'évolution des glaciers a traditionnellement été réalisée à l'aide d'approches empiriques ou physiques, dont l'optimisation est de plus en plus difficile compte tenu de la quantité croissante de données disponibles. Ici, nous présentons, à notre connaissance, le premier effort jamais entrepris pour appliquer l'apprentissage profond (i.e. des réseaux neuronaux artificiels profonds) pour simuler l'évolution des glaciers. Comme les systèmes climatique et glaciaire sont tous deux fortement non linéaires, les modèles traditionnels linéaires de bilan de masse offrent une représentation limitée des interactions entre le climat et les glaciers. Nous montrons comment des non-linéarités importantes liées au bilan de masse des glaciers sont capturées par une méthode d'apprentissage profond, ce qui améliore considérablement les performances des modèles par rapport aux méthodes linéaires.

Cette nouvelle méthode a été appliquée pour la première fois dans une étude visant à reconstruire les changements annuels du bilan de masse de tous les glaciers des Alpes françaises pour la période 1967-2015. En utilisant des réanalyses climatiques, des données topographiques et des inventaires de glaciers, nous démontrons comment une telle approche peut être utilisée avec succès pour reconstruire les changements de bilan de masse à grande échelle à partir d'observations. Cette étude a également apporté de nouveaux éclairages sur l'évolution des glaciers dans les Alpes françaises au cours du dernier demi-siècle, confirmant les taux de bilan de masse observés plutôt neutres dans les années 1980 et montrant une accélération bien marquée de la perte de masse à partir des années 2000. On constate des différences importantes entre les régions, le massif du Mont-Blanc présentant la perte de masse la plus faible et le Chablais étant le plus touché. Ensuite, nous avons appliqué ce cadre de modélisation pour simuler l'évolution future de tous les glaciers de la région selon de multiples scénarios de changement climatique (N=29). Nos estimations indiquent que la plupart du volume de glace dans la région sera perdue d'ici la fin du XXIe siècle, indépendamment des scénarios climatiques futurs. Nous prévoyons des pertes moyennes de volume des glaciers de 75%, 80% et 88% dans le cadre des scénarios RCP 2.6 (n=3), RCP 4.5 (n=13) et RCP 8.5 (n=13), respectivement. D'ici la fin du XXIe siècle, les Alpes françaises seront en grande partie libres de glace, avec des glaciers ne subsistant que dans les massifs du Mont-Blanc et du Pelvoux. Nous avons ensuite utilisé ces résultats comme un cas d'étude pour analyser les effets de la réponse non linéaire des glaciers au forçage climatique. Nous montrons que les modèles linéaires de bilan de masse de glaciers ignorent une grande partie des non-linéarités dans le bilan de masse par rapport à l'apprentissage profond non linéaire, en sur-estimant et sous-estimant les taux positifs et négatifs extrêmes du bilan de masse respectivement. En fonction des scénarios climatiques futurs extrêmes, ce comportement peut potentiellement introduire un biais significatif dans les projections de bilan de masse des glaciers dans les dernières décénnies du XXIe siècle. Cela pourrait donc avoir des conséquences remarquables sur les projections de l'évolution future des glaciers, ce qui suggère que les modèles globaux actuels des glaciers basés sur des relations linéaires de bilan de masse pourraient potentiellement donner des estimations de l'élévation future du niveau des mers qui sont trop faibles pour les scénarios climatiques avec les plus

fortes et plus faibles émissions de gaz à effet de serre.

Ce recul marqué des glaciers dans les Alpes françaises aura un ensemble de conséquences avec notamment un impact sur les ressources en eau pendant les mois les plus chauds de l'année. Les glaciers fournissent des ressources en eau douce froide bien après la fonte des neiges en été, ce qui est essentiel pour les habitants de la région qui en dépendent pour l'agriculture, l'industrie, les stations de ski, la production d'énergie hydroélectrique et l'utilisation domestique. En outre, plusieurs écosystèmes aquatiques et terrestres dépendent de ces ressources en eau de fin d'été, qui maintiennent la température de l'eau à un niveau bas et l'humidité des écosystèmes tout au long de l'année. La prévision de ces changements est d'une importance capitale pour anticiper correctement les impacts qui en résulteront et pour concevoir des stratégies d'atténuation adéquates. Les modèles hydrologiques actuellement utilisés en France souffrent généralement d'une représentation simplifiée des glaciers, les modélisant comme des réservoirs de glace statiques. Cette représentation est très problématique dans le contexte actuel de recul rapide des glaciers. Nous présentons ici une représentation dynamique actualisée des glaciers pour le modèle hydrologique J2K, validée dans une étude de cas dans le bassin versant partiellement englacé de l'Arvan. En prenant en compte l'évolution quotidienne de la surface des glaciers, ce modèle hydrologique basé sur les processus représente un excellent outil pour évaluer les conséquences hydrologiques du recul des glaciers à l'échelle des Alpes françaises.

Mots clés: Alpes françaises, glaciers, apprentissage automatique, apprentissage profond, modélisation, hydrologie

Acknowledgements

This PhD work has been, by all means, a collective effort. I would have never been able to accomplish this without the help, kind words or time from a multitude of people. I am extremely grateful for that, for this project has been an incredible human experience. There are a lot of people that I would like to thank, and I sincerely hope I will not forget anyone. First of all, I would like to thank my parents, for giving me the opportunity and freedom to pursue my studies, which gave me the independence to control my professional career and aim it towards the things I love and matter to me. All of this would not have been possible without Kadia, my closest companion, the hidden co-author, who took care of me during these years despite the long rants on glaciers, climate and machine learning. I am also extremely grateful for the family I have. Laia, Mariona, Andrew, for all the time shared together, especially in New Zealand; and my grandparents, particularly avi Robert, who taught me maths and physics, and who I wish I could show this work.

Then, I would like to thank my supervisors, who gave me the possibility to do this work, and who always respected my vision and way of working. Antoine, for his availability, dedicating whatever time needed to my problems, and protecting me from several ordeals regarding French paperwork. Being able to discuss in Spanish at the beginning of the PhD was a great way to engage in deep discussions on glaciers, and improved my confidence as a total newcomer to the field. Isabelle, who guided me in the most kind way, and provided invaluable insights on climatology and hydrology, especially during the last hectic weeks of the PhD debugging the hydrological model. I particularly appreciate the freedom I was given to work on the ideas that drive me, knowing the cost that this represented on her research part. For that, I am grateful, but also sorry for not having managed to include them in a better way. Eric and Thomas, who provided insightful comments throughout my work, and whose hydrological expertise helped me during the last part of this work. Special thanks go to Clovis Galiez, who has played the role of a bonus supervisor. I learnt so much about machine learning from him, and our discussions have been to me some of the most stimulating ones during these three years, including several times when his suggestions unlocked problems that I had for weeks. Sven Kralisch has also provided me with guidance on hydrological modelling during the last months. Despite finally not being able to visit Jena, I have always been surprised by his sincere kindness, availability and will to help.

My PhD companions have proved to be my best allies for such a long journey, with many people I would like to thank. Julien, Joseph, Gabi and Nathan shared with me some of the most memorable adventures on two wheels, from the Alps to Utah. Maria, Gabi, both Juliens, Jai, Jonathan, Joseph and Ambroise shared many hours of skinning up and skiing down snowy mountains, reminding us why we love them so much. Ugo, for the long discussions in the office, attempting to solve the world's problems besides finishing our PhDs, and for the amazing time in Stiappa. Lucas, Olivier and Juan Pedro, for being excellent office partners, and for the stimulating conversations. Romain, Marion, Astrid, Amber, Diego, Hans, Foteini, Isabelle, Albane, Sammy, Jinwha, Laura, Pedro, Peter, Sarah, Claudio, Maxim, Fanny and Marco, for the great times shared in the lab, in conferences, in the mountains or at the bar. I acknowledge the long term help and support from Molts Ànims, my good old friends in Sant Cugat, who have always been there and who always make me feel home despite the long seven years living abroad. And particularly Edu, who besides sharing almost all the university years with me, provided me with lots of insight on machine learning at the beginning of my PhD.

I am also grateful to Delphine, Olivier and Bruno, who taught me how to measure glacier mass balance in the field, in some of the most breathtaking landscapes I have ever seen. I had so much fun doing that, but I will particularly remember the day when, together with Delphine, we measured

all the ablation stakes in Mer de Glace in one long and arduous push. I am especially thankful to the members of my PhD jury for accepting to review this work. I have been lucky enough to have exactly the jury I wished for, and I really appreciate the time and effort that it involves. Moreover, I would also like to thank Christian, Thomas and Agnès, for taking part in my thesis committee, and guiding me with insightful comments and making it feel more like a conversation than an evaluation. There are many people in the lab(s) that I would also like to thank, for the friendly and interesting conversations in the cafeteria and for the shared small talk: Jérémie, Nico, Sophie, Patrick, Jean-Manu, Gilles, Martin, Manon, Lionel and Vincent.

Finally, I am grateful for the many scientific interactions I had outside the lab, particularly during conferences and paper reviews. I would like to thank Fabien Maussion, Ben Marzeion and Matthias Huss, who besides being an inspiration to me, provided constructive feedback that truly managed to improve my work. I can only hope to have the same luck with reviewers in the future. I am also very thankful to Daniel Farinotti, who always showed kind interest in my work from the beginning, and who is currently helping me to pursue my scientific ideas for a postdoc. I had the chance to meet Fernando Pérez in San Francisco last year, resulting in stimulating discussions on scientific modelling. I hope we will be able to collaborate in the future, once the currently troubled times calm down. I have very fond memories of my winter school in Mendoza, Argentina. I learnt a lot from Lucas Ruiz, Pierre Pitte, Lidia Ferri, Laura Zalazar, Maxi Viale and Mariano Masiokas, and I met some lovely people with whom I experienced the beauty of the Andes. I also had the pleasure to be part of the NASA ICESat-2 Hackweek, which despite having a virtual format, allowed me to learn from, interact and collaborate with great people from all around the world. At last, I am also thankful for the discussions and feedback from Harry Zekollari for my latest paper, with whom I share very similar research interests and the pleasure of writing long e-mails with lots of figures.

I acknowledge the funding of my PhD work by INRAE, the Labex OSUG@2020 (Investissement d'Avenir, ANR ANR10 LABX56), the Auvergne-Rhône-Alpes region through the BERGER project, the VIP Mont-Blanc project (ANR-14 CE03-0006-03) and the CNES (KALEIDOS-Alpes and ISIS projects grants).

I like to believe that these three years have been a small taste of what science is about: a diverse, inclusive, open and collective discussion on the investigation and discovery of nature.

This manuscript has mostly been written and assembled in the beautiful small village of Stiappa, Tuscany (Italy).

Contents

Chapter 1

Introduction

Even in science, the object of research is no longer nature itself, but man's investigation of nature.
Werner Heisenberg

1.1 On the importance of glaciers

Glaciers are fascinating natural systems to study. Their beauty originates from complex interactions between climate and topography, creating unique natural features that shape landscapes, influence ecosystems and even climates wherever they flow. These perennial ice masses originate in places allowing the accumulation of snow, that over the course of years gradually transform into firn and eventually ice. Due to gravity, this ice flows downwards, reaching lower elevations with higher temperatures where ice is lost through different processes of ablation, such as ice melting or calving (IPCC, 2018). The sum of all accumulation and ablation in a glacier determines its mass balance, which is essential to monitor the evolution of glaciers through time and their contribution to sea level rise (Fig. 1.1). Glaciers are excellent climate proxies, adjusting their geometry and size to changes in climate. They represent a large part of the cryosphere, covering some 10% of the Earth's land surface and storing about 69% of the world's fresh water (Cuffey and Paterson, 2010). In their study, glaciers are often divided into mountain glaciers (Fig. 1.1) and ice-sheets, which differ in size and geographical location, with ice-sheets being much larger than mountain glaciers and situated in Greenland and Antarctica (Benn and Evans, 2014).

Mountains are the water towers of the world, acting as buffers that store solid precipitation and distribute fresh water resources throughout the year (Immerzeel et al., 2020). Seasonal and long-term cryospheric changes in mountain environments regulate water, nutrient and sediment supply downstream (Huss et al., 2017). Glaciers play a major role in this, providing water resources during the warmest or driest months well after all snow has melted. This late summer runoff is essential to many ecosystems requiring cold water and humid habitats throughout the year (Cauvy-Fraunié and Dangles, 2019; Carlson et al., 2020). About 10% of the global population live in mountain areas and the contiguous plains, depending on these water resources for agriculture, industry, hydropower, recreation activities or domestic use (Huss and Hock, 2018; Farinotti et al., 2019b). Mountain areas are amongst the most affected regions by anthropogenic climate change, outpacing global warming with an increase of +0.3°C per decade (IPCC, 2018). These rapid changes in climate are causing a widespread retreat of glaciers (Fig. 1.1), with many regions already having reached "peak water", i.e. the maximum

glacier runoff. Once this point is reached, glaciers progressively reduce their water contributions, altering the hydrological regime of glacierized watersheds (Huss and Hock, 2018). The disappearance of glaciers produces an early release of accumulated solid precipitation in spring and early summer, with potential droughts in late summer (Brunner et al., 2019). This represents a transition from a nivo-glacial hydrological regime towards a nival hydrological regime. These fast changes in mountain glaciers also result in glaciers currently being important contributors to sea level rise (0.92 ± 0.39 mm a^{-1}), as much as the massive Antarctic and Greenland ice-sheets combined over the 20^{th} century, despite representing less than 1% of the ice on Earth (Zemp et al., 2019; Hock et al., 2019a).

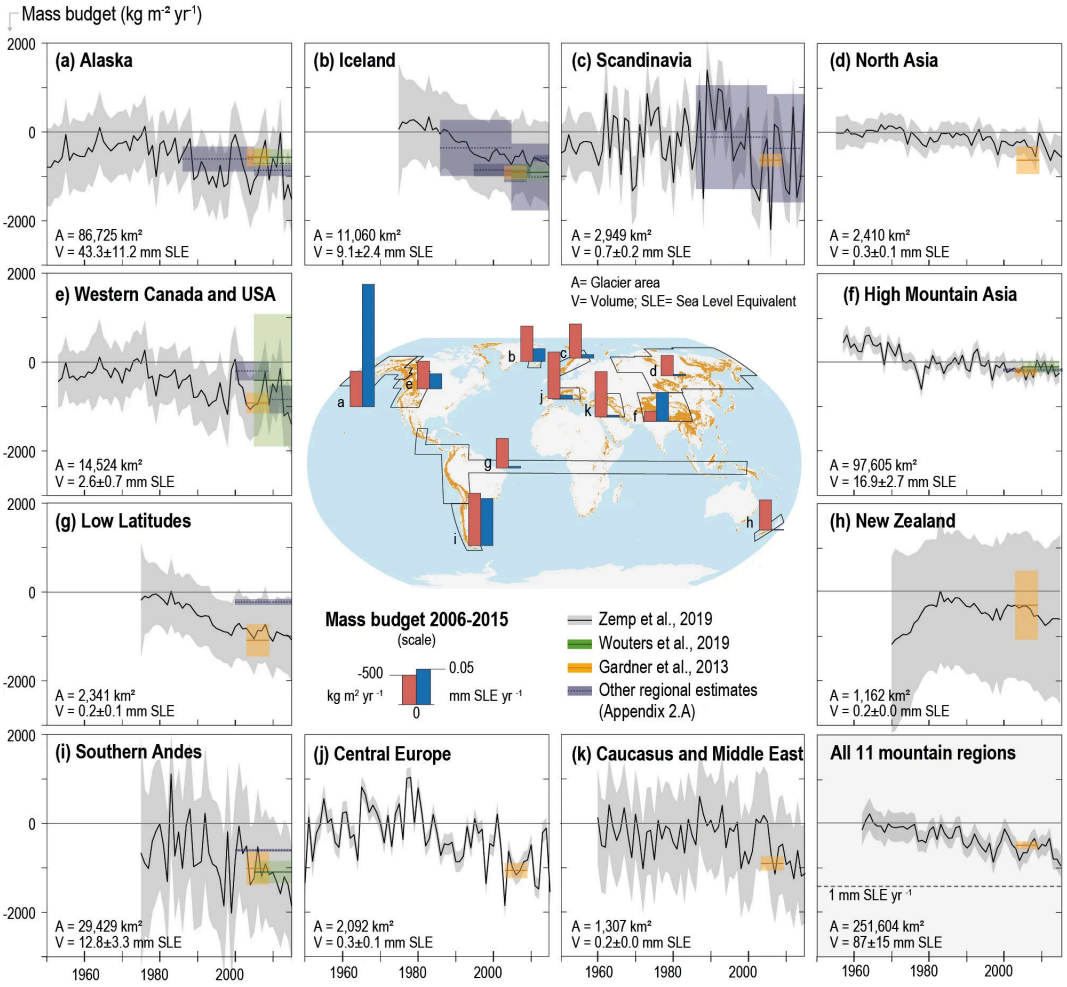

Figure 1.1: Glacier mass budgets for eleven different mountain regions and their combined results. Regional time series of annual mass change are based on glaciological and geodetic balances (Zemp et al., 2019). Superimposed are multi-year averages by Wouters et al. (2019) based on the Gravity Recovery and Climate Experiment (GRACE), only shown for the regions with glacier area > 3,000 km^2. Estimates by Gardner et al. (2013) were used in the IPCC 5th Assessment Report (AR5). Annual and time-averaged mass-budget estimates include the errors reported in each study. Glacier areas (A) and volumes (V) are based on RGI Consortium (2017) and Farinotti et al. (2019), respectively. Red and blue bars on map refer to regional budgets averaged over the period 2006–2015 in units of kg $m^{\check{}2}$ $a^{\check{}1}$ and mm sea level equivalent (SLE) $a^{\check{}1}$, respectively, and are derived from each region's available mass-balance estimates. *Figure from IPCC's Special Report on the Ocean and Cryosphere in a Changing Climate (SROCC, 2019).*

Mountain glaciers are predicted to lose an important fraction of their overall mass by the end of the 21^{st} century, with great differences between regions (Hock et al., 2019a). An accurate assessment of future glacier evolution is essential to understand and quantify the environmental and social consequences of their retreat. Since glaciers have become an icon of climate change, accurate predictions

paired with effective communication can prove a great way to raise awareness on climate change. Despite scientific efforts to precisely quantify and understand glacier retreat, the main driver of future uncertainty in long-term predictions are anthropogenic greenhouse emissions (Marzeion et al., 2020). Scientific studies on glaciers must find their way into a wider audience in order to effectively contribute to their conservation (Moser, 2010). By combining an improved understanding of glacier processes with targeted communication of relevant results, we can aim at preserving our very own subject of study.

1.2 Glaciers in the French Alps

The French Alps are located in the westernmost part of the European Alps, between 44° and 46°13'N and 5.08 and 7.67°E. Their geographical location amidst the Mediterranean sea and continental Europe produces a particular climate gradient, from south-east to north-west. The southern massifs are more influenced by a Mediterranean climate, receiving less precipitation than their northern counterparts. West Atlantic fluxes bring higher amounts of precipitation to north-western massifs, whereas eastern glaciers close to the Italian border receive most precipitation from east returns (Durand et al., 2009). These different climatic patterns, together with altitudes ranging from sea level to 4810 m at the summit of Mont-Blanc, create an array of sub-climates that influence the evolution of glaciers. A total area of 231 km^2 was covered by glaciers in the year 2015 the French Alps (Gardent et al., 2014, with 2015 update).

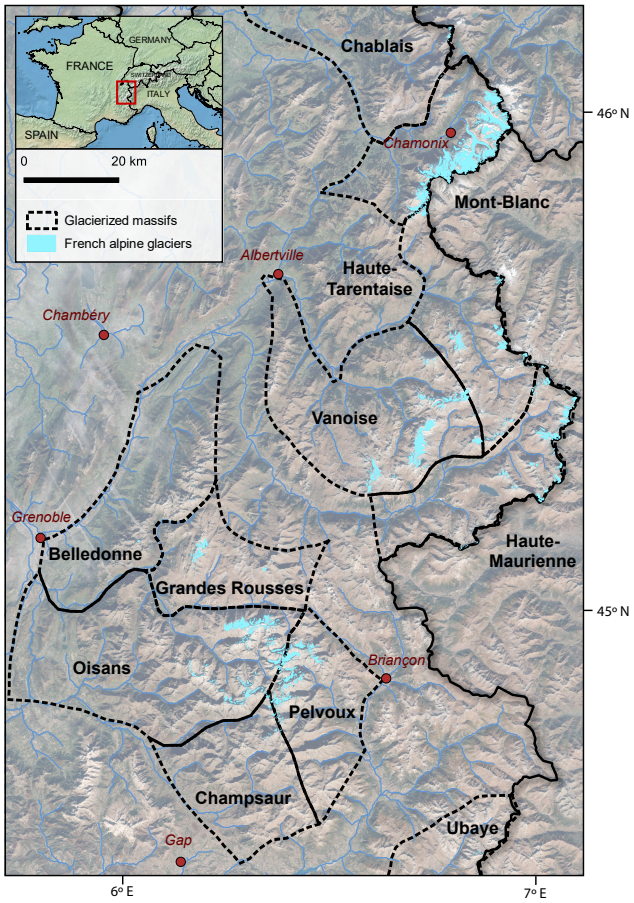

Figure 1.2: Glacierized massifs in the French Alps, with the extent of glaciers for the year 2015.

Like most of the European Alps, the French Alps have been inhabited for many centuries, developing a close relationship between alpine society and mountains. As for mountain peaks, the general social attitude towards glaciers has strongly evolved in the last centuries, transitioning from disdain and terror to awe and curiosity (Zryd, 2008). During the Little Ice Age, glaciers in the Mont-Blanc massif used to reach the valley, threatening villages and settlements (Fig. 1.3). During this time, glaciers were regarded as monsters, which were even exorcised to stop their advance (Ponchaud et al., 2012). This relationship between society and glaciers progressively changed in the first half of the 18^{th} century, integrating them as an important cultural elements, thus becoming symbols of identity for alpine societies throughout the European Alps. This means that the loss of glaciers has an additional social consequence in the French Alps, on top of the environmental ones

found in all glacierized regions (Smit et al., 2019).

These long-term interactions between people and glaciers resulted in some of the earliest studies and observations on glaciers in the world. From the 18^{th} century, the first mountain expeditions were seen as scientific endeavours, providing valuable observations of unknown natural sites (Richalet, 2001). This tradition has continued ever since in the whole European Alps, with the longest observation series of glacier change in the world (GLAMOS, 2019). In France, the GLACIOCLIM national observatory is now responsible for this task, providing uninterrupted multiple glacier measurements from the field every year since the 1950's. These long-term observations, combined with the rather easy access to glaciers, provide an excellent testbed for glaciological studies. The European and French Alps are some of the regions in the world with a strongest observed glacier mass loss (Fig. 1.1), a trend that is expected to make them one of the regions with the highest mass loss for this century (Marzeion et al., 2020).

Figure 1.3: The Mer de Glace in 1822, during the Little Ice Age. By then, its tongue reached the valley, receiving the name of Glacier des Bois, due to the fact that it reached the low-lying forests. *Painting by Jean Dubois*

In many aspects, people in the French Alps have built their lives around mountains and glaciers, whose vast forecasted retreat will impact their socioeconomic model (Mourey and Ravanel, 2017; Spandre et al., 2019). Emblematic regions such as the Mont-Blanc massif depend on glaciers for tourism (Schut, 2013), water resources and hydropower generation (Laurent et al., 2020). Moreover, natural hazards derived from glacier retreat might potentially impact populations in valleys (Magnin et al., 2020). All these effects demand deep changes in the socio-economic model of these regions in order to correctly adapt to these changes in time. This adaptation is impossible without accurate predictions of future glacier evolution. Models can provide answers to these questions, allowing the anticipation and prioritization of actions.

1.3 Modelling large-scale glacier evolution

"At last, combining the three causes which contribute to the maintenance of glaciers, it would be interesting to arrive at the mass which is supplied to them each year; but one feels that it is only possible to have on this subject more or less probable conjectures; it is especially here that we lack and will always lack observations, which must be the first element to lead to the intelligence of nature."

Like an oracle, Louis Rendu stated in 1840 in his book "Théorie des glaciers de la Savoie" what all

modern glacier modellers are still struggling with (Rendu and Bischof, 1840). First and foremost, observations are a key element in our understanding of glacier processes. Past observations enable the creation of equations and models to represent in an approximate manner the complex behaviour of glaciers. All glacier models, independently from their approach, will have to solve the two main processes that determine the evolution of glaciers: (a) Glacier mass balance, as the consequence of the mass gained via accumulation (e.g., snowfall, avalanche deposition) and the mass lost through ablation (e.g., ice melting, calving). Mass balance can be seen as the main consequence of climate-glacier interactions (Benn and Evans, 2014); (b) Glacier ice dynamics, that govern the movement of ice downwards due to gravity. Since ice is a viscoelastic material, this movement can occur as a combination of plastic deformation of the ice (also known as creep), sliding of ice over the bed and the deformation of the bed itself (Cuffey and Paterson, 2010). The interplay of mass balance and ice dynamics determines the advance or retreat of glaciers, as a consequence of climate and topography. Past observations of these two main processes have enabled the development of a variety of glacier models of different complexities, used to simulate glacier evolution at different geographical scales. As for any geophysical problem, the larger the study area the more simplifications are used in models. This holds especially for glaciers, for which several parameterizations and simplifications are needed for models to operate at regional or global scale (e.g., Marzeion et al., 2012; Huss and Hock, 2015; Maussion et al., 2019).

Predicting the future of glaciers is a complex task. It demands a correct representation of past observed glacier changes, accompanied with the hypothesis that the past observed relationships used in the modelling framework will remain constant in the future. This hypothesis would not be necessary with a detailed-enough representation of the physical processes involved in glacier evolution, but a large geographical scale hinders this level of detail in current models. Most importantly, future climate and therefore glacier evolution depend on future anthropogenic greenhouse emissions, introducing large uncertainties in projections that cannot be avoided (Marzeion et al., 2020). Therefore, the quest of the modern glacier modeller is to strike a balance between data availability, model complexity and geographical scale.

1.4 Teaching machines about glaciers

Regional and global glacier evolution models have been developed following a wide variety of approaches. The detailed representation of glacier processes is still a huge challenge, so modellers approach simplifications in different manners.

The complex physics involved in glacier processes can be simplified using empirical parameterizations, based on assumptions derived from observations. Despite their simplicity, these parameterizations often display a better performance than more complex approaches, since they are well adapted to large-scale problems where some physical processes become less important compared to others (Réveillet et al., 2018). Parameterizations have been applied to both glacier mass balance (e.g., a temperature-index model) and ice dynamics (e.g., area-volume scaling, Δh parameterization), providing the tools for the vast majority of regional and global glacier evolution models (e.g., Marzeion et al., 2012; Huss and Hock, 2015; Maussion et al., 2019; Hock et al., 2019a).

Alternatively, statistical models approach simplifications from a purely data-driven perspective. Relationships found in past observations can be used to create statistical models, used to analyse these relationships and performing predictions for unseen cases. Traditional linear statistical models have been applied in glaciology for more than 50 years (Hoinkes, 1968; Martin, 1974). In the last decades,

statistics have seen a massive increase in both their popularity and research output with the advent of machine learning. The ever-growing amount of data stored by humans is becoming increasingly challenging to use, process and interpret, leading to the development of advanced methods in data science (Mjolsness, 2001). As in many research fields, machine learning has made its way into glaciology (Fig. 1.4), albeit with much less intensity than other fields in Earth sciences such as climatology (e.g., Liu et al., 2016; Ham et al., 2019; Jiang et al., 2018) or oceanography (e.g., Ducournau and Fablet, 2016; Lguensat et al., 2019). Linear machine learning models have been applied to regression problems in order to interpret climate-glacier interactions (Maussion et al., 2015), and a shallow neural network was applied to model a glacier's mass balance and length (Steiner et al., 2005, 2008).

In the last years, neural networks have been revolutionized with new methods enabling the training of deep neural networks (i.e. deep learning), composed of multiple intermediate layers. This depth allows the neural networks to capture more complex non-linear patterns in data, resulting in improved performance in a wide range of problems (Wang and Raj, 2017). Nonetheless, very few efforts have been made in this direction in glaciology in the recent years, with most recent research focusing on classification problems (Mohajerani et al., 2019; Baumhoer et al., 2019; Zhang et al., 2019). Classification problems offer a more straightforward problem to validate in geosciences, avoiding the tricky question of reproducing physical processes with a "black box" approach (Karpatne et al., 2017). Applying deep learning to geophysical regression problems is a complex task, demanding a solid validation of the results in order to avoid pitfalls related to spatiotemporal data independence (Roberts et al., 2017).

The "black box" effect

Machine learning is a relatively new research field, with a lot of complicated jargon that is in constant evolution due to the high research output of the last years. This rapid evolution, often displaying rather spectacular results in particular applications, has nonetheless been counterbalanced by a reputation that machine learning models act essentially as "black boxes". They are regarded as opaque models, taking input data, training on them in order to reproduce the patterns in the dataset, and spitting out the results without the possibility of understanding what is going on inside them. While this might be true for certain situations, this general statement is quite misleading, and it can be the source of a great deal of confusion. Deep learning, being a particular family of machine learning, can often act as a black box as I am going to show in this work, but this is not the case for many other algorithms. The so-called "accuracy *vs* interpretability" tradeoff tells us that, as a rule of thumb, methods with the strongest predictive power are also the most complex ones to interpret. Therefore, machine learning can still be used to interpret relationships in data, at the cost of sacrificing some predictive power (Bratko, 1997). Nonetheless, this notion is currently being challenged by a new wave of interpretable machine learning methods, spearheaded by interpretable deep learning (e.g., Dong et al., 2017; Zhang et al., 2018; Rackauckas et al., 2020). These new methods, as I am going to elaborate in the last chapter, have a huge potential to overcome the current limitations of machine learning.

In this manuscript, I introduce my attempt to apply deep learning to model glacier evolution at a regional scale. The French Alps are used as a case study, for which their evolution is studied from the late 1960's until the end of the 21^{st} century. As it often happens in science, this investigation on deep learning was not included in my original PhD project. Initial tests with a simple statistical glacier mass balance model slowly evolved into more complex linear

machine learning and eventually into deep learning. A great deal of what is included in this manuscript are the lessons learnt from numerous problems, mistakes and dilemmas that I encountered during these three years.

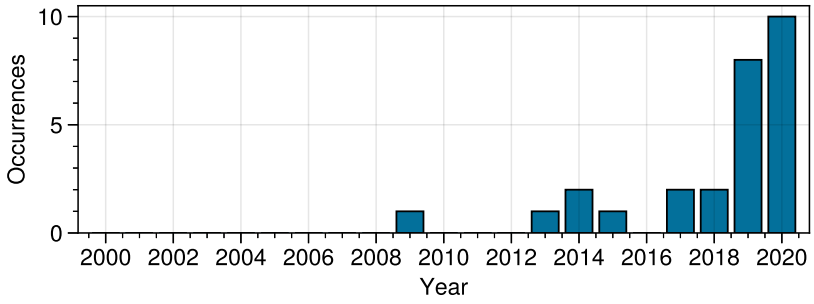

Figure 1.4: Number of scientific articles containing the words "glacier machine learning", based on queries on Web of Science in August 26 2020.

1.5 Modelling glacierized mountain catchments

The correct assessment of the consequences of glacier retreat requires not only an understanding of the evolution of glaciers, but a hydrological, ecological and social perspective of their role at the catchment scale. In the French Alps, this type of studies are only found at the scale of the whole European Alps (Coppola et al., 2018) or the Mont-Blanc massif (Laurent et al., 2020). The J2K hydrological model (Krause, 2002), developed at the University of Jena (Germany), has been applied and co-developed for many years by hydrologists in many countries, including France, in a wide variety of catchment configurations (Branger et al., 2012; Braud et al., 2017; Horner et al., 2020). Among these studies, a special focus was placed in glacierized catchments, with a few glacio-hydrological modelling studies in Himalayan mountain catchments (Gao et al., 2012; Nepal et al., 2014). The current representation of glaciers in J2K takes into account a wide variety of processes, including snow accumulation, sublimation, ageing and melt; and ice melt under different conditions including debris cover (Nepal et al., 2014). Nonetheless, the absence of glacier geometry evolution hinders its application for long-term projections in glacierized mountain catchments. Indeed, in the current version of J2K, glaciers are included as static objects, acting as unchanging ice reservoirs (Nepal et al., 2014). This approach is highly problematic in the current context of rapid glacier retreat. Other hydrological models in France (e.g., GR rainfall-runoff models, Coron et al. (2017)) suffer from a lack of representation of glaciers, highlighting the gap in knowledge on the fate of glacierized catchments in the French Alps.

In this manuscript, I introduce an attempt to bridge this gap, using output data from a glacier evolution model developed during this project (Bolibar, 2020), in order to take into account glacier evolution in the J2K hydrological model. The initial objective of my PhD was to correctly assess the future glacio-hydrological changes in the French Alps and the whole Rhône river catchment. It combined a first part on regional glacier modelling with a second part about glacio-hydrological modelling at the scale of the whole Rhône river catchment. This initial objective was driven by the BERGER project funded by the Auvergne-Rhône-Alpes region. This project, which partially funded my PhD work, aims at understanding the impacts of future glacier retreat in the French Alps on aquatic communities living in glacier-fed streams. By providing accurate estimates of future glacier evolution and glacier runoff, ecologists will be able to extrapolate how changes in runoff intensity, water temperature and seasonality might affect these communities (Robinson et al., 2014; Cauvy-Fraunié and Dangles, 2019). Due to

the unexpected turn of events during the three years of this project, a great fraction of the time was focused on machine learning applications for glacier evolution modelling (Sect. 1.4). This impacted the original objectives, leaving less time to work on regional glacio-hydrological modelling. Therefore, efforts on glacio-hydrological modelling have been focused on a technical implementation of glacier dynamics in a well-documented glacierized catchment, and the assessment of glacier retreat and its hydrological effects over the recent past. This work provides a validated novel methodology, ready to be applied at a larger geographical scale in future studies.

Objectives of this PhD work

The work of my PhD has contributed to two main research axes: (a) the methods, where I introduce a first effort to apply deep learning to model glacier evolution at a regional scale, and the addition of glacier evolution into a process-based hydrological model; (b) the results, where I analyse and present the results of numerical simulations of the evolution of all glaciers in the French Alps from the late 1960's to the end of the 21^{st} century. With the combination of these two axes I attempt to address the following scientific questions:

Question 1 - Can deep learning be applied to model annual glacier mass balance changes at a regional scale? What are the benefits of using nonlinear deep learning models compared to linear machine learning?

Question 2 - What are the annual glacier changes of all glaciers in the French Alps for the last half century?

Question 3 - How will French alpine glaciers evolve during the 21^{st} century? How does glacier retreat affect the climate signal on glaciers? What are the main factors that determine glacier survival in the French Alps? What are the benefits of using a nonlinear mass balance model for future glacier projections?

Question 4 - What are the current limitations in the representation of glaciers in hydrological models in France? How can this be improved?

After answering these questions during this work, a new one arose, setting the direction of future research venues:

Question 5 - What are the caveats of the deep learning modelling approach used in this work? What improvements are needed to overcome these limitations for glaciological studies?

A short note to the reader

This manuscript consists of three parts: one dedicated to regional glacier evolution modelling, another one to glacio-hydrological modelling of glacierized alpine catchments and a final one as an outlook. Part I, being the largest one, is built around three papers: two published and one in preparation. Each paper is included as a dedicated chapter, with a small preface giving the necessary context to the reader. This regional glacier modelling part follows a logical structure found in most publications: a first paper dedicated to the methods (Chapter 2), a second paper dedicated to the results of the application of this method to reconstruct past mass balance changes in the French Alps (Chapter 3), and a third paper dedicated to the future evolution of French alpine glaciers under different scenarios of climate change (Chapter 4). Part II, dedicated to glacio-hydrological modelling of glacierized catchments, is included as a single chapter (Chapter 5) with a section detailing the modelling approach, and a re-

sults section presenting the preliminary results. At last, Part III, with Chapter 6, serves as a conclusion, where various relevant topics of this manuscript are discussed and some perspectives are laid down regarding the most promising future research venues of this work.

Part I

Glaciers

Chapter 2

Deep learning applied to glacier evolution modelling

All models are wrong, but some are useful.
George Box

Preface

Models are becoming increasingly important in science. The ever growing amount of data is fostering the development of more and more complex models, that can be used to interpret relationships and structures in data, but also to make predictions for unobserved cases. Nonetheless, as stated in this famous quote by George Box, all models are just more or less acceptable approximations of nature. The most important element in scientific modelling, is therefore to understand the characteristics needed for a certain study, and to develop a model tailored to its needs. This implies being aware of the model's deficiencies, but also trying to achieve the most accurate results for the right reasons. In this chapter, I introduce a first effort to apply deep learning to model glacier evolution at a regional scale. This method was developed purely out of curiosity, starting with a simple statistical modelling and slowly escalating complexity in order to tailor the methods to the needs of the data. This exploratory process implied interactions with many people, and particularly a fruitful collaboration with Clovis Galiez from the Laboratoire Jean Kuntzmann, from whom I learnt so much. Investigating these ideas involved a great deal of dead ends, complications and tradeoffs. A shadow of doubt was present throughout the development of this method, with many results taking weeks to be fully understood. I believe the main effort in this work has been to attempt to achieve the best results for the right reasons. With this, I mean trying to validate (and cross-validate) with all resources at hand the results obtained, in order to be as sure as possible of the reasons explaining them. I am also grateful for the insightful comments by Fabien Maussion and an anonymous reviewer during the open peer review of this work. Their comments helped address many weak aspects of the paper, and resulted in highly stimulating discussions on glacier evolution modelling. With this chapter, and the resulting discussion in Chapter 6, I aim at explaining why certain aspects worked, what are the pitfalls of this method, and most importantly, how it should be improved in the future.

Based on Bolibar, J., Rabatel, A., Gouttevin, I., Galiez, C., Condom, T., and Sauquet, E.: Deep learning applied to glacier evolution modelling, The Cryosphere, 14, 565–584, doi: 10.5194/tc-14-565-2020, URL

https://www.the-cryosphere.net/14/565/2020/, 2020a.

2.1 Abstract

We present a novel approach to simulate and reconstruct annual glacier-wide surface mass balance (SMB) series based on a deep artificial neural network (*i.e.* deep learning). This method has been included as the SMB component of an open-source regional glacier evolution model. While most glacier models tend to incorporate more and more physical processes, here we take an alternative approach by creating a parameterized model based on data science. Annual glacier-wide SMBs can be simulated from topo-climatic predictors using either deep learning or Lasso (regularized multilinear regression), whereas the glacier geometry is updated using a glacier-specific parameterization. We compare and cross-validate our nonlinear deep learning SMB model against other standard linear statistical methods on a dataset of 32 French alpine glaciers. Deep learning is found to outperform linear methods, with improved explained variance (up to +64% in space and +108% in time) and accuracy (up to +47% in space and +58% in time), resulting in an estimated r^2 of 0.77 and RMSE of 0.51 m.w.e. Substantial nonlinear structures are captured by deep learning, with around 35% of nonlinear behaviour in the temporal dimension. For the glacier geometry evolution, the main uncertainties come from the ice thickness data used to initialize the model. These results should encourage the use of deep learning in glacier modelling as a powerful nonlinear tool, capable of capturing the nonlinearities of the climate and glacier systems, that can serve to reconstruct or simulate SMB time series for individual glaciers in a whole region for past and future climates.

2.2 Introduction

Glaciers are arguably one of the most important icons of climate change, being climate proxies which can depict the evolution of climate for the global audience (IPCC, 2018). In the coming decades, mountain glaciers will be some of the most important contributors to sea level rise and will most likely drive important changes in the hydrological regime of glaciarized catchments (Beniston et al., 2018; Vuille et al., 2018; Hock et al., 2019a). The reduction in ice volume may produce an array of hydrological, ecological and economic consequences in mountain regions which requires to be properly predicted. These consequences will strongly depend on the future climatic scenarios, which will determine the timing and magnitude for the transition of hydrological regimes (Huss and Hock, 2018). Understanding these future transitions is key for societies to adapt to future hydrological and climate configurations.

Glacier and hydro-glaciological models can help answer these questions, giving several possible outcomes depending on multiple climate scenarios. (a) Surface mass balance (SMB) and (b) glacier dynamics both need to be modelled to understand glacier evolution on regional and sub-regional scales. Models of varying complexity exist for both processes. In order to model these processes at large scale (*i.e.* on several glaciers at a catchment scale), some compromises need to be made, which can be approached in different ways:

(a) Regarding SMB:

1. Empirical models, like the temperature-index model (e.g. Hock, 2003), simulate glacier SMB through empirical relationships between air temperature and melt and snow accumulation.
2. Statistical or machine learning models describe and predict glacier SMB based on statistical re-

lationships found in data from a selection of topographical and climate predictors (e.g. Martin, 1974; Steiner et al., 2005).

3. Physical and Surface Energy Balance (SEB) models take into account all energy exchanges between the glacier and the atmosphere, and can simulate the spatial and temporal variability of snowmelt and the changes in albedo (e.g. Gerbaux et al., 2005).

(b) Regarding glacier dynamics:

1. Parameterized models do not explicitly resolve any physical processes, but implicitly take them into account using parameterizations, based on statistical or empirical relationships, in order to modify the glacier geometry. This type of models range from very simple statistical models (e.g. Carlson et al., 2014) to more complex ones based on different approaches, such as a calibrated equilibrium-line altitude (ELA) model (e.g. Zemp et al., 2006), a glacier retreat parameterization specific for glacier size groups (Huss and Hock, 2015) or volume/length-area scaling (e.g. Marzeion et al., 2012; Radić et al., 2014).
2. Process-based models, like GloGEMflow (e.g. Zekollari et al., 2019) and OGGM (e.g. Maussion et al., 2019), approximate a number of glacier physical processes involved in ice flow dynamics using the shallow ice approximation.
3. Physics-based models, like the finite elements Elmer/Ice model (e.g. Gagliardini et al., 2013), approach glacier dynamics by explicitly simulating physical processes and solving the full Stokes equations (e.g. Jouvet et al., 2009; Réveillet et al., 2015).

At the same time, the use of these different approaches strongly depend on available data, whose spatial and temporal resolutions have an important impact on the results' quality and uncertainties (e.g., Réveillet et al., 2018). Parameterized glacier dynamics models and empirical and statistical SMB models require a reference or training dataset to calibrate the relationships, which can then be used for projections with the hypothesis that relationships remain stationary in time. On the contrary, process-based and specially physics-based glacier dynamics and SMB models have the advantage of representing physical processes, but they require larger datasets at higher spatial and temporal resolutions with a consequently higher computational cost (Réveillet et al., 2018). For SMB modelling, meteorological reanalyses provide an attractive alternative to sparse point observations, although their spatial resolution and suitability to complex high-mountain topography are often not good enough for high-resolution physics-based glacio-hydrological applications. However, parameterized models are much more flexible, equally dealing with fewer and coarser meteorological data as well as the state of the art reanalyses, which allows to work at resolutions much closer to glaciers' scale and to reduce uncertainties. The current resolution of climate projections is still too low to adequately drive most glacier physical processes, but the ever-growing datasets of historical data are paving the way for the training of parameterized machine learning models.

In glaciology, statistical models have been applied for more than half a century, starting with simple multiple linear regressions on few meteorological variables (Hoinkes, 1968; Martin, 1974). Statistical modelling has made enormous progress in the last decades, specially thanks to the advent of machine learning. Compared to other fields in geosciences, such as oceanography (e.g., Ducournau and Fablet, 2016; Lguensat et al., 2018), climatology (e.g., Rasp et al., 2018; Jiang et al., 2018) and hydrology (e.g., Marçais and de Dreuzy, 2017; Shen, 2018), we believe that the glaciological community has not yet exploited the full capabilities of these approaches. Despite this fact, a number of studies have taken steps towards statistical approaches. Steiner et al. (2005) pioneered the very first study to use artificial neural networks (ANNs) in glaciology to simulate mass balances of the Grosse Aletschgletscher in Switzerland. They showed that a nonlinear model is capable of better simulating glacier mass bal-

ances compared to a conventional stepwise multiple linear regression. Furthermore, they found a significant nonlinear part within the climate/glacier mass balance relationship. This work was continued in Steiner et al. (2008) and Nussbaumer et al. (2012) for the simulation of glacier length instead of mass balances. Later on, Maussion et al. (2015) developed an empirical statistical downscaling tool based on machine learning in order to retrieve glacier surface energy and mass balance (SEB/SMB) fluxes from large-scale atmospheric data. They used different machine learning algorithms, but all of them were linear, which are not necessarily the most suitable for modelling the nonlinear climate system (Houghton et al., 2001). Nonetheless, more recent developments in the field of machine learning and optimization enabled the use of deeper network structures than the 3-layer ANN of Steiner et al. (2005). These deeper ANNs, which remain unexploited in glaciology, are capable of capturing more nonlinear structures in the data even for relatively small datasets (Ingrassia and Morlini, 2005; Olson et al., 2018).

Here, we present a parameterized regional open-source glacier model: the ALpine Parameterized Glacier Model (ALPGM, Bolibar, 2020). When most glacier evolution models tend to incorporate more and more physical processes in SMB or ice dynamics (e.g., Maussion et al., 2019; Zekollari et al., 2019), ALPGM takes an alternative approach based on data science for SMB modelling and parameterizations for glacier dynamics simulation. ALPGM simulates annual glacier-wide SMB and the evolution of glacier volume and surface area over time scales from a few years to a century at a regional scale. Glacier-wide SMBs are computed using a deep ANN, fed by several topographical and climatic variables, an approach which is compared to different linear methods in the present paper. In order to distribute these annual glacier-wide SMBs and to update the glacier geometry, a refined version of the Δh methodology (e.g., Huss et al., 2008) is used, for which we dynamically compute glacier-specific Δh functions. In order to validate this approach, we use a case study with 32 French alpine glaciers for which glacier-wide annual SMBs are available over the period 1984-2014 and 1959-2015 for certain glaciers. High resolution meteorological reanalyses for the same time period are used (SAFRAN, Durand et al., 2009) while the initial ice thickness distribution of glaciers are taken from Farinotti et al. (2019a), for which we performed a sensitivity analysis based on field observations.

In the next section, we present an overview of the proposed glacier evolution model framework with a detailed description of the two components used to simulate the annual glacier-wide SMB and the glacier geometry update. Then, a case study using French alpine glaciers is presented, which enables to illustrate an example of application of the proposed framework including a rich dataset, the parameterized functions, as well as the results and their performance. In the end, several aspects regarding machine and deep learning modelling in glaciology are discussed, from which we make some recommendations and draw the final conclusions.

2.3 Model overview and methods

In this section we present an overview of the ALPGM glacier model. Moreover, the two components of this model are presented in detail: the Glacier-wide SMB Simulation component and the Glacier Geometry Update component.

2.3.1 Model overview and workflow

ALPGM is an open-source glacier model coded in Python. The source code of the model is accessible in the project repository (see Code availability). It is structured in multiple files which execute specific sep-

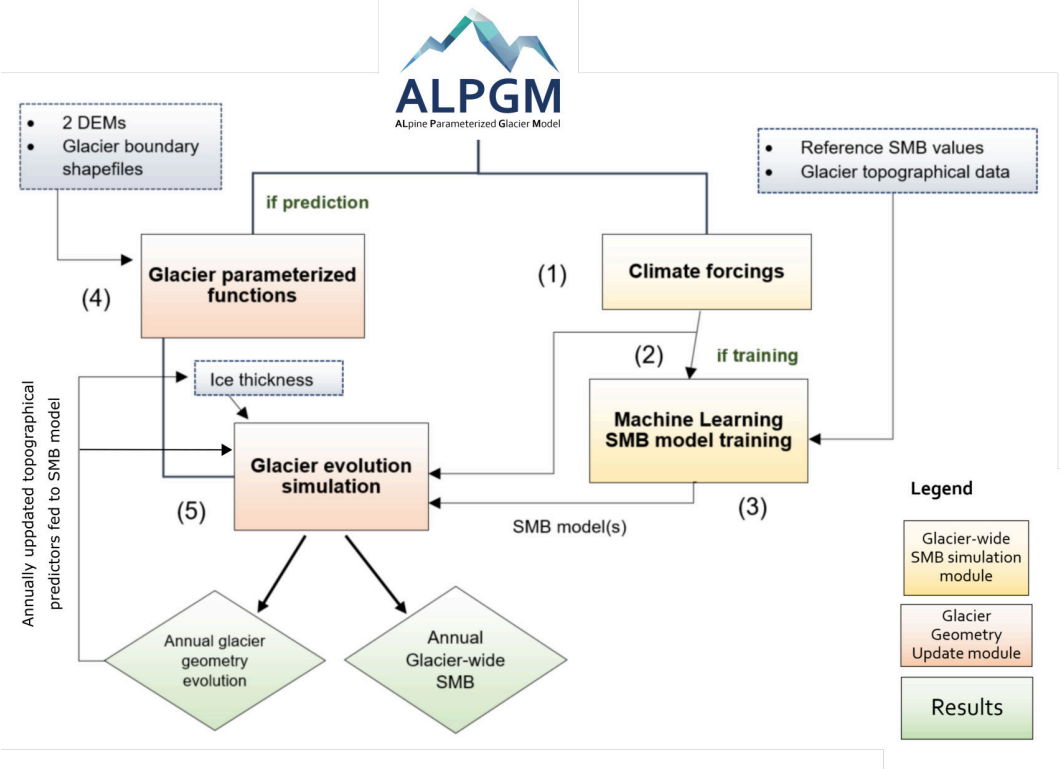

Figure 2.1: ALPGM structure and workflow

arate tasks. The model can be divided into two main components: (1) the Glacier-wide SMB Simulation and (2) the Glacier Geometry Update. The Glacier-wide SMB Simulation component is based on machine learning, taking both meteorological and topographical variables as inputs. The Glacier Geometry Update component generates the glacier-specific parameterized functions and modifies annually the geometry of the glacier (*e.g.*, ice thickness distribution, glacier outline) based on the glacier-wide SMB models generated by the Glacier-wide SMB simulation component.

Figure 2.1 presents ALPGM's basic workflow. The workflow execution can be configured via the model interface, allowing to run or skip any of the following steps:

1. The meteorological forcings are preprocessed in order to extract the necessary data closest to each glacier's centroid. The meteorological features are stored in intermediate files in order to reduce computation times for future runs, automatically skipping this preprocessing step when the files have already been generated.
2. The SMB machine learning component retrieves the preprocessed climate predictors from the stored files, retrieves the topographical predictors from the multitemporal glacier inventories, and then it assembles the training dataset by combining all the necessary topo-climatic predictors. A machine learning algorithm is chosen for the SMB model, which can be loaded from a previous run or it can be trained again with a new dataset. Then, the SMB model(s) are trained with the full topo-climatic dataset. These model(s) are stored in intermediate files, allowing to skip this step for future runs.
3. Performances of the SMB models can be evaluated with a leave-one-glacier-out (LOGO) or a leave-one-year-out (LOYO) cross-validation. This step can be skipped when using already established models. Basic statistical performance metrics are given for each glacier and model, as well as plots with the simulated cumulative glacier-wide SMBs compared to their reference

values with uncertainties for each of the glaciers from the training dataset.

4. The Glacier Geometry Update component starts with the generation of the glacier specific parameterized functions, using a raster containing the difference of the two pre-selected digital elevation models (DEMs) covering the study area for two separate dates, as well as the glacier contours. These parameterized functions are then stored in individual files to be used in the final simulations.
5. Once all previous steps have been run, the glacier evolution simulations are launched. For each glacier, the initial ice thickness and DEM rasters and the glacier geometry update function are retrieved. Then, in a loop, for every glacier and year, the topographical data is computed from these raster files. The climate predictors at the glacier's current centroid are retrieved from the climate data (e.g. reanalysis or projections) and with all this data the input topo-climatic data for the glacier-wide SMB model is assembled. Afterwards, the glacier-wide SMB for this glacier and year is simulated, which combined with the glacier-specific geometry update function allows to update the glacier's ice thickness and DEM rasters. This process is repeated in a loop, therefore updating the glacier's geometry with an annual timestep and taking into account the glacier's morphological and topographical changes in the glacier-wide SMB simulations. For the simulation of the following year's SMB, the previously updated ice thickness and DEM rasters is used to re-compute the topographical parameters, which in turn are used as input topographical predictors for the glacier-wide SMB machine learning model. If all the ice thickness raster pixels of a glacier become zero, the glacier is considered as disappeared and is removed from the simulation pipeline. For each year, multiple results are stored in data files as well as the raster DEM and ice thickness values for each glacier.

2.3.2 Glacier-wide surface mass balance simulation

Annual glacier-wide SMBs are simulated using machine learning. Due to the regional characteristics and specificities of topographical and climate data, this glacier-wide SMB modelling method is, for now, a regional approach.

Selection of explanatory topographical and climatic variables

In order to narrow down which topographical and climatic variables best explain glacier-wide SMB in a given study area, a literature review as well as a statistical sensitivity analysis are performed. Typically used topographical predictors are longitude, latitude, glacier slope and mean altitude. As for meteorological predictors, cumulative positive degree days (CPDD), but also mean monthly temperature, snowfall and possibly other variables that influence the surface energy budget are often used in the literature. Examples of both topographic and meteorological predictors can be found in the case study in Sect. 2.4. A way to prevent biases when making predictions with different climate data is to work with anomalies, calculated as differences of the variable with respect to its average value over a chosen reference period.

For the machine learning training, the relevant predictors must be selected, so we perform a sensitivity study of the annual glacier-wide SMB to topographical and climatic variables over the study training period. This can be performed with individual linear regressions between each variable and glacier-wide SMB data. After identification of the topographical and climatic variables that can potentially explain annual glacier-wide SMB variability for the region of interest, a training dataset is built. An effective way of expanding the training dataset in order to dig deeper into the available data is to

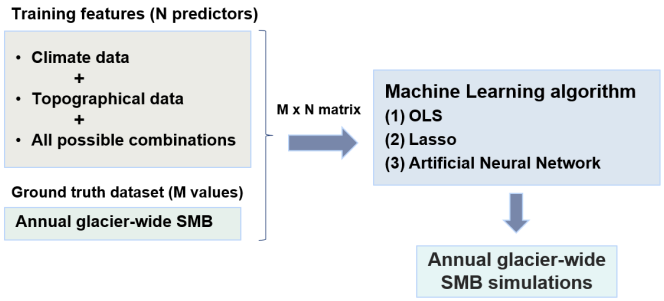

Figure 2.2: Glacier-wide SMB simulation component workflow. Machine learning models are dynamically created based on training data

combine the climatic and topographical input variables (Weisberg, 2014). Such combinations can be expressed following equation 2.1

$$SMB_{g,y} = f(\hat{\Omega}, \hat{C}) + \varepsilon_{g,y} \tag{2.1}$$

Where $\hat{\Omega}$ is a vector of the selected topographical predictors, $\hat{C}$ is a vector with the selected climatic features and $\varepsilon_{g,y}$ is the residual error for each annual glacier-wide SMB value, $SMB_{g,y}$.

Once the training dataset is created, different algorithms f (two linear and one nonlinear, for the case of this study) can be chosen to create the SMB model: (1) OLS (Ordinary Least Squares) all-possible multiple linear regressions; (2) Lasso (Least absolute shrinkage and selection operator) (Tibshirani, 1996); and (3) a deep Artificial Neural Network (ANN). ALPGM uses some of the most popular machine learning Python libraries: StatsModels (Seabold and Perktold, 2010), Scikit-learn (Pedregosa et al., 2012) and Keras (Chollet, 2015) with a TensorFlow backend. The overall workflow of the machine learning glacier-wide SMB model production in ALPGM is summarized in Fig. 2.2.

All-possible multiple linear regressions

With the ordinary least squares (OLS) all-possible multiple linear regressions, we attempt to find the best subset of predictors in Eq. 2.1 based on the resulting r^2 adjusted, while at the same time avoiding overfitting (Hawkins, 2004) and collinearity, and limiting the complexity of the model. As its name indicates, the goal is to minimize the residual sum of squares for each subset of predictors (Hastie et al., 2009). n models are produced by selecting all possible subsets of k predictors. It is advisable to narrow down the number of predictors for each subset in the search to reduce the computational cost. Models with low performance are filtered out, keeping only models with highest r^2 adjusted possible, a variance inflation factor (VIF) < 1.2 and a p-value < $0.01/n$ (in order to ensure the Bonferroni correction). Retained models are combined by averaging their predictions, thereby avoiding the pitfalls related to stepwise single model selection (Whittingham et al., 2006). These criteria ensure that the models explain as much variability as possible, avoid collinearity and are statistically significant.

Lasso

The Lasso (Least absolute shrinkage and selection operator) (Tibshirani, 1996) is a shrinkage method which attempts to overcome the shortcomings of the simpler step-wise and all-possible regressions. In these two classical approaches, predictors are discarded in a discrete way, giving subsets of variables which have the lowest prediction error. However, due to its discrete selection, these different

subsets can exhibit high variance, which does not reduce the prediction error of the full model. The Lasso performs a more continuous regularization by shrinking some coefficients and setting others to zero, thus producing more interpretable models (Hastie et al., 2009). Because of its properties, it strikes a balance between subset selection (like all-possible regressions) and Ridge regression (Hoerl and Kennard, 1970). All input data is normalized by removing the mean and scaling to unit variance. In order to determine the degree of regularisation applied to the coefficients used in the linear OLS regression, an alpha parameter needs to be chosen using cross-validation. ALPGM performs different types of cross-validations to choose from: the Akaike Information Criterion (AIC), the Bayes Information Criterion (BIC) and a classical cross-validation with iterative fitting along a regularization path (used in the case study). Alternatively, a Lasso model with Least Angle Regression, also known as Lasso Lars (Tibshirani et al., 2004), can also be chosen with a classical cross-validation.

Deep artificial neural networks

Artificial neural networks (ANNs) are nonlinear statistical models inspired by biological neural networks (Fausett, 1994; Hastie et al., 2009). A neural network is characterized by: (1) the architecture or pattern of connections between units and the number of layers (input, output and hidden layers); (2) the optimizer: which is the method for determining the weights of the connections between units; and (3) its (usually nonlinear) activation functions (Fausett, 1994). When ANNs have more than one hidden layer (*e.g.* Fig. 2.3), they are referred to as deep ANNs or deep learning. The description of neural networks is beyond the scope of this study, so for more details and a full explanation please refer to Fausett (1994), Hastie et al. (2009), as well as Steiner et al. (2005, 2008) where the reader can find a thorough introduction to the use of ANNs in glaciology. ANNs gained recent interest thanks to improvements of optimization algorithms enabling the training of deep neural networks, that lead to better representation of complex data patterns. As their learnt parameters are difficult to interpret, ANN are adequate tools when the quality of predictions prevails over the interpretability of the model (the latter likely involving causal inference, sensitivity testing or modelling of ancillary variables). This is precisely the case in our study context here, where abundant knowledge about glacier physics further helps choosing adequate variables as input to deep learning. Their ability to model complex functions of the input parameters makes them particularly suitable for modelling complex nonlinear systems such as the climate system (Houghton et al., 2001) and glacier systems (Steiner et al., 2005).

ALPGM uses a feedforward fully-connected ANN (Fig. 2.3). In such an architecture, the processing units - or neurons - are grouped into layers where all the units of a given layer are fully connected to all units of the next layer. The flow of information is directional, from the input layer (*i.e.*. in which each neuron corresponds to one of the N explanatory variables) to the output neuron (*i.e.*. corresponding to the target variable of the model, the SMB). For each connection of the ANN, weights are initialized in a random fashion following a specific distribution (generally centred around 0). In each unit of each hidden layer, the weighted values are summed before going through a nonlinear activation function, responsible for introducing the nonlinearities in the model. Using a series of iterations known as epochs, the ANN will try to minimize a specific loss function (the mean squared error (MSE) in our case) comparing the processed values of the output layer with the ground truth (y). In order to avoid falling into local minima of the loss function, some regularisation is needed to prevent the ANN from overfitting (Hastie et al., 2009). To prevent overfitting during the training process (*i.e.*. to increase the ability of the model to generalize to new data), we used a classical regularization method called dropout, consisting in training iteratively smaller subparts of the ANN by randomly disconnecting a certain amount of connections between units. The introduction of Gaussian noise at the input of

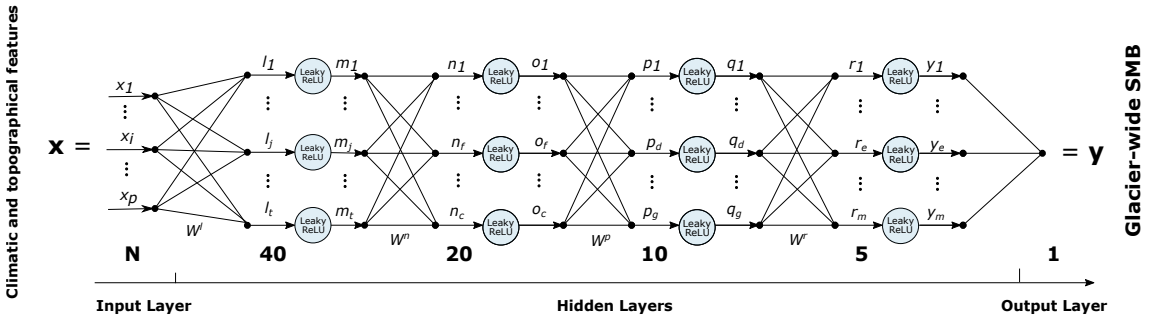

Figure 2.3: Deep Artificial Neural Network architecture used in ALPGM. The numbers indicate the number of neurons in each layer

the ANN also helped to generalize, as it performs a similar effect to data augmentation. The main consequence of regularisation is generalization, for which the produced model is capable of better adapting to different configurations of the input data.

The hyperparameters used to configure the ANN are determined using cross-validation, in order to find the best performing combination of number of units, hidden layers, activation function, learning rate and regularisation method. Due to the relatively small size of our dataset, we encountered the best performances with a quite small deep ANN, with a total of 6 layers (4 hidden layers) with a (N, 40, 20, 10, 5, 1) architecture (Fig. 2.3), where N is the number of selected features. Since the ANN already performs all the possible combinations between features (predictors), we use a reduced version of the training matrix from Eq. 2.1, with no combination of climatic and topographical features. Due to the relatively small size of the architecture, the best dropout rates are small (Srivastava et al., 2014), and range between 0.3 and 0.01 depending on the number of units of each hidden layer. Leaky ReLUs have been chosen as the activation function, because of their widespread reliability and the fact they help prevent the "dead ReLU" problem, where certain neurons can stop "learning" (Xu et al., 2015). The He uniform initialization (He et al., 2015) has been used as it is shown to work well with Leaky ReLUs, and all unit bias were initialized to zero. In order to optimize the weights of the gradient descent, we used the RMSprop optimizer, for which we fine-tuned the learning rate, obtaining the best results at 0.0005 in space and 0.02 in time. Each batch was normalized before applying the activation function in order to accelerate the training (Ioffe and Szegedy, 2015).

Like for many other geophysical processes found in nature, extreme annual glacier-wide SMB values occur much less often than average values, approximately following an unbounded Gumbel-type distribution (Thibert et al., 2018). From a statistical point of view, this means that ANN will "see" few extreme values and will accord less importance to them. For future projections in a warmer climate, extreme positive glacier-wide SMB balances should not be the main concern of glacier models. However, extreme negative annual glacier-wide SMB values should likely increase in frequency, so it is in the modeller's interest to reproduce them as well as possible. Setting the sample weights as the inverse of the probability density function during the ANN training can partly compensate for the imbalance of a dataset. This boosts the performance of the model for the extreme values, at the cost of sacrificing some performance on more average values, which can be seen as a r^2/RMSE trade-off (Fig. 2.6 and 2.9 from the case study). The correct setting of the sample weights allows the modeller to adapt the ANN to each dataset and application.

2.3.3 Glacier geometry update

Since the first component of ALPGM simulates annual glacier-wide SMBs, these changes in mass need to be redistributed over the glacier surface-area in order to reproduce glacier dynamics. This redistribution is applied using the Δh parameterization. The idea was first developed by Jóhannesson et al. (1989) and then adapted and implemented by Huss et al. (2008). The main idea behind it is to use two or more DEMs covering the study area. These DEMs should have dates covering a period long enough (which will be later discussed in detail). By subtracting them, the changes in glacier surface elevation over time can be computed, which corresponds to a change in thickness (considering no basal erosion). Then, these thickness changes are normalized and considered as a function of the normalized glacier altitude. This Δh function is specific for each glacier and represents the normalized glacier thickness evolution over its altitudinal range. One advantage of such a parametrized approach is that it implicitly considers the ice flow which redistributes the mass from the accumulation to the ablation area. In order to make the glacier volume evolve in a mass-conserving fashion, we apply this function to the annual glacier-wide SMB values in order to scale and distribute its change in volume.

As discussed in Vincent et al. (2014), the time period between the two DEMs used to calibrate the method needs to be long enough to show important ice thickness differences. The criteria will of course depend on each glacier and each period, but it will always be related to the achievable signal-to-noise ratio. Vincent et al. (2014) concluded that for their study on the Mer de Glace glacier (28.8 km^2, mean altitude = 2868 m.a.s.l.) in the French Alps, the 2003-2008 period was too short, due to the delayed response of glacier geometry to a change in surface mass balance. Indeed, the results for that 5-year period diverged from the results from longer periods. Moreover, the period should be long enough to be representative of the glacier evolution, which will often encompass periods with strong ablation and others with no retreat or even with positive SMBs.

Therefore, by subtracting the two DEMs, the ice thickness difference is computed for each specific glacier. These values can then be classified by altitude, thus obtaining an average glacier thickness difference for each pixel altitude. As a change to previous studies (Vincent et al., 2014; Huss and Hock, 2015; Hanzer et al., 2018; Vincent et al., 2019), we no longer work with altitudinal transects, but with individual pixels. In order to filter noise and artefacts coming from the DEM raster files, different filters are applied to remove outliers and pixels with unrealistic values, namely at the border of glaciers or where the surface slopes are high (refer to Supplements for detailed information). Our methodology thus allows to better exploit the available spatial information based on its quality, and not on arbitrary location within transects.

2.4 Case study: French alpine glaciers

2.4.1 Data

All data used in this case study is based on the French Alps (Fig. 2.4), located in the westernmost part of the European Alps, between 5.08° and 7.67°E, and 44° and 46°13'N. This region is particularly suited for the validation of a glacier evolution model because of the wealth of available data. Moreover, ALPGM has been developed as part of a hydro-glaciological study to understand the impact of the retreat of French alpine glaciers in the Rhône river catchment (97,800 km^2).

Glacier-wide surface mass balance

An annual glacier-wide SMB dataset, reconstructed using remote sensing based on changes in glacier volume and the snow line altitude, is used (Rabatel et al., 2016). This dataset is constituted by annual glacier-wide SMB values for 30 glaciers in the French Alps (Fig. 2.4) for 31 years, between 1984-2014. The great variety in topographical characteristics of the glaciers included in the dataset, with a good coverage of the three main clusters or groups of glaciers in the French Alps (Fig. 2.4), makes them an ideal training dataset for the model. Each of the clusters represents a different setup of glaciers with different contrasting latitudes (Écrins and Mont-Blanc), longitudes (Écrins and Vanoise), glacier size (smaller glaciers in Écrins and Vanoise vs larger ones in Mont-Blanc) and climatic characteristics with a Mediterranean influence towards the south of the study region. For more details regarding this dataset refer to Rabatel et al. (2016). Data from the Mer de Glace, Saint-Sorlin, Sarennes and Argentière glaciers is also used, coming from field observations from the GLACIOCLIM observatory. For some of these glaciers, glacier-wide SMB values are available since 1949, although only values from 1959 onwards were used to match the meteorological reanalysis. This makes a total of 32 glaciers (Argentière and Saint-Sorlin glaciers belonging to the two datasets), representing 1048 annual glacier-wide SMB values (taking into account some gaps in the dataset).

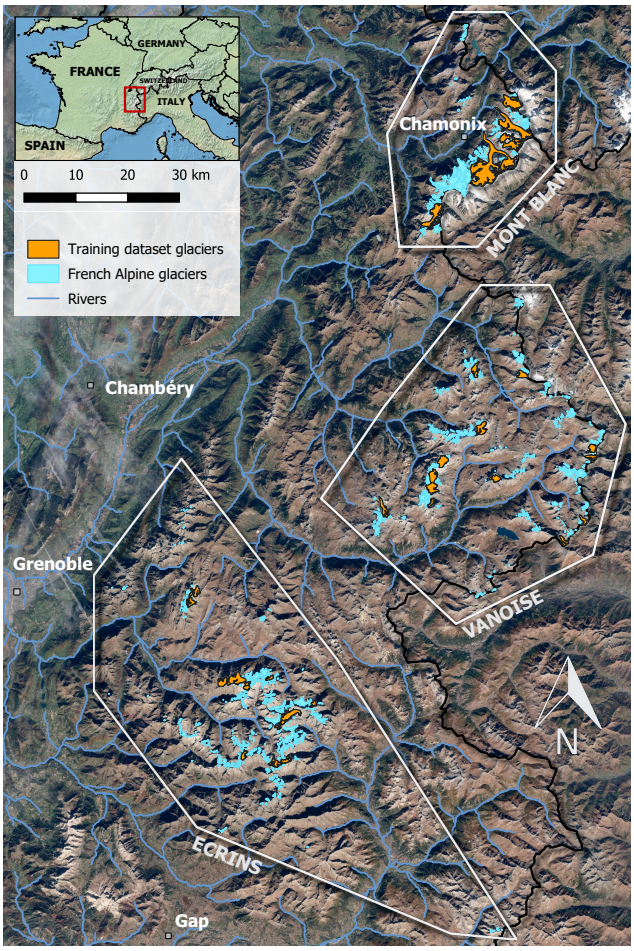

Figure 2.4: French alpine glaciers used for model training and validation and their classification into 3 clusters/regions (Écrins, Vanoise, Mont-Blanc). Coordinates of bottom left map corner: 44°32'N, 5°40'E, coordinates of the top right map corner: 46°08'N, 7°17'E.

Topographical glacier data and altimetry

The topographical data used for the training of the glacier-wide SMB machine learning models is taken from the multitemporal inventory of the French Alps glaciers (e.g., Gardent et al., 2014) partly available through the GLIMS Glacier Database (NSIDC, 2005). We worked with the 1967, 1985, 2003 and 2015 inventories (Gardent et al., 2014, with 2015 update). Between these dates, the topographical predictors are linearly interpolated. On the other hand, in the glacier evolution component of ALPGM (Fig. 2.1, step 5), the topographical data is re-computed every year for each glacier from the evolving and annually updated glacier-specific ice thickness and DEM rasters (Sect. 2.4.1). Since these raster files are estimates for the year 2003 (Farinotti et al. (2019a) for the ice thickness), the full glacier evolution

simulations can start the earliest at this date. For the computation of the glacier-specific geometry update functions, two DEMs covering the whole French Alps have been used: (1) one from 2011 generated from SPOT5 stereo-pair images, acquired on 15 October 2011; and (2) a 1979 aerial photogrammetric DEM from the French National Geographic Institute (Institut Géographique National, IGN), processed from aerial photographs taken around 1979. Both DEMs have an accuracy between 1 and 4 meters (Rabatel et al., 2016), and their uncertainties are negligible compared to many other parameters in this study.

Glacier ice thickness

Glacier ice thickness data come from Farinotti et al. (2019a), hereafter F19, based on the Randolph Glacier Inventory v6.0 (RGI, Consortium, 2017). The ice thickness values represent the latest consensus estimate, averaging an ensemble of different methods based on the principles of ice flow dynamics to invert the ice thickness from surface characteristics.

We also have ice thickness data acquired by diverse field methods (seismic, ground penetrating radar or hot water drilling, Rabatel et al., 2018) for four glaciers of the GLACIOCLIM observatory. We compared these in situ thickness data, with the simulated ice thicknesses from F19 (refer to Supplements for detailed information). Although differences can be found (locally up to 100% in the worst cases), no systematic biases were found with respect to glacier local slope nor glacier altitude; therefore, no systematic correction was applied to the dataset. The simulated ice thicknesses for Saint-Sorlin (2 km^2, mean altitude = 2920 m.a.s.l., Écrins cluster) and Mer de Glace (28 km^2, mean altitude = 2890 m.a.s.l., Mont-Blanc cluster) glaciers are satisfactorily modelled by F19. Mer de Glace's tongue presents local errors of about 50 m, peaking at 100 m (30% error) around 2000-2100 m.a.s.l, but the overall distribution of the ice is well represented. Saint Sorlin glacier follows a similar pattern, with maximum errors of around 20 m (20% error) at 2900 m.a.s.l. and a good representation of the ice distribution. The ice thicknesses for Argentière Glacier (12.8 km^2, mean altitude = 2808 m.a.s.l., Mont-Blanc cluster) and Glacier Blanc (4.7 km^2, mean altitude = 3196 m.a.s.l., Écrins cluster) are underestimated by F19 with an almost constant bias with respect to altitude, as seen in Rabatel et al. (2018). Therefore, a manual correction was applied to the F19 datasets for these two glaciers based on the field observations from the GLACIOCLIM observatory. A detailed plot (Fig. 2.13) presenting these results can be found in the supplementary material.

Climate data

In our French Alps case study, ALPGM is forced with daily mean near-surface (2 m) temperatures, daily cumulative snowfall and rain. The SAFRAN dataset is used to provide this data close to the glaciers' centroids. SAFRAN meteorological data (Durand et al., 2009) is a reanalysis of weather data including observations from different networks, and specific to the French mountain regions (Alps, Pyrenees and Corsica). Instead of being structured as a grid, data is provided at the scale of massifs, which are in turn divided into altitude bands of 300 meters and into 5 different aspects (north, south, east, west and flat).

2.4.2 Glacier-wide surface mass balance simulations: validation and results

In this section, we go through the selection of SMB predictors, we introduce the procedure for building machine learning SMB models, we assess their performance in space and time and we show some results of simulations using the French alpine glaciers dataset.

Selection of predictors

Statistical relationships between meteorological and topographical variables with respect to glacier-wide SMB are frequent in the literature for the European Alps (Hoinkes, 1968). Martin (1974) performed a sensitivity study on the SMB of the Saint-Sorlin and Sarennes glaciers (French Alps) with respect to multi-annual meteorological observations for the 1957-1972 period. Martin (1974) obtained a multiple linear regression function based on annual precipitation and summer temperatures, and he concluded that it could be further improved by differentiating winter and summer precipitations. Six and Vincent (2014) studied the sensitivity of the SMB to climate change in the French Alps from 1998 until 2014. They found that the variance of summer SMB is responsible for over 90% of the variance of the annual glacier-wide SMB. Rabatel et al. (2013, 2016) performed an extensive sensitivity analysis of different topographical variables (slope of the lowermost 20% of the glacier area, mean elevation, surface area, length, minimum elevation, maximum elevation, surface area change and length change) with respect to glacier ELA and annual glacier-wide SMBs of French alpine glaciers. Together with Huss (2012), who performed a similar study with SMB, the most significant statistical relationships were found for the lowermost 20% area slope, the mean elevation, glacier surface area, aspect and easting and northing. Rabatel et al. (2013) also determined that the climatic interannual variability is mainly responsible for driving the glacier equilibrium-line altitude temporal variability, whereas the topographical characteristics are responsible for the spatial variations in the mean ELA.

Summer ablation is often accounted for by means of cumulative positive degree days (CPDD). However, in the vast majority of studies, accumulation and ablation periods are defined between fixed dates (*e.g.*, 1st October - 30th April for the accumulation period in the northern mid-latitudes) based on optimizations. As discussed in Zekollari and Huybrechts (2018), these fixed periods may not be the best to describe SMB variability through statistical correlation. Moreover, the ablation season will likely evolve in the coming century, due to climate warming. In order to overcome these limitations, we dynamically calculate each year the transition between accumulation and ablation seasons (and vice-versa) based on a chosen quantile in the CPDD. We found higher correlations between annual SMB and ablation-period CPDD calculated using this dynamical ablation season. On the other hand, it was not the case for the separation between summer and winter snowfall. Therefore, we decided to keep constant periods to account for winter (1st October-1st May) and summer (1st May-1st October) snowfalls, and to keep them dynamical for the CPDD calculation.

Following this literature review, vectors $\hat{\Omega}$ and $\hat{C}$ from (Eq. 2.1) read as:

$$\hat{\Omega} = \left[\begin{array}{ccccccc} \overline{Z} & Z_{\max} & \alpha_{20\%} & \text{Area} & \text{Lat} & \text{Lon} & \Phi \end{array} \right] \tag{2.2}$$

$$\widehat{C} = \left[\begin{array}{ccccc} \Delta CPDD & \Delta WS & \Delta SS & \Delta \overline{T}_{\text{mon}} & \Delta \overline{S}_{\text{mon}} \end{array} \right] \tag{2.3}$$

Where:
$\overline{Z}$: Mean glacier altitude
$Z_{\max}$: Maximum glacier altitude
$\alpha_{20\%}$: Slope of the lowermost 20% glacier altitudinal range
$Area$: Glacier surface area
Lat: Glacier latitude
Lon: Glacier longitude
Φ: Cosine of the glacier's aspect (North = 0°)

$\Delta CPDD$: CPDD (Cumulative Positive Degree Days) anomaly
ΔWS: Winter snow anomaly
ΔSS: Summer snow anomaly
$\Delta\overline{T}_{\text{mon}}$: Average temperature anomaly for each month for the hydrological year
$\Delta\overline{S}_{\text{mon}}$: Average snowfall anomaly for each month for the hydrological year

For the linear machine learning models training, we chose a function f that linearly combines $\hat{\Omega}$ and $\hat{C}$, generating new combined predictors (Eq. 2.4.2). In $\hat{C}$, only $\Delta CPDD$, ΔWS, and ΔSS are combined, to avoid generating an unnecessary amount of predictors with the combination of $\hat{\Omega}$ with $\Delta\overline{T}_{\text{mon}}$ and $\Delta\overline{S}_{\text{mon}}$.

$$\begin{aligned} SMB_{g,y} = ((&a_1\overline{Z} + a_2 Z_{\max} + a_3\alpha_{20\%} + a_4 Area + a_5 Lat + a_6 Lon + a_7\Phi + a_8)\Delta CPDD + \\ &(b_1\overline{Z} + b_2 Z_{\max} + b_3\alpha_{20\%} + b_4 Area + b_5 Lat + b_6 Lon + b_7\Phi + b_8)\Delta SS + \\ &(c_1\overline{Z} + c_2 Z_{\max} + c_3\alpha_{20\%} + c_4 Area + c_5 Lat + c_6 Lon + c_7\Phi + c_8)\Delta WS + \\ &d_1\overline{Z} + d_2 Z_{\max} + d_3\alpha_{20\%} + d_4 Area + d_5 Lat + d_6 Lon + d_7\Phi + d_8 + d_n\Delta\overline{T}_{\text{mon}} + d_m\Delta\overline{S}_{\text{mon}} + \varepsilon)_{\text{g,y}} \end{aligned} \tag{2.4}$$

32 glaciers over variable periods between 31 and 57 years result in 1048 glacier-wide SMB ground truth values. For each glacier-wide SMB value, 55 predictors were produced following Eq. 2.4.2 33 combined predictors, with $\Delta\overline{T}_{\text{mon}}$ and $\Delta\overline{S}_{\text{mon}}$ accounting for 12 predictors each, one for each month of the year. All these values combined produce a 1048x55 matrix, given as input data to the OLS and Lasso machine learning libraries. Early Lasso tests (not shown here) using only the predictors from Eq. 2.2 and 2.3 demonstrated the benefits of expanding the number of predictors, as it is later shown in Fig. 2.5. For the training of the ANN, no combination of topo-climatic predictors is done as previously mentioned (Sect. 2.3.2), since it is already done internally by the ANN.

Causal analysis

By running the Lasso algorithm on the dataset based on Eq. 2.2 and 2.3, we obtain the contribution of each predictor in order to explain the annual glacier-wide SMB variance. Regarding the climatic variables, accumulation-related predictors (winter snowfall, summer snowfall as well as several winter, spring and even summer months), appear as the most important predictors. Ablation-related predictors also seem to be relevant, mainly with CPDD and summer and shoulder season months (Fig. 2.5). Interestingly, meteorological conditions in the transition months are crucial for the annual glacier-wide SMB in the French Alps: (1) October temperature is determinant for the transition between the ablation and the accumulation season, favouring a lengthening of melting when temperature remains positive, or conversely allowing snowfalls that protect the ice and contribute to the accumulation when temperatures are negative; (2) March snowfall has a similar effect: positive anomalies contribute to the total accumulation at the glacier surface, and a thicker snow pack will delay the snow/ice transition during the ablation season leading to a less negative ablation rate (e.g. Fig. 2.6b, Réveillet et al., 2018). Therefore, meteorological conditions of these transition months seem to strongly impact the annual glacier-wide SMB variability, since their variability oscillates between positive and negative values, unlike the months in the heart of summer or winter.

In a second term, topographical predictors do play a role, albeit a secondary one. The slope of the 20% lowermost altitudinal range, the glacier area, the glacier mean altitude and aspect help to modulate the glacier-wide SMB signal, which unlike point or altitude-dependent SMB, partially depends on glacier topography (Huss et al., 2012). Moreover, latitude and longitude are among the most relevant topographical predictors, which for this case study are likely to be used as bias correctors of precipitation of the SAFRAN climate reanalysis. SAFRAN is suspected of having a precipitation bias, with higher uncertainties for high altitude precipitations (Vionnet et al., 2016). Since the French Alps present an altitudinal gradient, with higher altitudes towards the eastern and the northern massifs, we found that the coefficients linked to latitude and longitude enhanced glacier-wide SMBs with a north-east gradient.

Spatial predictive analysis

In order to evaluate the performance of the machine learning SMB models in space, we perform a leave-one-glacier-out (LOGO) cross-validation. For relatively small datasets like the one used in this study, cross-validation ensures that the model is validated on the full dataset. Such validation aims at understanding the model's performance for predictions on other glaciers for the same time period as during the training.

An important aspect is the comparison between linear and nonlinear machine learning algorithms used in this study. Steiner et al. (2005) already proved that a nonlinear ANN improved the results with respect a classic stepwise multiple linear regression. Here, we draw a similar comparison using more advanced methods for a larger dataset: OLS and Lasso as linear machine learning algorithms and a deep ANN as a nonlinear one. We observed significant differences between OLS, Lasso and deep learning, both in terms of explained variance (r^2) and accuracy (RMSE) of predicted glacier-wide SMBs. On average, we found improvements between +55% and +61% in the explained variance (from 0.49 to 0.76-0.79) using the nonlinear deep ANN compared to Lasso, whereas the accuracy was improved up to 45% (from 0.74 to 0.51-0.62). This means that 27% more variance is explained with a nonlinear model in the spatial dimension for glacier-wide SMB in this region (Fig. 2.6). An interesting consequence of the nonlinearity of the ANN is the fact that it better captures extreme SMB values compared to a linear model. A linear model can correctly approximate the main cluster of values around the median, but the linear approximation

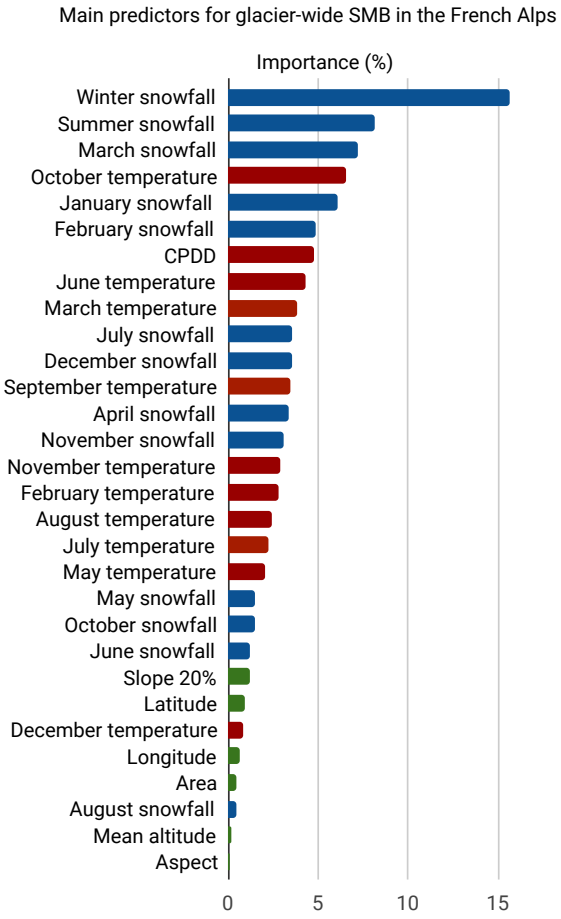

Figure 2.5: Contribution to the total variance of the 30 top topo-climatic predictors out of 55 predictors using Lasso. Green bars indicate predictors including topographical features, blue ones including accumulation-related features, and red ones including ablation-related features

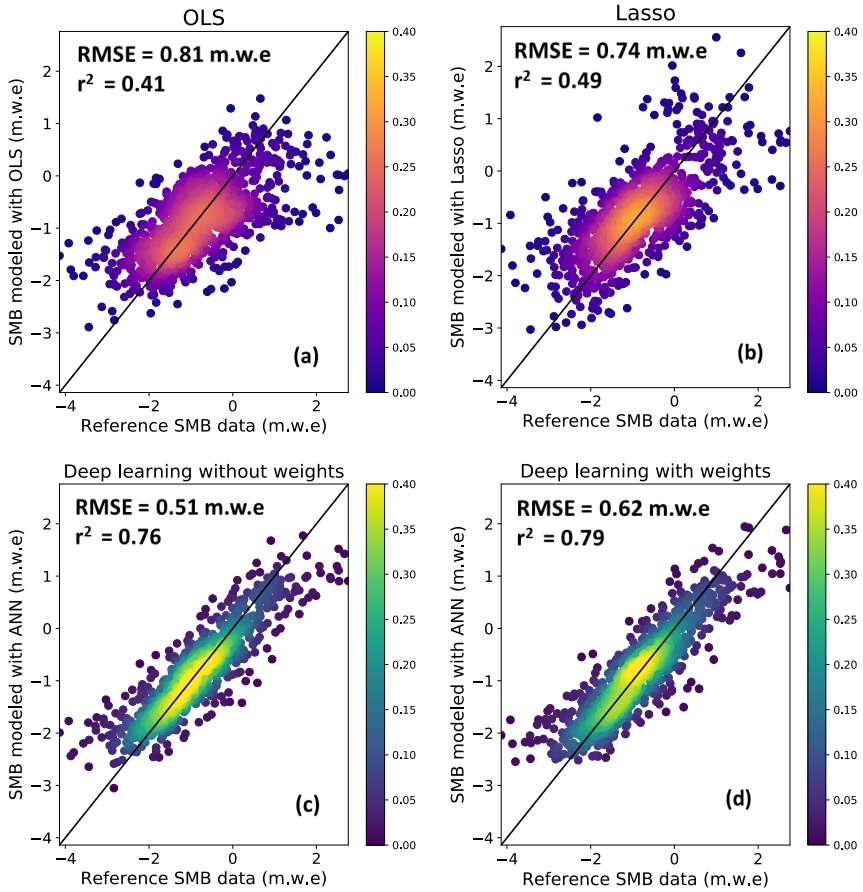

Figure 2.6: Evaluation of modelled annual glacier-wide SMB against the ground truth SMB data (both in m.w.e. a^{-1}) using Leave-One-Glacier-Out cross-validation. The colour (purple-orange for linear; blue-green for nonlinear) indicates frequency based on the probability density function. The black line indicates the reference one-to-one line. a) Scatter plot of the OLS model results; b) Scatter plot of the Lasso linear model results; Scatter plots of the deep artificial neural network nonlinear models without (c) and with sample weights (d)

performs poorly for extreme annual glacier-wide SMB values. The ANN solves this problem, with an increased explained variance which translates into a better accuracy for extreme SMB values, even without the use of sample weights (Fig. 2.6).

As a consequence, the added value of deep learning is especially relevant on glaciers with steeper annual changes in glacier-wide SMB (Fig. 2.7a). The use of sample weights can scale up or down this factor, thus playing with a performance trade-off depending on how much one wants to improve the model's behaviour for extreme SMB values.

Overall, deep learning results in a lower error throughout all the glaciers in the dataset when evaluated using LOGO cross-validation (Fig. 2.8). Moreover, the bias is also systematically reduced, but it is strongly correlated to the one from Lasso.

Temporal predictive analysis

In order to evaluate the performance of the machine learning SMB models in time, we perform a leave-one-year-out (LOYO) cross-validation. This validation serves to understand the model's performance for past or future periods outside the training time period. The best results achieved for Lasso make no use of any monthly average temperature or snowfall, suggesting that these features are not relevant

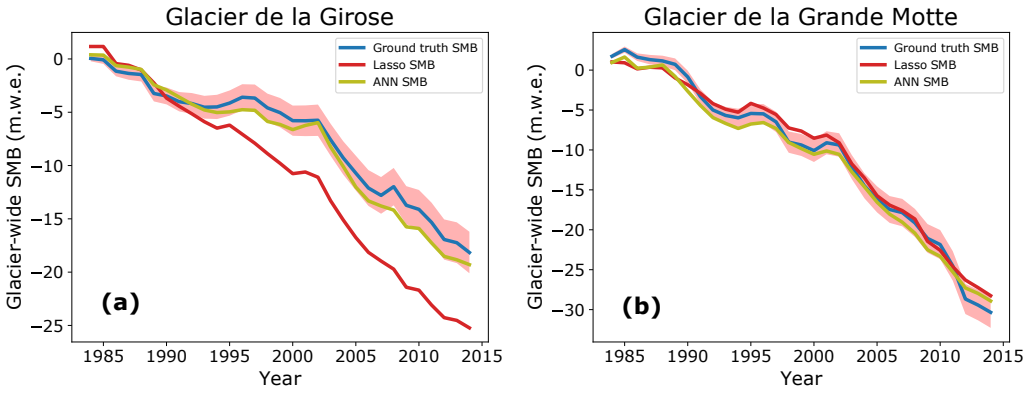

Figure 2.7: Examples of cumulative glacier-wide SMB (m.w.e.) simulations against the ground truth SMB data. The pink envelope indicates the accumulated uncertainties from the ground truth data. The deep learning SMB model has not been trained with sample weights in these illustrations.

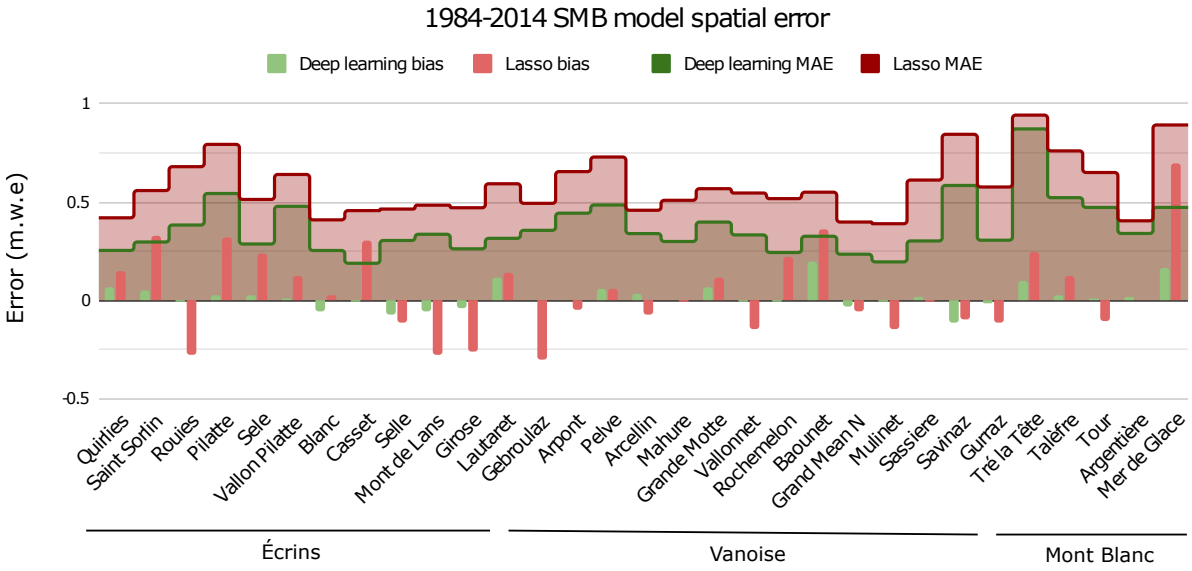

Figure 2.8: Mean average error (MAE) and bias (vertical bars) for each glacier of the training dataset structured by clusters for the 1984-2014 LOGO glacier-wide SMB simulation. No clear regional error patterns arise

for temporal predictions unlike the spatial case.

As in Sect. 2.4.2, the results between the linear and nonlinear machine learning algorithms were compared. Interestingly, using LOYO, the differences between the different models were even greater than for spatial validation, revealing the more complex nature of the information in the temporal dimension. As illustrated by Fig. 2.9, we found remarkable improvements between the linear Lasso and the nonlinear deep learning in both the explained variance (between +94% and +108%) and accuracy (between +32% and +58%). This implies that 35% more variance is explained using a nonlinear model in the temporal dimension for glacier-wide SMB balance in this region. Deep learning manages to keep very similar performances between the spatial and temporal dimensions, whereas the linear methods see their performance affected most likely due to the increased nonlinearity of the SMB reaction to meteorological conditions.

A more detailed year by year analysis reveals interesting information about the glacier-wide SMB data structure. As seen in Fig. 2.10, the years with the worst deep learning precision are 1984, 1985 and 1990. All these three hydrological years present a high spatial variability in observed (or remotely-

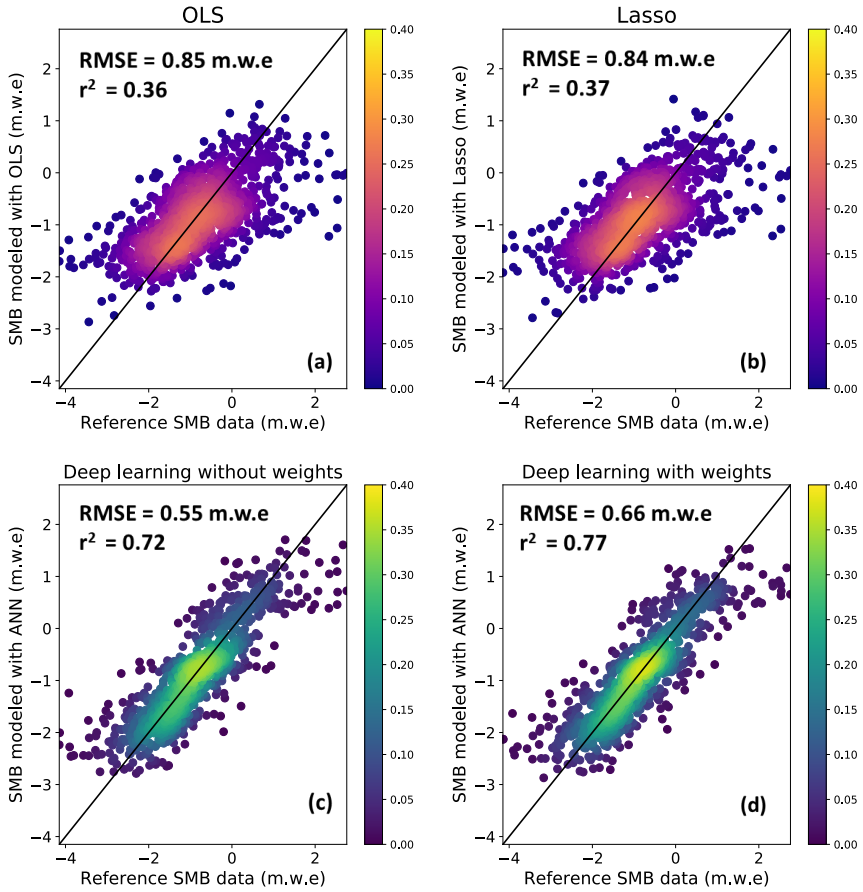

Figure 2.9: Evaluation of modelled annual glacier-wide SMB against the ground truth SMB data (both in m.w.e. a^{-1}) using Leave-One-Year-Out cross-validation. The colour (purple-orange for linear; blue-green for nonlinear) indicates frequency based on the probability density function. The black line indicates the reference one-to-one line. a) Scatter plot of the OLS model results; b) Scatter plot of the Lasso linear model results; Scatter plots of the deep artificial neural network nonlinear models without (c) and with sample weights (d).

sensed) SMBs: very positive SMB values in general for 1984 and 1985 with few slightly negative values, and extremely negative SMB values in general for 1990 with few almost neutral values. These complex configurations are clearly outliers within the dataset, which push the limits of the nonlinear patterns found by the ANN. The situation becomes even more evident with Lasso, which struggles to resolve these complex patterns and often performs poorly where the ANN succeeds (*e.g.*, years 1996, 2012 or 2014). The important bias present only with Lasso is representative of its lack of complexity towards nonlinear structures, which results in an underfitting of the data. The average error is not bad, but it shows a high negative bias for the first half of the period, which mostly has slightly negative glacier-wide SMBs, and a high positive bias for the second half of the period, which mostly has very negative glacier-wide SMB values.

Spatiotemporal predictive analysis

Once the specific performances in the spatial and temporal dimensions have been assessed, the performance in both dimensions at the same time is evaluated using Leave-Some-Years-and-Glaciers-Out (LSYGO) cross-validation. 64 folds were built, with test folds being comprised of data for 2 random glaciers on 2 random years, and train folds of all the data except the 2 years (for all glaciers) and the 2 glaciers (for all years) present in the test fold. These combinations are quite strict, implying that

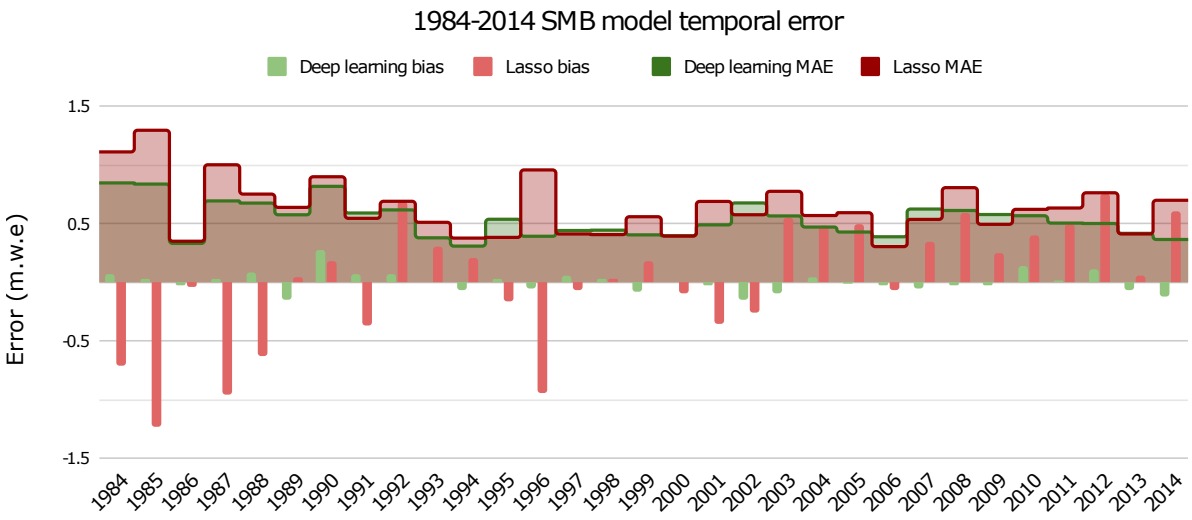

Figure 2.10: Mean average error (MAE) and bias (vertical bars) for each year of the training dataset for the 1984-2014 LOYO glacier-wide SMB simulation.

for every 4 tested values we need to drop between 123 and 126 values for training, depending on the glacier and year, to respect the spatiotemporal independence (Roberts et al., 2017).

The performance of LSYGO is similar to LOYO, with a RMSE of 0.51 m.w.e. and a coefficient of determination of 0.77 (Fig. 2.16). This is reflected in the fact that very similar ANN hyperparameters were used for the training. This means that the deep learning SMB model is successful in generalizing and it does not overfit the training data.

2.4.3 Glacier geometry evolution: Validation and results

As mentioned in Sect. 2.3.3, the h parameterization has been widely used in many studies (e.g., Huss et al., 2008, 2010; Vincent et al., 2014; Huss and Hock, 2015, 2018; Hanzer et al., 2018; Vincent et al., 2019). It is not in the scope of this study to evaluate the performance of this method, but we present the approach developed in ALPGM to compute the Δh functions and show some examples for single glaciers to illustrate how these glacier-specific functions perform compared to observations. For the studied French alpine glaciers, the 1979-2011 period is used. This period was proved by Vincent et al. (2014) to be representative of Mer de Glace's secular trend. Other sub-periods could have been used, but it was shown that they did not necessarily improve the performance. In addition, the 1979 and 2011 DEMs are the only ones available that cover all the French alpine glaciers. Within this period, some years with neutral to even positive surface mass balances in the late 1970s and early 1980s can be found, as well as a remarkable change from 2003 onward with strongly negative surface mass balances, following the heatwave that severely affected the western Alps in summer 2003.

The glacier-specific Δh functions are computed for glaciers $\geq$ 0.5 km^2, which represented about 80% of the whole glaciarized surface of the French Alps in 2015 (some examples are illustrated in the Supplement Fig. 2.15). For the rest of very small glaciers (< 0.5 km^2), a standardized flat function is used in order to make them shrink equally at all altitudes. This is done to simulate the fact that generally, the equilibrium line of very small glaciers has surpassed the glacier's maximum altitude, thus shrinking from all directions and altitudes in summer. Moreover, due to their reduced size and altitudinal range, the ice flow no longer has the same importance as for larger or medium sized glaciers.

In order to evaluate the performance of the parameterized glacier dynamics of ALPGM, coupled with the glacier-wide SMB component, we compared the simulated glacier area of the 32 studied glaciers with the observed area in 2015 from the most up-to-date glacier inventory in the French Alps. Simulations were started in 2003, for which we used the F19 ice thickness dataset. In order to take into account the ice thickness uncertainties, we ran three simulations with different versions of the initial ice thickness: the original data, -30% and +30% of the original ice thickness in agreement with the uncertainty estimated by the authors. Moreover, in order to take into account the uncertainties in the Δh glacier geometry update function computation, we added a ±10% variation in the parameterized functions (Fig. 2.11).

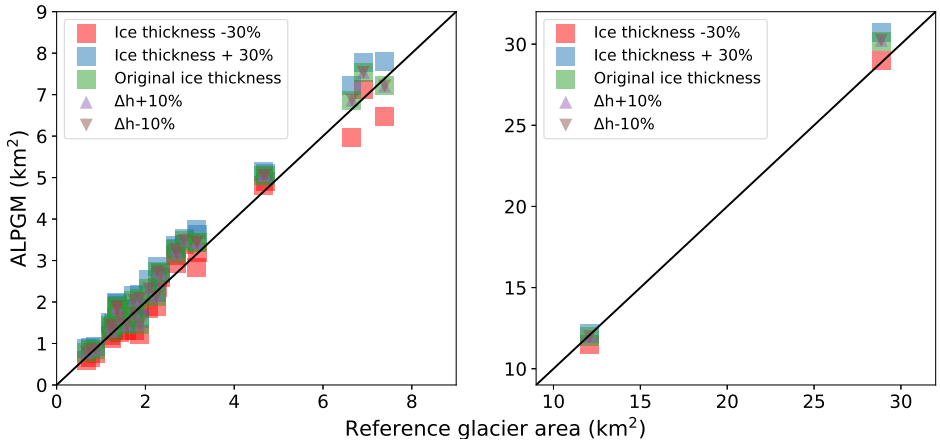

Figure 2.11: Simulated glacier areas for the 2003-2015 period for the 32 study glaciers using a deep learning SMB model without weights. Squares indicate the different F19 initial ice thicknesses used taking into account their uncertainties and triangles indicate the uncertainties linked to the glacier-specific geometry update functions. For better visualisation, the figure is split in two with the two largest French glaciers on the right.

Overall, the results illustrated in Fig. 2.11 show a good agreement with the observations. Even for a 12-year period, the initial ice thickness remains the largest uncertainty, with almost all glaciers falling within the observed area when taking it into account. The mean error in simulated surface area was of 10.7% with the original F19 ice thickness dataset. Other studies using the Δh parameterization already proved that the initial ice thickness is the most important uncertainty in glacier evolution simulations, together with the choice of a GCM for future projections (Huss and Hock, 2015).

2.5 Discussion and perspectives

2.5.1 Linear methods still matter

Despite the fact that deep learning often outperforms linear machine learning and statistical methods, there is still a place for such methods in modelling. Indeed, unlike ANNs, simpler regularised linear models such as Lasso allow an easy interpretation of the coefficients associated to each input feature, which helps to understand the contribution of each of the chosen variables to the model. This means that linear machine learning methods can be used for both prediction and causal analysis. Training a linear model in parallel to an ANN has therefore the advantage to provide a simpler linear alternative which can be used to understand the dataset. Moreover, seeing the contribution of each coefficient, one can reduce the complexity of the dataset by keeping only the most significant predictors. Finally, a linear model serves as well as a reference to highlight and quantify the nonlinear gains obtained by

deep learning.

2.5.2 Training deep learning models with spatiotemporal data

The creation and training of a deep ANN requires a certain knowledge and strategy with respect to the data and study focus. When working with spatiotemporal data, the separation between training and validation becomes tricky. The spatial and temporal dimensions in the dataset cannot be ignored, and strongly affect the independence between training and validation data (Roberts et al., 2017; Oliveira et al., 2019). Depending on how the cross-validation is performed, the obtained performance will be indicative of one of these two dimensions. As it is shown in Sect. 2.4.2, the ANNs and especially the linear modelling approaches had more success in predicting SMB values in space than in time. This is mostly due to the fact that the glacier-wide SMB signal has a greater variability and nonlinearities in time than in space, with climate being the main driver of the annual fluctuations in SMB, whereas geography, and in particular the local topography, modulates the signal between glaciers (Huss, 2012; Rabatel et al., 2016; Vincent et al., 2017). Consequently, linear models find it easier to make predictions on a given period of time for other glaciers elsewhere in space, than for time periods outside the training. Nonetheless, the deep learning SMB models were capable of equally capturing the complex nonlinear patterns in both the spatial and temporal dimensions.

In order to cope with the specific challenges related to each type of cross-validation, there are several hyperparameters that can be modified to adapt the ANN's behaviour. Due to the long list of hyperparameters intervening in an ANN, it is not advisable to select them using brute force with a grid search or cross-validation. Instead, initial tests are performed in a subset of random folds to narrow down the range of best performing values, before moving to the full final cross-validations for the final hyperparameter selection. Moreover, the ANN architecture plays an important role: the number of neurons as well as the number of hidden layers will determine the ANN's complexity and its capabilities to capture hidden patterns in the data. But the larger the architecture, the higher are the chances to overfit the data. This undesired effect can be counterbalanced using regularization. The amount of regularization (dropout and Gaussian noise in our case, see Sect. 2.3.2) used in the training of the ANN necessarily introduces some trade-offs. The greater the dropout, the more we will constrain the learning of the ANN so the higher the generalization will be, until a certain point, where relevant information will start to be lost and performance will drop. On the other hand, the learning rate to compute the stochastic gradient descent, which tries to minimize the loss function, also plays an important role: smaller learning rates generally result in a slower convergence towards the absolute minima, thus producing models with better generalization. By balancing all these different effects, one can achieve the accuracy versus generalization ratio that best suits a certain dataset and model in terms of performance. Nonetheless, one key aspect in machine learning models is data: expanding the training dataset in the future will enable an increase in the complexity of the model and its performance. Consequently, machine learning models see their performance improved as time goes by, with new data becoming available for training.

Although the features used as input for the model are classical descriptors of the topographical and meteorological conditions of the glaciers, it is worth mentioning that applying the model in different areas or with different data sources would likely require a re-training of the model due to possible biases: different regions on the globe may have other descriptors of importance but also different measuring techniques will likely have different biases.

2.5.3 Perspectives on future applications of deep learning in glaciology

The currently used meteorological variables in the deep ANN of ALPGM's SMB component are based on the classic degree-day approach, which relies only on temperature and precipitation. However, the model could be trained with variables involved in more complex models, such as SEB-type models, for which the longwave and shortwave radiation, as well as the turbulent fluxes and albedo intervene. The current model framework allows flexibility in the choice and number of input variables that can reflect different degrees of complexity for the resolved processes. Despite the fact that it has been shown that for glaciers in the European Alps there is almost no added value in transitioning from a simple degree-day to a SEB model for annual glacier-wide SMB simulations (e.g., Réveillet et al., 2017), it could be an interesting way to expand the training dataset for glaciers in tropical and subtropical regions, where shortwave radiation plays a much more important role (Benn and Evans, 2014). Maussion et al. (2015) followed a similar approach with linear machine learning in order to calibrate a regression-based downscaling model that linked local SEB/SMB fluxes to atmospheric reanalysis variables.

In this work, we also evaluated the resilience of the deep learning approach: since many glacierized regions in the world do not have the same amount of data used in this study, we trained an ANN only with monthly average temperature and snowfall, without any topographical predictors, to see until which point the algorithm is capable of learning from minimal data. The results were quite interesting, with a coefficient of determination of 0.68 (against 0.76 from the full model) and a RMSE of 0.59 m.w.e. a^{-1} (against 0.51 from the full model). These results indicate that meteorological data is the primary source of information, determining the interannual high frequency variability of the glacier-wide SMB signal. On the other hand, the "bonus" of topographical data helps to modulate the high frequency climate signal, by adding a low frequency component to better differentiate glaciers and the topographical characteristics included in the glacier-wide SMB data (Huss et al., 2012). The fact that glacier-wide SMB is influenced by glacier topography poses the question of determining if the simulated glacier geometries can correctly reproduce topographical observations, needed to represent the topographical feedback present in glacier-wide SMB signals. These aspects are analyzed and discussed in Sect. 2.4 of the Supplementary material, showing small differences between the observed and simulated topographical parameters for the 2003-2015 period (Table S1). Additionally, the simulated glacier-wide SMBs using simulated topographical parameters show very small differences (0.069 m.w.e. a^{-1} on average) compared to simulations using topographical observations (Fig. 2.17). Since glacier ice thickness estimates date from the year 2003 (Farinotti et al., 2019a), our validation period can only encompass 12 years. According to all the available data for validation, our model seems to be able to correctly reproduce the glacier geometry evolution, but since the 2003-2015 validation period is quite short, the validation performance might not be representative when dealing with future glacier evolution projections of several decades. Consequently, these aspects will have to be taken into account for future studies using this modelling approach for projections. Moreover, the cross-validation results of the SMB model(s) (Fig. 2.6-2.10) are representative of the performance of predictions using topographical observations. Despite the small differences found between simulated and observed topographical parameters, the SMB model's performance might be slightly different than the performance found in the cross-validation analysis. Therefore, it would be interesting for future studies to investigate the use of point SMB data, which could avoid the complexities related to the influence of glacier topography in glacier-wide SMB.

A nonlinear deep learning SMB component like the one used for ALPGM could provide an interesting alternative to classical SMB models used for regional modelling. The comparison with other SMB models is beyond the scope of this study, but it would be worth investigating to quantify the spe-

cific gains that could be achieved by switching to a deep learning modelling approach. Nonetheless, the linear machine learning models trained with the CPDD and cumulative snowfall used in this study behave in a similar way to a calibrated temperature-index model. Even so, we believe that future efforts should be taken towards physics-informed data science glacier SMB and evolution modelling. Adding physical constraints in ANNs, with the use of physics-based loss functions and/or architectures (e.g., Karpatne et al., 2018), would allow improving our understanding and confidence in predictions, reduce our dependency on big datasets, and to start bridging the gap between data science and physical methods (Karpatne et al., 2017; de Bezenac et al., 2018; Lguensat et al., 2019; Rackauckas et al., 2020). Deep learning can be of special interest once applied in the reconstruction of SMB time series. More and more SMB data is becoming available thanks to the advances in remote sensing (e.g., Brun et al., 2017; Zemp et al., 2019; Dussaillant et al., 2019), but these datasets often cover limited areas and the most recent time period in the studied regions. An interesting way of expanding a dataset would be to use a deep learning approach to fill the data gaps, based on the relationships found in a subset of glaciers as in the case study presented here. Past SMB time series of vast glaciarized regions could thereby be reconstructed, with potential applications in remote glaciarized regions such as the Andes or High Mountain Asia.

2.6 Conclusions

We presented a novel approach to simulate and reconstruct glacier-wide SMB series using deep learning for individual glaciers at a regional scale. This method has been included as a SMB component in ALPGM (Bolibar, 2020), a parameterized regional glacier evolution model, following an alternative approach to most physical and process-based glacier models. The data-driven glacier-wide SMB modelling component is coupled with a glacier geometry update component, based on glacier-specific parameterized functions. Deep learning is shown to outperform linear methods for the simulation of glacier-wide SMB with a case study of French alpine glaciers. By means of cross-validation, we demonstrated how important nonlinear structures (up to 35%) coming from the glacier and climate systems in both the spatial and temporal dimensions are captured by the deep ANN. Taking into account this nonlinearity substantially improved the explained variance and accuracy compared to linear statistical models, especially in the more complex temporal dimension. As we have shown in our case study, deep ANNs are capable of dealing with relatively small datasets, and they present a wide range of configurations to generalize and prevent overfitting. Machine learning models benefit from the increasing number of available data, which makes their performance constantly improve as time goes by.

Deep learning should be seen as an opportunity by the glaciology community. Its good performance for SMB modelling in both the spatial and temporal dimensions shows how relevant it can be for a broad range of applications. Combined with in situ or remote sensing SMB estimations, it can serve to reconstruct SMB time series for regions or glaciers with already available data for past and future periods, with potential applications in remote regions such as the Andes or the high mountains of Asia. Moreover, deep learning can be used as an alternative to classical SMB models as it is done in ALPGM: important nonlinearities from the glacier and climate systems are potentially ignored by these mostly linear models, which could give an advantage to deep learning models in regional studies. It might still be too early for the development of such models in certain regions which lack consistent datasets with a good spatial and temporal coverage. Nevertheless, upcoming methods adding physical knowledge to constrain neural networks (e.g., Karpatne et al., 2018; Rackauckas et al., 2020) could

provide interesting solutions to the limitations of our current method. By incorporating prior physical knowledge in neural networks, the dependency on big datasets would be reduced, and it would enable a transition towards more interpretable physics-informed data science models.

2.7 Supplementary material

2.7.1 Filtering of DEM rasters

Before computing the glacier-specific Δh parameterized functions, some preprocessing is done to the regional French Alps DEM raster files in order to filter artefacts and noise. The processing chain works as follows:

1. The regional DEM files are cropped using the 2003 glacier inventory shapefile outlines, thus obtaining glacier-specific rasters with the DEMs from 1979 and 2011.
2. The glacier surface altitude difference for this period (so-called dh/dt) which corresponds to the change in ice thickness is computed glacier by glacier by subtracting the two previously mentioned DEM rasters.
3. A first empirical filter is applied to all rasters to filter unrealistic values coming from artefacts (e.g., presence of clouds or saturation on the images used to generate de DEMs).
4. The filtered ice thickness difference (dh/dt) and DEM rasters are paired together as in Figure 12, and a low-order polynomial fit is applied in order to get the main trend of the scatterplot between the ice thickness difference vs. altitude.
5. A dynamic envelope/buffer around the polynomial fit line is computed for each glacier based on a quantile between maximum and minimum values for each altitude. In order to smooth the computed envelope for each altitude, a convolutional filter is applied to these values in order to smooth them and to follow the polynomial fit. A dynamic sliding window size is used to adjust the averaging process to the characteristics of each glacier.
6. A second filter is then applied using the computed smoothed envelope buffer to remove outliers
7. A final polynomial fit is computed with a variable order depending on the number of remaining data values of each glacier.
8. The percentage of pixels of information available for computing the polynomial fit (the parameterized function) is displayed for each glacier at the end of the processing chain.

2.7.2 SMB statistical error analysis

In order to determine the error due to each predictor, a Lasso model was trained with the same training matrix as the ANN, but instead of using SMB as ground truth data the errors generated by the ANN without weights were used. As discussed in section 2.5.1, Lasso performs a regularization on the training dataset, thus keeping only certain predictors and removing the rest. By looking at the resulting coefficients of the model, we can estimate the linear contribution of each predictor to the final model error. Latitude and longitude appear as the most important error predictors, but their contribution might in fact indicate the different magnitude of errors between glaciers or regions, since the pair of coordinates specifically identifies each glacier. October, August and March temperature follow behind, indicating that changes in temperature during these months have an influence in the simulation errors. It is not surprising that two of these months appear as top predictors (Fig. 2.5), as

changes in temperature during these months at the transition between the accumulation and ablation season can have a strong importance on the surface mass balance processes.

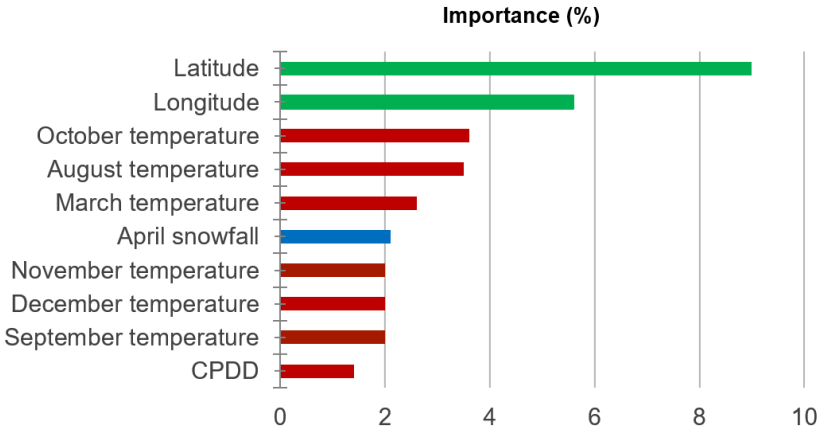

Figure 2.12: Importance (%) of the first 10 predictors using Lasso to predict residual error from the ANN SMB model. Green bars indicate topographical features, red bars temperature-related features and blue bars precipitation-related features.

Such an approach to analyze the influence of the different predictors into the quantification of uncertainties is of course limited, since a linear model is trained with nonlinear results. But these results are useful to determine the main contributors to errors rather than quantifying these errors, which has been done with the LOGO, LOYO and LSYGO cross-validations.

2.7.3 Topographical glacier-wide SMB predictors

Since topography plays a role in the glacier-wide SMB signal, besides the climate, the representation of the glacier's topography is important in order to correctly simulate its glacier-wide SMB and its geometrical evolution. As explained in Sect. 2.3 "Model overview and workflow" and Sect. 2.4.1 "Topographical glacier data and altimetry", the source of the topographical predictors used for the simulation of glacier-wide SMB is different at different steps of the glacier evolution simulation chain. Two cases exist:

1. For the machine learning training of the glacier-wide SMB models, which is performed on historical data, all topographical data comes from the multitemporal glacier inventories (Gardent et al., 2014, with 2015 update). In order to have an annual timestep, topographical data from these inventories are linearly interpolated.
2. For the full glacier evolution simulation, coupling the glacier-wide SMB component with the glacier geometry evolution component, the model must be capable of generating all the input topographical predictors even for non-observed glaciers and future periods. For every glacier and year, all the topographical predictors are computed from the updated glacier-specific ice thickness and DEM raster files from Farinotti et al. (2019), which then are used to simulate a single glacier-wide SMB for that glacier and year. Then, this glacier-wide SMB together with the glacier-specific geometry update function are used to update the glacier's geometry and their respective ice thickness and DEM rasters. For the next year, all the topographical predictors are recomputed with the updated raster files, and this process is repeated in a loop with an annual timestep. Therefore, the glacier-wide SMB model is called with an annual timestep, simulating only single values in order to take into account the evolution of the glacier's topography.

In order to show that the glacier geometry update component, coupled with the glacier-wide SMB simulation component can successfully simulate the evolution of the topographical characteristics of glaciers in the region, a specific test was designed. Using the same validation period as in Sect. 2.4.2 (2003-2015), we ran parallel simulations of glacier-wide SMB for all the 32 case study glaciers. The first simulation was done using case (1), with the multitemporal glacier inventories data, and the second one was done following case (2), with the full glacier evolution model and the Farinotti et al. (2019) raster files. The results of both simulations were really similar, revealing only small differences. On average, the simulated glacier-wide SMBs for this period differed on 0.069 m.w.e. a^{-1}, due to the differences in the input topographical predictors, which are computed from different datasets (Fig. 2.17). Moreover, the performances of both simulations for this period are very similar, with a RMSE of 0.49 m.w.e. a^{-1} for case (1) and 0.52 m.w.e. a^{-1} for case (2). The results with all the differences between the simulated glacier-wide SMB values and input topographical values are summarized in Table 2.1:

Variable (multitemporal inventories vs. full glacier evolution)	SMB simulated	Slope	Average glacier elevation	Area
MAE or mean difference	0.069 m.w.e a^{-1}	1.8°	31.3 m	0.2 km^2

Table 2.1: Differences on simulated glacier-wide SMB and topographical predictors between a simulation using interpolated topographical predictors from the multitemporal glacier inventories and the full glacier evolution simulations including the coupling of the glacier-wide SMB with the glacier geometry update.

The only striking difference is perhaps the difference in simulated areas. This is mainly due to the fact that the Farinotti et al. (2019) dataset uses the RGI v6, which for the largest glaciers of Argentière and Mer de Glace, overestimates its surface area (from 32 to 34 km2 for Mer de Glace in 2003). The differences in slope are explained by the fact that this variable is not included in the multitemporal glacier inventories (Gardent et al., 2014), therefore it has been computed once with a global DEM and kept constant for each glacier throughout the years for the training of the SMB model. On the other hand, in order to include the long term effects of glacier morphology changes in the glacier evolution simulations (glacier-wide SMB simulation + glacier geometry update), the glacier slope is re-computed with an annual timestep and it evolves through time. Therefore, there are small differences for certain glaciers whose slope has evolved during this period, thus accounting for the differences with the fixed value used for the training of the SMB model. This test serves to prove that the full glacier evolution simulations in ALPGM are capable of reproducing the topographical predictors used for the training of the glacier-wide SMB machine learning models. Moreover, this test also helps to prove that ALPGM can correctly simulate the topographical evolution of glaciers, which allows to capture the topography induced feedback, which plays a role in the simulation of glacier-wide SMBs.

2.7.4 Supplementary figures

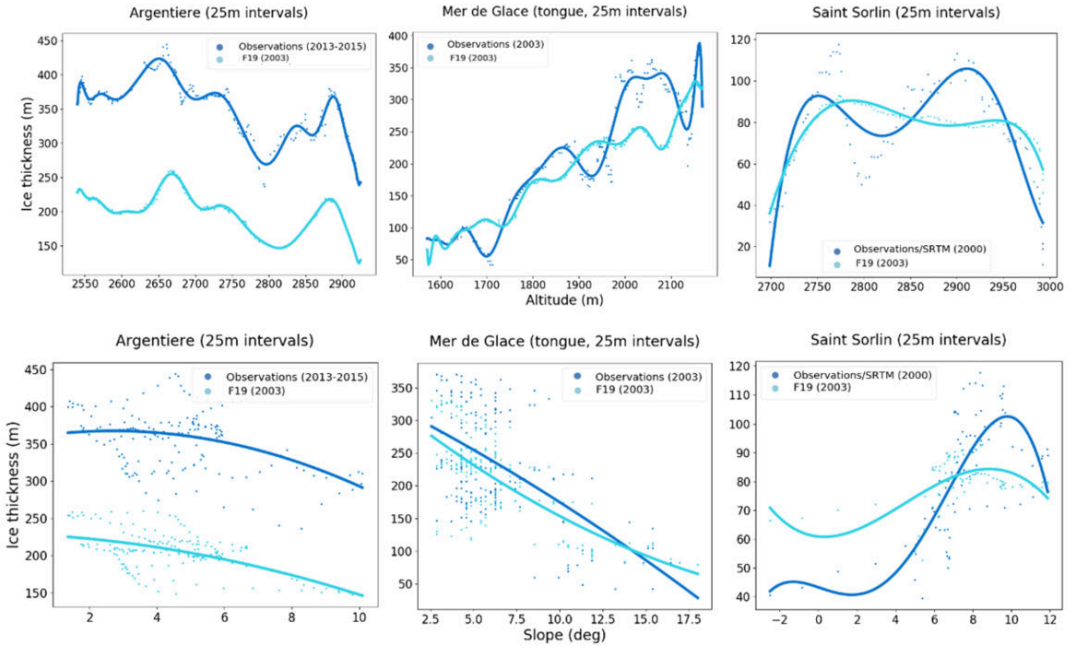

Figure 2.13: Comparison of simulated glacier ice thicknesses from F19 with observations from the GLACIOCLIM observatory. Points are compared at 25 m intervals on the glacier flowline. The polynomial fits have less degrees of freedom for the slope plots. Note that for some glaciers the dates are not the same

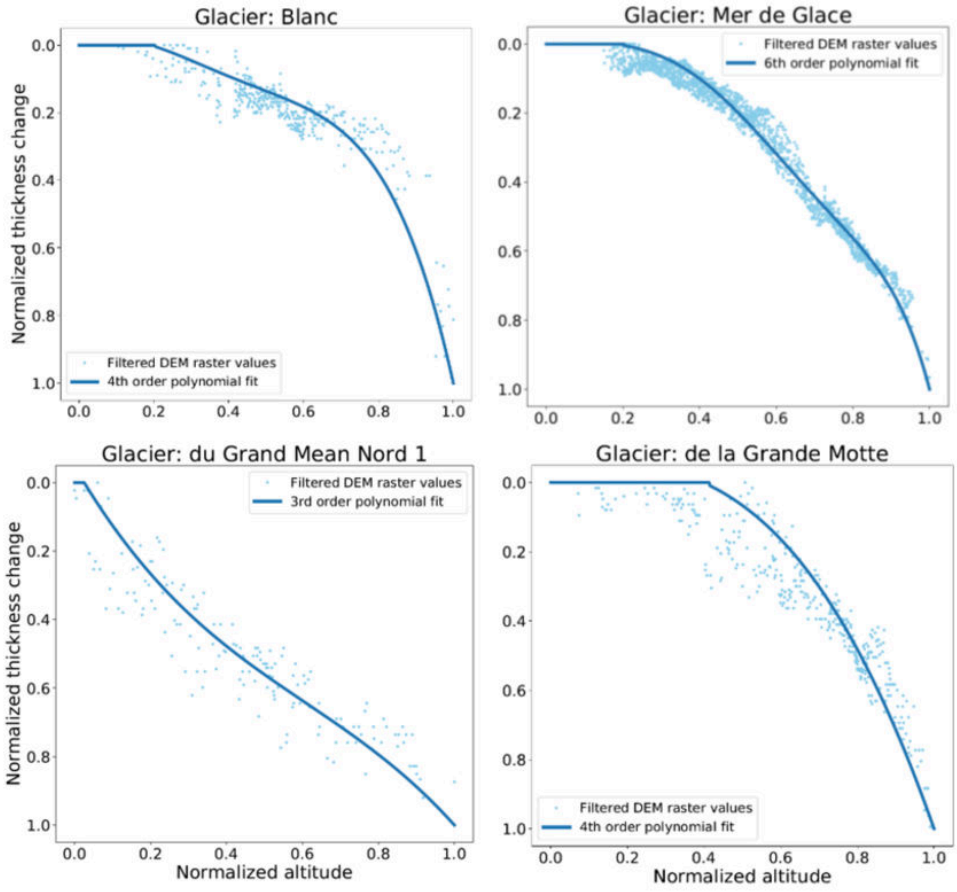

Figure 2.14: Examples of glacier specific Δh parameterized functions generated by ALPGM. The order of the polynomial fit depends on the number of available pixels.

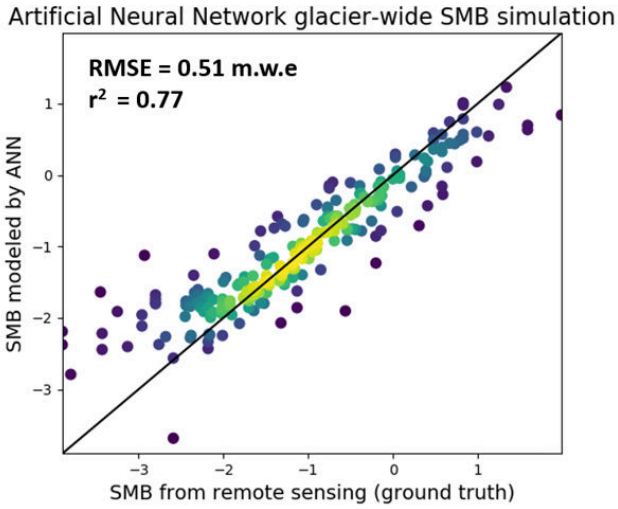

Figure 2.15: Results for the spatiotemporal cross-validation using Leave-Some-Glaciers-and-Years-Out (LSYGO). SMB values are in m.w.e. Compared to the other scatter plots from 3.2, there are less values available for test due to the severity of the spatiotemporal independence.

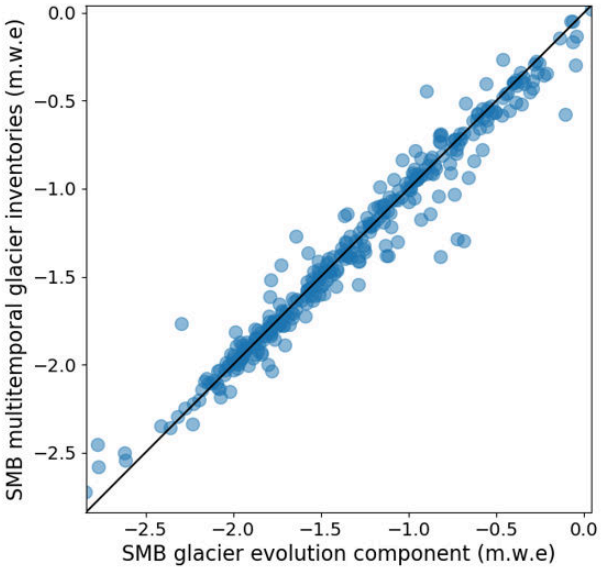

Figure 2.16: Comparison of glacier-wide SMB simulations (2003-2015, 32 case study glaciers) using topographical predictors from the multitemporal glacier inventories (Y axis) vs. using the full glacier evolution simulations in ALPGM with the Farinotti et al. (2019) ice thickness and DEM rasters (X axis). Average difference = 0.069 m.w.e. a^{-1}

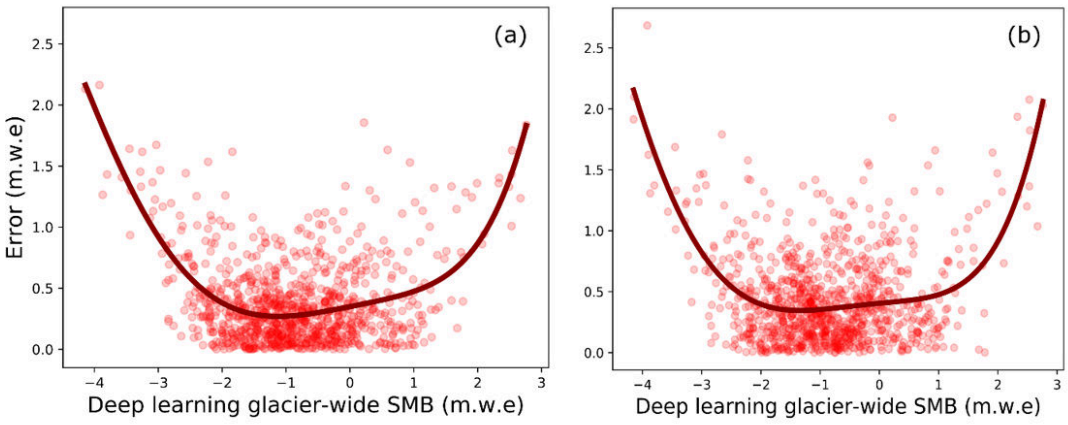

Figure 2.17: Error distribution of deep learning (without weights) glacier-wide SMB simulations for the 1984-2015 period for the 32 case study glaciers. (a) Performance in the spatial dimension using LOGO cross-validation; (b) performance in the temporal dimension using LOYO cross-validation. The red line corresponds to a 5th order polynomial fit.

Chapter 3

A deep learning reconstruction of mass balance series for all glaciers in the French Alps: 1967-2015

In using the present in order to reveal the past, we assume that the forces in the world are essentially the same through all time; for these forces are based on the very nature of matter.

James Dwight Dana

Preface

After the development of the deep learning modelling approach, it was clear that the initial objectives of this PhD project regarding the glacio-hydrological modelling of the Rhône catchment would be transformed. In order to properly apply this new method to a regional-scale scientific problem, we decided to use all climate, topographical and glaciological data available during the last 50 years in the French Alps, in order to reconstruct annual mass balance series for all French alpine glaciers. This new study, served as a proof of concept of the methodology, but also enabled the presentation of a new open reference dataset of mass balance changes in the French Alps. Despite the high quality and availability of data for this region and period, as it always happens in science, inference is based on hypotheses. Empirical and statistical approaches can suffer when applied to largely different conditions, proving wrong the words of James Dwight Dana. Following the philosophy of the previous chapter, we tried again to be as sure as possible that we were obtaining the good results for the right reasons. This dataset carries indeed important uncertainties, particularly for very small glaciers, but it represents, to our knowledge, the best approximation on how the mass balance of French alpine glaciers evolved through the last half century. I am very grateful for the reviews by Matthias Huss and Ben Marzeion during the open peer review of this paper. I cannot think of more qualified people to judge my work, and I was greatly pleased with their constructive and thoughtful comments, that helped to improve this study in many ways. A common thread throughout this PhD work has been to render this work as transparent and open as possible. By sharing the source-code used for simulations, and publishing the results in open-access journals and repositories, I aim at doing my part to make science a more accessible and transparent collective enterprise.

Based on Bolibar, J., Rabatel, A., Gouttevin, I. and Galiez, C.: A deep learning reconstruction of mass balance series for all glaciers in the French Alps: 1967–2015, Earth Syst. Sci. Data, 12(3), 1973–1983, doi:10.5194/essd-12-1973-2020, 2020

3.1 Abstract

Glacier mass balance (MB) data are crucial to understand and quantify the regional effects of climate on glaciers and the high-mountain water cycle, yet observations cover only a small fraction of glaciers in the world. We present a dataset of annual glacier-wide mass balance of all the glaciers in the French Alps for the 1967-2015 period. This dataset has been reconstructed using deep learning (i.e. a deep artificial neural network), based on direct MB observations and remote sensing annual estimates, meteorological reanalyses and topographical data from glacier inventories. The method's validity was assessed previously through an extensive cross-validation against a dataset of 32 glaciers, with an estimated average error (RMSE) of 0.55 m.w.e. a^{-1}, an explained variance (r^2) of 75% and an average bias of -0.021 m.w.e. a^{-1}. We estimate an average regional area-weighted glacier-wide MB of -0.69±0.21 (1σ) m.w.e. a^{-1} for the 1967-2015 period, with negative mass balances in the 1970s (-0.44 m.w.e. a^{-1}), moderately negative in the 1980s (-0.16 m.w.e. a^{-1}), and an increasing negative trend from the 1990s onwards, up to -1.26 m.w.e. a^{-1} in the 2010s. Following a topographical and regional analysis, we estimate that the massifs with the highest mass losses for the 1967-2015 period are the Chablais (-0.93 m.w.e. a^{-1}), Champsaur (-0.86 m.w.e. a^{-1}) and Haute-Maurienne and Ubaye ranges (-0.84 m.w.e. a^{-1} both), and the ones presenting the lowest mass losses are the Mont-Blanc (-0.68 m.w.e. a^{-1}), Oisans and Haute-Tarentaise ranges (-0.75 m.w.e. a^{-1} both). This dataset - available at: https://doi.org/10.5281/zenodo.3925378 (Bolibar et al., 2020a) - provides relevant and timely data for studies in the fields of glaciology, hydrology and ecology in the French Alps, in need of regional or glacier-specific annual net glacier mass changes in glacierized catchments.

3.2 Introduction

Among all the components of the Earth system, glaciers are some of the most visibly affected by climate change, with an overall worldwide shrinkage despite important differences between regions (Zemp et al., 2019). The European Alps are among the regions with the strongest glacier mass loss over recent decades, with expected mass losses between 60% and 95% by the end of the 21st century (Zekollari et al., 2019). These major glacier mass changes are likely to have an impact on water resources, society and alpine ecosystems (e.g. Huss and Hock, 2018; Immerzeel et al., 2020; Cauvy-Fraunié and Dangles, 2019). In order to study and quantify all these potential consequences, the availability of glacier mass balance data is of high relevance. Therefore, open historical datasets are crucial for the understanding of the driving processes and the calibration of models used for projections. Unlike glacier length, glacier mass balance (MB) provides a more direct indicator of the climate-glacier interactions (Marzeion et al., 2012). Glacier surface mass balance (SMB) is classically measured using the direct or glaciological method, by separately determining the ablation and accumulation totals. Direct measurements quantify the surface mass balance at different points of the glacier, and these values must be integrated at the glacier scale in order to assess the glacier-wide SMB (Benn and Evans, 2014). These different point SMB measurements can show a high nonlinear variability, which can complicate this integration process towards glacier-wide estimates (Vincent et al., 2018). Moreover, field measurements require a lot of manpower, time and economic resources in order to be sustained for

a meaningful period of time. On the other hand, recent advances in remote sensing allow estimating glacier MB changes at a regional level with unprecedented efficiency using geodetic and gravimetric methods (Kääb et al., 2012; Fischer et al., 2015; Berthier et al., 2016; Brun et al., 2017; Dussaillant et al., 2019). Due to constraints related to the availability of digital elevation models (DEMs) or airborne data, these mass balance estimates normally encompass several years or decades. Some studies are bridging the gap towards an annual temporal resolution (Rabatel et al., 2005, 2016; Rastner et al., 2019), but the coverage is still limited to glaciers without cloud cover or acquisition-related artefacts. This means that these mass balance datasets are often restricted to certain glaciers and years within a region. All these new datasets are extremely beneficial for data-driven approaches, fostering the training of machine learning models capable of capturing the regional characteristics and relationships (Bolibar et al., 2020c). This type of approach allows to fill the spatiotemporal gaps in the MB datasets, therefore, it can be seen as a complement to remote sensing and direct observations.

On the other hand, MB reconstructions have already been carried out in the European Alps, providing a basis for comparison between different approaches (see Hock et al. (2019a) for a compilation). Two studies include reconstructions in the European Alps, including the French Alps, over a substantial period of the recent past: Marzeion et al. (2012, 2015) reconstructed annual MB series of all glaciers in the Randolph Glacier Inventory for the last century. They used a minimal model relying only on temperature and precipitation data, based on a temperature-index method, with two parameters to calibrate the temperature sensitivity and the precipitation lapse rate. Huss (2012) presented an approach to extrapolate SMB series of a limited number of glaciers to the mountain-range scale. By comparing multiple methods, he found the best results with a multiple linear regression based on 6 topographical parameters. From this relationship he reconstructed area-averaged SMB series of all the glaciers of the European Alps between 1900-2100 and analysed the trends for the different alpine nations and different glacier sizes.

Here, we introduce a dataset of annual glacier-wide MB of all the glaciers in the French Alps (Bolibar et al., 2020a), located in the westernmost part of the European Alps, between 5.08° and 7.67°E, and 44° and 46°13'N. Glacier-wide MBs have been reconstructed for the 1967-2015 period, using deep learning (i.e. a deep artificial neural network) (Fig. 3.1). This approach was introduced in Bolibar et al. (2020c), for which a deep artificial neural network (ANN) was trained with data from 32 French alpine glaciers, as part of the ALpine Parametrized Glacier Model (ALPGM) (Bolibar, 2020). Annual glacier-wide MB values are reported for each glacier in the French Alps found in the 2003 glacier inventory (Gardent et al., 2014). An overview of the methodology used to produce the dataset and a review of the associated uncertainties is presented in Sect. 3.3, followed by a dataset overview in Sect. 3.4, where the data structure and regional trends are described and where the dataset is compared to a previous study and observations.

3.3 Data and methods

3.3.1 Training data

For the reconstruction presented here, a dataset of 32 French alpine glaciers has been used for training, covering most of the massifs within the French Alps, which exhibit a great variability of topographical characteristics. The French Alps are located in the westernmost part of the European Alps, rising from the Mediterranean sea northwards between 44 and 46°13' N, 5.08 and 7.67° E. Due to its particular geographical setup, glacierized mountain ranges in the French Alps have distinct climatic signatures.

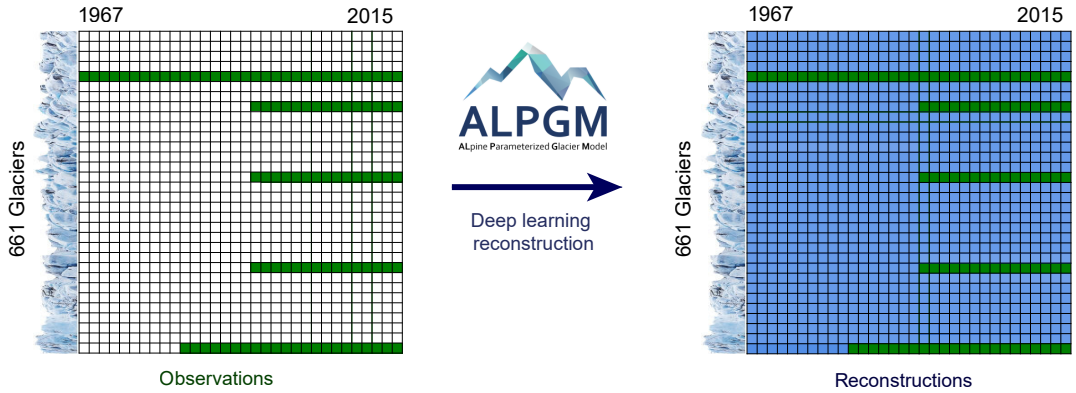

Figure 3.1: Summary of the deep learning regional MB reconstruction approach. From the available annual glacier-wide MB data, a deep learning model is used to reconstruct the full dataset, thus filling the spatiotemporal gaps in the observational dataset. Green indicates glaciers and years with MB observations and remote sensing estimates, and blue indicates reconstructed MB values. Glacier ice cliffs in the vertical axis indicate rows representing individual glaciers. The grid size with glaciers and years is schematic and only serves to illustrate the concept.

Southern glaciers exhibit a Mediterranean influence, whereas northern glaciers are mostly affected by western fluxes from the Atlantic, except for eastern glaciers close to the Italian border, which are more influenced by east returns.

Out of the 32 glaciers from this dataset, four glaciers include direct MB measurements from the GLACIOCLIM observatory, some of which since 1949. These direct observations have been calibrated using photogrammetric geodetic MB (Vincent et al., 2017). On the other hand, 28 glaciers include estimates of annual glacier-wide MB from remote sensing between 1984 and 2014 (Rabatel et al., 2016). These remote sensing estimates were computed using (1) the end-of-summer snowline for every year, which in the European Alps is a proxy of the equilibrium-line altitude (ELA); and (2) geodetic MB for the 1984-2014 period quantified from two high-resolution DEMs. Both data sources are used to reconstruct the annual glacier-wide MB of each individual glacier for the same period of the geodetic MB.

This dataset of 32 glaciers, with a total of 1048 annual glacier-wide MB values, is used as a reference. Unlike point MB, glacier-wide MB is influenced by both climate and glacier geometry, producing complex interactions between climate and glacier morphology that need to be taken into account in the model. For each annual glacier-wide MB value available, the following data are compiled to train the ANN with an annual time step: (1) climate data from the SAFRAN meteorological reanalyses (Durand et al., 2009), with: cumulative positive degree days (CPDD), cumulative winter snowfall, cumulative summer snowfall, mean monthly temperature and mean monthly snowfall, all variables being quantified at the altitude of the glacier's centroid. In order to capture the climate signal at each glacier's centroid, temperatures are taken from the nearest SAFRAN 300 m altitudinal band and adjusted with a 6 °C/km lapse rate. The updated temperature is then used to update the rain-snow parts from the same 300 m altitudinal band. Snowfall is considered as all precipitation fallen at temperatures equal or lower than 0° C. (2) annually interpolated topographical data between the 1967, 1985, 2003 and 2015 glacier inventories in the French Alps (update of Gardent et al., 2014), with: mean and maximum glacier altitude, slope of the lowermost 20% altitudinal range of the glacier, surface area, latitude, longitude and aspect. Therefore, the topographical feedback of the shrinking glaciers is captured from these annually interpolated topographical predictors. These topoclimatic parameters were identified

as relevant for glacier-wide MB modelling in the French Alps (Bolibar et al., 2020c), and the dates of the glacier inventories determined the time interval for the reconstructions presented here.

For more details on the choice of predictors, the reader can find a more detailed analysis in Bolibar et al. (2020c).

3.3.2 Methods

The annual glacier-wide MB dataset for the 661 French alpine glaciers has been reconstructed using a deep artificial neural network (ANN), also known as deep learning. ANNs are nonlinear statistical models inspired by biological neural networks (Fausett, 1994; Hastie et al., 2009). Recent developments in the field of machine learning and optimization enabled the use of deeper ANN architectures, which allows capturing more nonlinear and complex patterns in data even for small datasets (Ingrassia and Morlini, 2005). This modelling approach is part of the MB component of ALPGM (Bolibar, 2020), an open-source data-driven parameterized glacier evolution model. For a detailed explanation of the methodology, please refer to Bolibar et al. (2020c). For the final reconstructions presented here, a cross-validation ensemble approach was used based on 60 Leave-Some-Years-and-Glaciers-Out (LSYGO) cross-validation models. Individual predictions of each of the members were averaged to produce a single output. An ensemble approach has the advantage of further improving generalization, and reducing overfitting as well as the inter-model high variance typical from neural networks (Krogh and Vedelsby, 1995). A weighted bagging approach (Hastie et al., 2009) was used in order to balance the dataset, giving more weight to under-represented data samples from the years 1967-1983. On the other hand, for the 32 glaciers with glacier-wide MB observations and remote sensing estimates used for training, an ensemble of 50 models trained with the full dataset was used, in order to achieve the best possible performance for this subset of glaciers, which represents a substantial fraction (45% in 2003) of the total glacierized surface area in the French Alps.

3.3.3 Uncertainty assessment

The uncertainties linked to the deep learning approach used in this study have been assessed through cross-validation, for which deep learning predictions were compared with observations and remote sensing estimates. A detailed presentation of the method's uncertainties and performance from the cross-validation study can be found in Bolibar et al. (2020c). Block cross-validation ensured that all the 32 glaciers in the dataset were evaluated, with spatiotemporal structures formed by glaciers and years being considered in order to prevent the violation of the assumption of independence (Roberts et al., 2017). This means that three different deep ANNs were produced: one for reconstructing glacier-wide MB in space, one for the reconstruction in time (future and past), and another one for both dimensions at the same time; each of these with a different calibration and performance. It was shown that the deep ANN performs better in the spatial dimension, in which the MB signal relationships with the predictors are the simplest. MB annual variability is mostly driven by climate, whereas geography and local topography (i.e. differences between glaciers) modulate the signal in space in a simpler way (Vincent et al., 2017; Bolibar et al., 2020c). Therefore, deep learning is capable of finding more structures in the spatial dimension, accounting for a better accuracy and explained variance compared to the temporal dimension. The deep ANN used in this study presents an RMSE of 0.55 m.w.e a^{-1} with an r^2 of 0.75 in LSYGO cross validation. The ANN MB reconstructions accurately reproduce the annual variability of glaciological observations from the GLACIOCLIM observatory (Figure S1). This reinforces the trust in the produced model ensemble, indicating that models trained with heterogeneous data

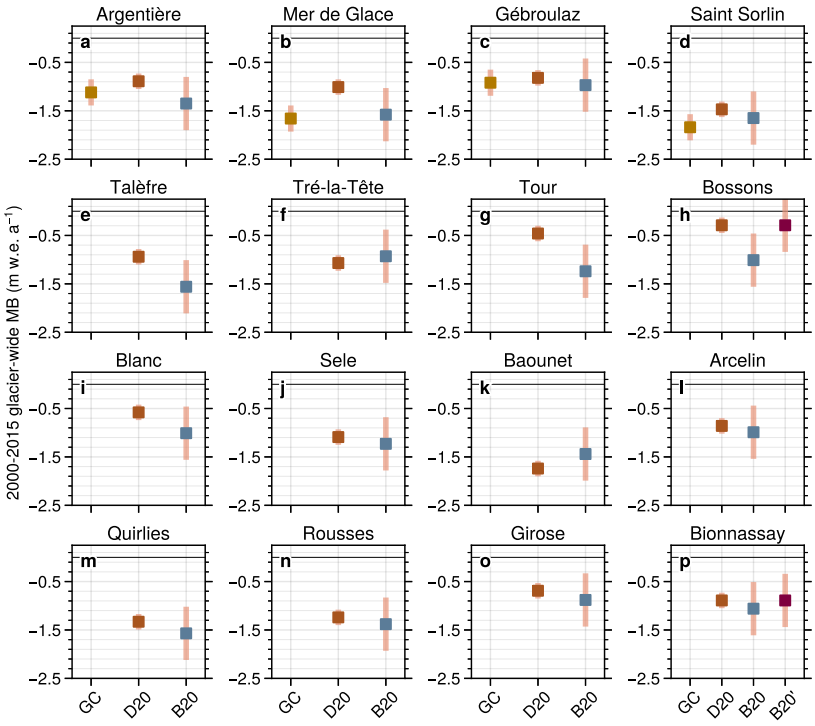

Figure 3.2: Comparison of average annual glacier-wide MB for the 2000-2015 period between the glaciological MB from the GLACIOCLIM observatory (GC), the ASTER-derived geodetic MB from Davaze et al., 2020 (D20), the MB reconstructions from this study (B20) and the reconstructions from this study recalibrated using the ASTER-derived geodetic MB (B20').

comprised by glaciological and remote sensing estimates can correctly reproduce direct annual observations.

Nonetheless, only one glacier in the training dataset is smaller than 0.5 km^2 (Glacier de Sarennes, 0.3 km^2 in 2003), implying that uncertainties for very small glaciers (< 0.5 km^2) might differ from those estimated using cross-validation. In 2015, very small glaciers in the French Alps represented about 80% of the total glacier number, but they accounted for only 20% of the total glacierized area. This means that their importance is relative, for example in terms of water resources, but a user of this dataset should bear in mind that MB from these very small glaciers might carry greater uncertainties than the ones assessed during cross-validation. This might be especially true for extremely small glaciers (< 0.05 km^2) which can be considered as spatial outliers for the deep ANN. Since there is only one glacier with MB observations for very small glaciers and none for extremely small glaciers, there is no precise way to quantify these uncertainties. On the other hand, the ANN is mostly trained with glacier-wide MB data between 1984 and 2014, with a reduced amount of values between 1967 and 1984 (986 and 62 values, respectively). Since this early period contains on average more positive and neutral glacier-wide MB values than the 1984-2014 period, the performance of the ANN was specifically assessed for this period. An additional cross-validation was performed with four folds, each with a glacier including glacier-wide MB data before 1984. For each fold, all MB data of that glacier and time period were hidden from the ANN, and the simulated glacier-wide MBs between 1967 and 1983 were tested in order to assess the model's performance. The results showed that the ANN is capable of correctly reconstructing glacier-wide MB for glaciers and years before 1984 (Fig. 3.11), with an estimated accuracy (RMSE) of 0.47 m.w.e. a^{-1} and an estimated explained variance (r^2) of 0.65. This uncertainty assessment is

based on roughly 10% of the full dataset, meaning that these estimates lack the robustness of the full cross-validation from Bolibar et al. (2020c), but they serve to show that the model can accurately reconstruct glacier-wide MB data outside the main cluster of years used during training.

In order to further validate the reconstructions presented here, a comparison against independent ASTER (Davaze et al., 2020) and Pléiades (Berthier et al., 2014) geodetic MB data was performed, that helps to assess the bias of the MB reconstructions for the 2000-2015 (Fig. 3.2) and 2003-2012 (Fig. 3.8) sub-periods. The photogrammetric geodetic MB used to calibrate the MB datasets from Rabatel et al. (2016) and the glaciological observations from GLACIOCLIM have a much higher resolution than ASTER-derived geodetic MB, but the comparison can bring interesting information for glaciers outside the training dataset. Our reconstructions show a good agreement with the geodetic MB for certain regions (e.g. Grandes Rousses), except for some particular steep large high-altitude glaciers (e.g. Bossons and Taconnaz in the Mont-Blanc massif) that substantially differ from most glaciers in the French Alps. A more detailed analysis and additional figures comparing the MB datasets can be found in Sect. 3.6.1 of the Supplementary. In order to exploit this additional geodetic MB dataset, we have recalibrated our MB reconstructions for the 2000-2015 period using the ASTER-derived geodetic MB from Davaze et al. (2020) for some glaciers outside our training dataset (i.e. B20' in Fig. 3.2). Since ASTER-derived geodetic MB present important uncertainties for small glaciers (i.e. < 1 km^2), we have only recalibrated MB series for 16 large glaciers outside the training dataset with uncertainties lower than 0.15 m.w.e. a^{-1}. The calibration has been performed by adding the average annual bias between Davaze et al. (2020) and this study for the 2000-2015 sub-period.

3.4 Dataset overview

3.4.1 Dataset format and content

The MB dataset is presented in two different formats: (a) A single netCDF file containing the MB reconstructions, the glacier RGI and GLIMS IDs and the glacier names. This file contains all the necessary information to correctly interact with the data, including some metadata with the authorship and data units. (b) A dataset comprised of multiple CSV files, one for each of the 661 glaciers from the 2003 glacier inventory (Gardent et al., 2014), named with its GLIMS ID and RGI ID with the following format: *GLIMS-ID_RGI-ID_SMB.csv*. Both indexes are used since some glaciers that split into multiple sub-glaciers do not have an RGI ID. Split glaciers have the GLIMS ID of their "parent" glacier and an RGI ID equal to 0. Every file contains one column for the year number between 1967 and 2015 and another column for the annual glacier-wide MB time series. Glaciers with remote sensing-derived estimates (Rabatel et al., 2016) include this information as an additional column. This allows the user to choose the source of data, with remote sensing data having lower uncertainties (0.35±0.06 (σ) m.w.e. a^{-1} as estimated in Rabatel et al. (2016)). Columns are separated by semicolon (;). All topographical data for the 661 glaciers can be found in the updated version of the 2003 glacier inventory included in the Supplementary material and in the dataset repository.

3.4.2 Overall trends

We estimate an average area-weighted regional glacier-wide MB of -0.69±0.21 (σ) m.w.e. a^{-1} between 1967 and 2015 (Fig. 3.3 and 3.4). As reported in previous studies (Huss, 2012; Rabatel et al., 2016; Vincent et al., 2017), our reconstructed MB data show a slightly negative average value during the 1970s, even less negative in the 1980s, and then increasingly negative values in recent decades with an abrupt

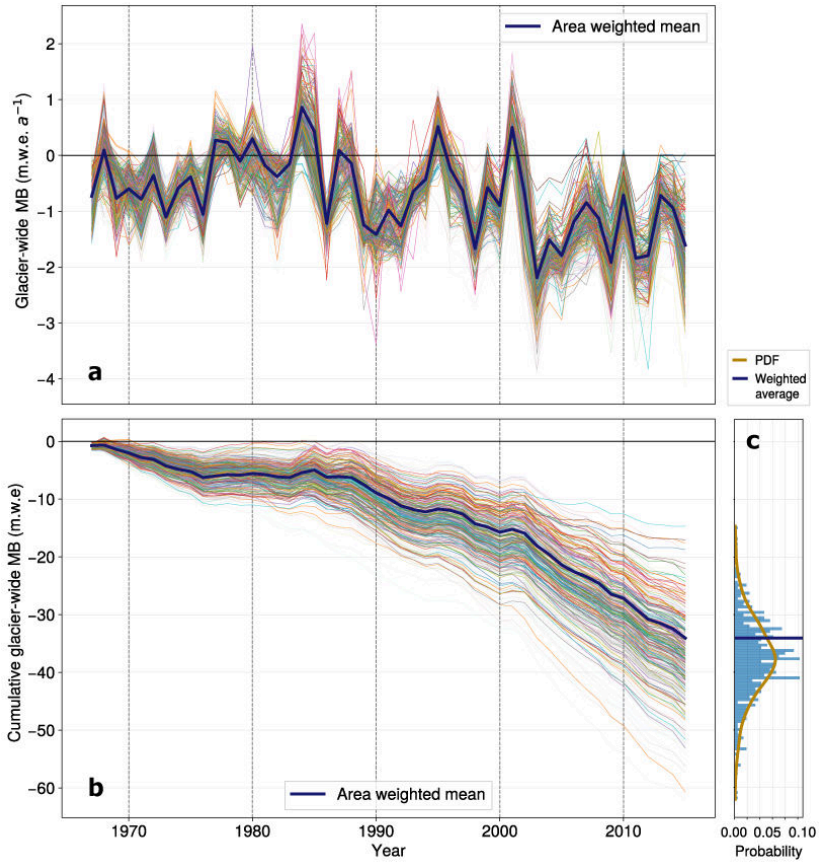

Figure 3.3: (a) Annual glacier-wide MB and (b) cumulative glacier-wide MB reconstructions of all the glaciers in the French Alps (N = 661) between 1967 and 2015. For each individual glacier, line thickness depends on glacier area, with smaller glaciers having thinner lines. The histogram (c) indicates the distribution and probability density function (PDF) of the 1967-2015 cumulative MB (m w.e.) of the dataset.

change in 2003 (Fig. 3.2). For this period (1967-2015), the year 2003 with its remarkable heatwave remains the most negative glacier-wide MB year (-2.26 m.w.e. a^{-1} on average), with 1984 being the most positive year of the study period (+0.85 m.w.e. a^{-1} on average). The area-weighted average MB is slightly less negative than the mean annual glacier-wide MB, showing a light asymmetry in the probability distribution function (PDF) (Fig. 3.3c).

3.4.3 Regional and topographical trends

Here we analyse the main trends for the glacierized massifs and for some relevant topographical parameters. The reported glacier-wide MBs are only area-weighted if specifically mentioned. Interesting differences appear once the dataset is divided into mountain ranges (Fig. 3.5). The Mont-Blanc massif presents the lowest mass loss over the entire study period, with an average cumulative loss over the 1967-2015 period of 33.5 m.w.e. This is probably due to its northern location within the French Alps and its large high altitude accumulation areas, which resulted in more positive or less negative MBs, especially during the 1980-2000s. Oisans is the massif with the second lowest average cumulative mass loss (37.20 m.w.e.). Its glaciers have average altitudes ranging from 2290 to 3470 m.a.s.l., with around 50% of them having mean altitudes over 3000 m.a.s.l. and with about 40% of glaciers (including most of the large ones) having a northern aspect. Glaciers in Haute-Tarentaise present similar characteristics to those from Oisans, with mean altitudes ranging between 2300 and 3600 m.a.s.l., with about

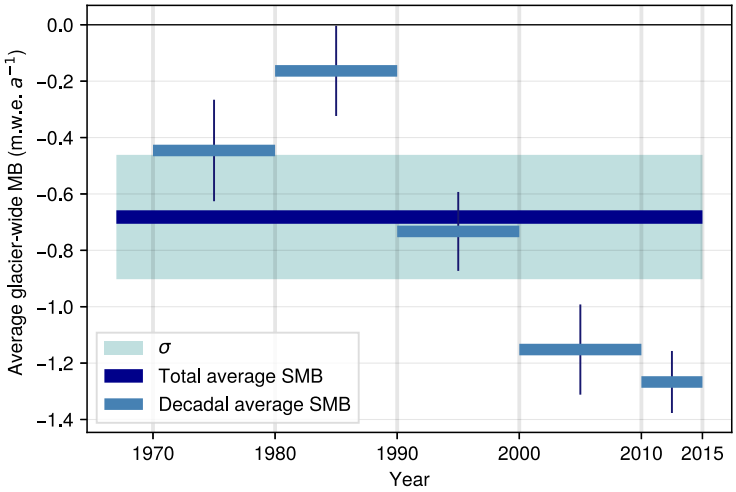

Figure 3.4: Averaged area-weighted decadal glacier-wide MB for the French Alps with decadal uncertainties. The total area-weighted glacier-wide MB is estimated for the 1967-2015 period.

60% of the glaciers above 3000 m.a.s.l. This less negative trend was especially important during the recent years with high mass losses from 2003 onwards. On the other hand, the Ubaye, Champsaur, Chablais and Haute-Maurienne massifs appear as the most affected mountain ranges with cumulative mass losses reaching between 41 and 46 m.w.e. for the four massifs over the 1967-2015 period. The Chablais range has a very small number of glaciers remaining, all of them at rather low altitudes (2200-2900 m.a.s.l.), relatively small (0.01 - 1.1 km^2), and with a northwestern aspect. Despite being the northernmost mountain range in the French Alps, its low altitude is most likely the main reason for the very negative MBs, which were under the regional average even during the positive years in the 1980s. The Champsaur range shows a similar situation, with very small glaciers (0.03 - 0.89 km^2) lying at relatively low altitudes (2300-3100 m.a.s.l.) in the southernmost latitudes of the Alps (44°7′). Finally, the situation of the Ubaye massif is quite similar to the one of Champsaur, being the southernmost glacierized massif in the French Alps, with a strong mediterranean influence. Such glaciers are remnants of the Little Ice Age, far from being in equilibrium with the warming climate, and can quickly lose a lot of mass through non-dynamic downwasting (Paul et al., 2004).

When classifying the MB time series by glacier surface area, we encounter the following patterns, with n being the number of glaciers in the subset and s its standard deviation: (1) Very small glaciers (< 0.5 km^2; n = 534; $\overline{MB}_{1967-2015}$ = -0.79 m.w.e. a^{-1}; s = 0.23 m.w.e. a^{-1}) present more negative glacier-wide MBs than (2) small/medium glaciers (ranging from 0.5 to 2 km^2; n = 93; $\overline{MB}_{1967-2015}$ = -0.74 m.w.e. a^{-1}; s = 0.18 m.w.e. a^{-1}) and (3) large glaciers (> 2 km^2; n = 34; $\overline{MB}_{1967-2015}$ = -0.68 m.w.e. a^{-1}; s = 0.14 m.w.e. a^{-1}) (Fig. 3.14). Very small glaciers present a larger spread of values than small/medium and large glaciers (s = 0.23 m.w.e. a^{-1} versus 0.18 and 0.14 m.w.e. a^{-1}, respectively). As explained in Sect. 3.3, the uncertainties for very small glaciers are greater due to their under-representation in the training dataset, meaning that analyses based on small glaciers have to be taken with greater care. The effects of these trends can be seen in the PDF of the cumulative MB reconstructions (Fig. 3.3c), where the area-weighted mean lies slightly outside the PDF maximum, showing how a great number of small glaciers are presenting higher losses. On the other hand, a clearer relationship between the glacier slope (computed here as the lowermost 20% altitudinal range slope) and glacier-wide MB arises, with steeper glaciers having less negative glacier-wide MBs (Fig. 3.12 and 3.15). Glaciers with

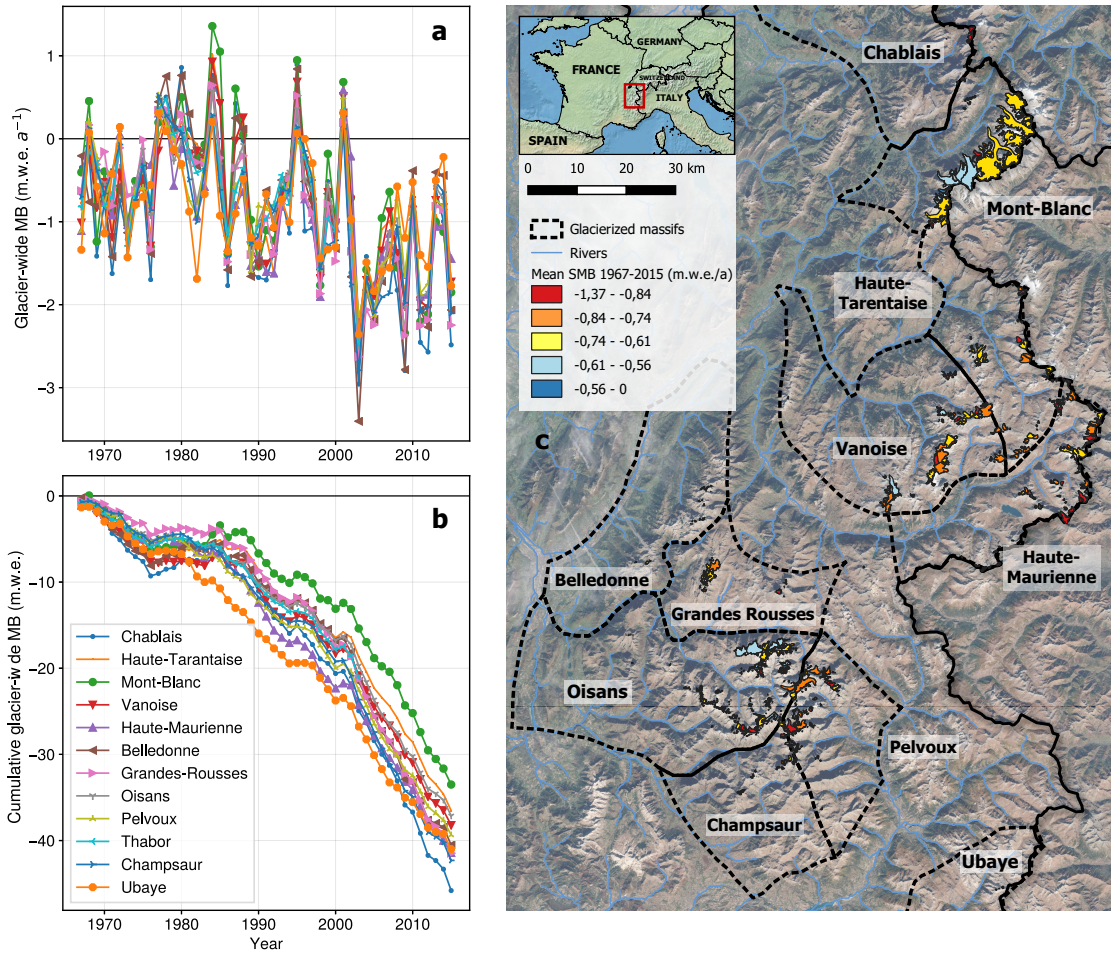

Figure 3.5: (a) Averaged annual glacier-wide MB and (b) cumulative averaged glacier-wide MB time series for each of the massifs in the French Alps between 1967 and 2015. (c) Glacierized massifs in the French Alps with the average glacier-wide MB for the 1967-2015 period. Coordinates of bottom left map corner: 44°32′ N, 5°40′ E. Coordinates of the top right map corner: 46°08′ N, 7°17′ E.

a gentle tongue slope generally present longer response times and higher ice thickness, which are associated with more negative mass balances (Hoelzle et al., 2003; Huss and Fischer, 2016; Zekollari et al., 2020). These results are in agreement with the findings by Fischer et al. (2015), who computed the geodetic mass balance of all the Swiss glaciers for the 1980-2010 period. Overall, the topographical relationships found here are similar, although more negative than for the Swiss Alps (Huss, 2012; Huss et al., 2015), showing how the southernmost glaciers in the Écrins and Vanoise regions present stronger glacier mass losses. This is mostly due to their mediterranean climatic influence compared to the more continental Swiss and Austrian glaciers, which results in more negative MB in a warming climate (Oerlemans and Reichert, 2000). Nonetheless, results from this type of bivariate analysis can show rather biased trends, since the topographical variables are highly intercorrelated, with for example small glaciers having steeper slopes and *vice versa* (Gardent et al., 2014). The position and evolution of the equilibrium line can totally reverse the trends of small or steep glaciers, so these relationships can strongly vary depending on the region or time period observed.

3.4.4 Comparison with previous studies and observations

In order to put into perspective the reconstructions presented in this study, we compare them to an updated version from the Marzeion et al. (2015) reconstructions (B. Marzeion, personal communication, October 2019 - January 2020), and to all the available glacier-wide MB observations and remote sensing estimates in the French Alps. The goal of this comparison is not to draw conclusions on the quality of either reconstruction, but to analyse the differences among them and to try to understand the causes. In the updated version of Marzeion et al. (2015) - referred as M_{15U} from now on - a global MB model relying on temperature and solid precipitation was used to reconstruct MB time series for all the glaciers in the world present in the Randolph Glacier Inventory (Consortium, 2017). This model was optimized based on five parameters: the temperature sensitivity of the glacier (local); and a precipitation correction factor, precipitation lapse rate, temperature threshold for solid precipitation and melt temperature threshold (global). As in Bolibar et al. (2020c), the approach by M_{15U} was cross-validated respecting the spatiotemporal independence in order to evaluate its performance for unobserved glaciers and years. Due to the highly different methodologies and forcings of the two models, a direct comparison is not possible, so the following analysis is focused on the overall trends and sensitivities in the reconstructions and their potential sources. All the specific differences and details between the two models can be found in Sect. 3.6.2 from the Supplement.

The annual variability (Fig. 3.6), driven by climate, is quite similar between the two reconstructions. Conversely, important differences are found for different subperiods in the amplitude of the area-weighted mean glacier-wide MB series. These differences are the greatest in the 1970s, 1980s and 2010s, with similar average values for the 1990s and 2000s (Fig. 3.6 and 3.13). M_{15U} presents less negative and more positive glacier-wide MB values in the 1970s, but on the contrary, it presents more negative values in the 1980s compared to our results. We believe there might be two potential reasons for this: (1) In 1976 there was a shift in the winter mass balance regime in the French Alps, with more humid winters bringing more accumulation; and in 1982 there was a shift in the summer mass balance, resulting in increased ablation (Thibert et al., 2013). Since both models use parameterized or statistical relationships for MB response to precipitation and temperature, they are likely to react differently to these changes. A similar situation is found from the year 2003 onwards, where there was a substantial increase in temperatures and mass loss (e.g. Six and Vincent, 2014). Our reconstructions show a marked change in 2003 (change of slope in the cumulative plot in Fig. 3.6), whereas M_{15U} present a rather linear trend. The fact that M_{15U} used a volume-area scaling compared to the interpolated topographical data from inventories from this study means that the topographical feedback of the models might differ as well throughout the reconstructed period. (2) For the 1967-1983 interval, the amount of available glacier-wide MB data for training is much lower than for the rest of the period (green numbers in Fig. 3.6). This is likely the reason why the differences between our reconstructions and training data are greater for that period (Fig. 3.6). On the other hand, the similarities between our reconstructions and the training data for the 1984-2014 period are explained by the fact that the 32 glaciers with observations represent around 45% of the total glacierized area in the French Alps in the year 2003. For the periods before and after this interval, differences and uncertainties in the reconstructed values are greater because of the smaller sample size.

In the following, we argue that similarities between observations, remote sensing estimates and the reconstructed glacier-wide MB values for the 1984-2015 period in this study (Fig. 3.6) are not due to overfitting. First, for the vast majority of the 661 French glaciers, the reconstructions are based on an ensemble of cross-validated models, which intrinsically limits overfitting (Sect. 3.3). Second, we analysed the deviation to the climatological mass-balance signal of the MB for each cluster of glacier-sizes.

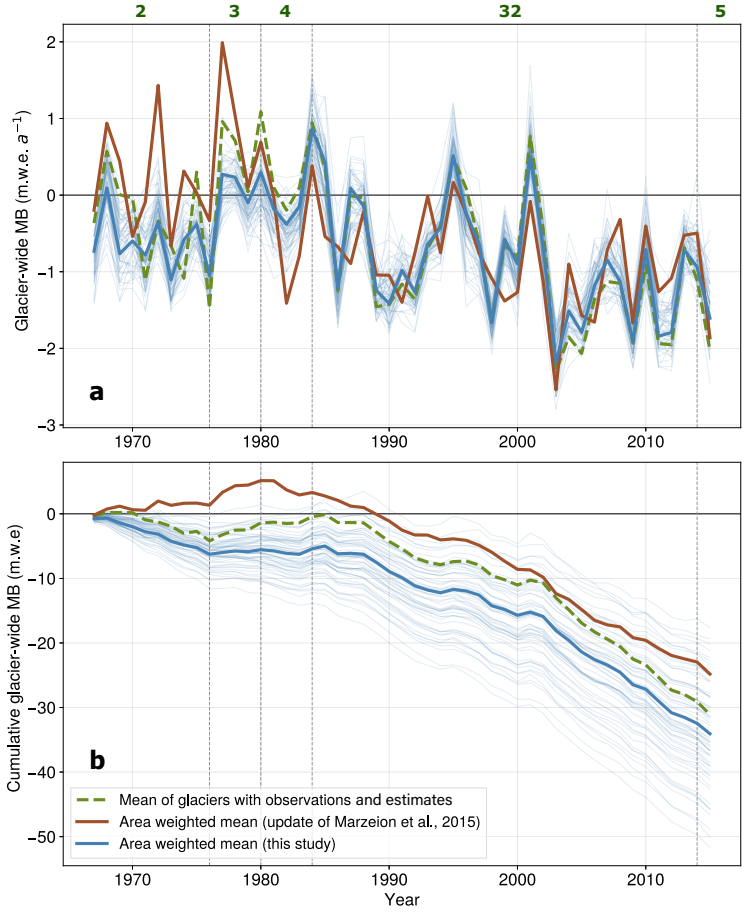

Figure 3.6: Comparison of (a) annual and (b) cumulative glacier-wide MB simulations in the French Alps between this study, reconstructions from an update from Marzeion et al. (2015) and the mean of all observations and remote sensing estimates available in the French Alps. Green numbers indicate the number of glaciers with MB observations and remote sensing estimates for each period and thin light blue lines indicate the area-weighted mean of each of the cross-validation ensemble members.

This analysis is presented in Sect. 3.6.3 of the supplementary material. It reveals that the similarities between the training data and the reconstructed glacier-wide MB values for the 1984-2015 period in Fig. 3.6 originate from big glaciers, that dominate both in the area-weighted reconstructions and in the training data (Fig. 3.9 and 3.10). However, for the other glacier-size classes, our reconstruction shows different patterns from the data in the training data, which suggests that the model is not overfitting (Fig. 3.9).

3.5 Conclusions

We presented a dataset of annual glacier-wide MB of all the glaciers in the French Alps (44° - 46°13'N, 5.08° - 7.67°E) for the 1967-2015 period (Bolibar et al., 2020a). This dataset has been reconstructed using deep learning (i.e. an artificial neural network), based on direct and remote sensing annual glacier-wide MB observations and estimates, climate reanalysis and topographical data from multi-temporal glacier inventories. The deep learning model is capable of reconstructing glacier-wide MB time series for unobserved glaciers in the same region based on patterns and structures learnt by the artificial neural network from the training data and their relationships with predictors. An extensive

cross-validation was implemented to understand the characteristics of the MB signal in the region and to assess the method's validity and uncertainty. The average accuracy (RMSE) of the dataset is estimated at 0.55 m.w.e. a^{-1} with an explained variance (r^2) of 75%. Reconstructions show a mean area-weighted glacier-wide MB of -0.69±0.21 (1 σ) m.w.e. a^{-1} for the 1967-2015 period. Important differences are found among different massifs, with the Mont-Blanc (-0.68 m.w.e. a^{-1}), Oisans (-0.75 m.w.e. a^{-1} both) presenting the lowest mass losses and the Chablais (-0.93 m.w.e. a^{-1}), Champsaur (-0.86 m.w.e. a^{-1}) and Haute-Maurienne and Ubaye (-0.84 m.w.e. a^{-1} both) showing the highest losses. In order to put these results into perspective, this reconstruction was compared to all available glacier-wide MB observations and remote sensing estimates in the French Alps as well as the physical/empirical reconstructions from another study (update from Marzeion et al., 2015). Interesting differences were found between the two methods, highlighting the different sensitivities and responses of different approaches to climate shifts that occurred during the study period. These differences are particularly relevant in the 1970s and 1980s, previous to a winter precipitation and summer temperature shift that occurred in the French Alps in the years 1976 and 1982, respectively. Moreover, after the famous 2003 European heatwave, glaciers experienced an acceleration in mass loss which is well captured by our reconstruction. This open glacier-wide MB dataset can be useful for hydrological or ecological studies in need of net glacier mass contributions of glacierized catchments in the French Alps. The publication of such open datasets is essential to future community-based data-driven scientific studies.

3.6 Supplementary material

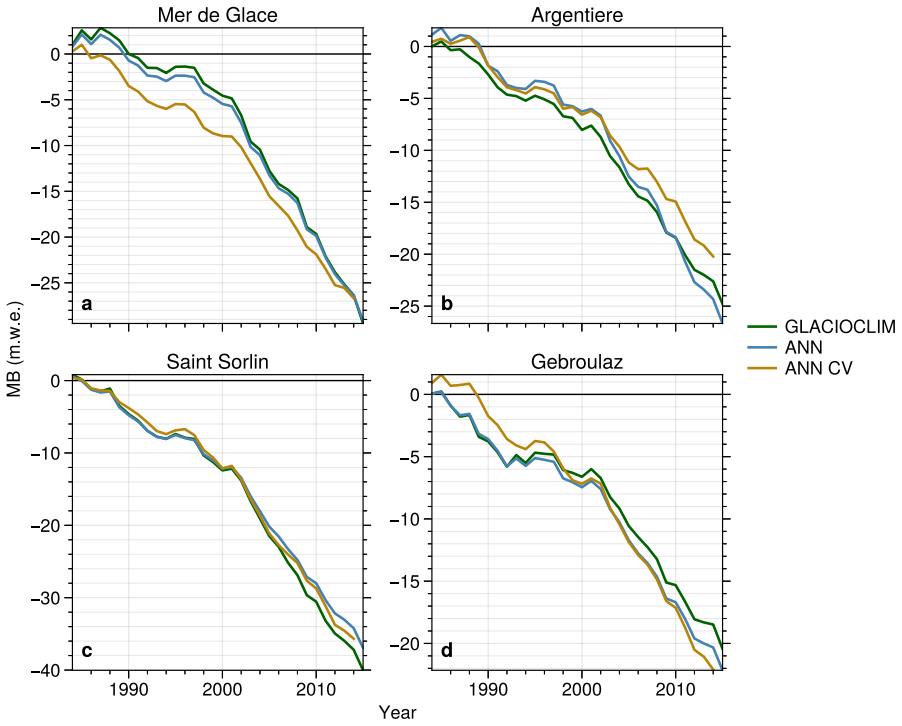

Figure 3.7: Comparison between glaciological observations from the GLACIOCLIM observatory, cross-validated MB reconstructions from this study (ANN CV) and fitted MB reconstructions (ANN). The cross-validated models are shown to display the out-of-sample performance. The fitted reconstructions display the actual reconstructions from the dataset, with models especially fitted for glaciers with data.

3.6.1 Comparison with independent geodetic mass balance data

All available annual glacier-wide MB data in the French Alps have been used to train the MB ANN of the present study. However, some multi-annual geodetic mass balance (MB) datasets exist that can provide a means to validate the reconstruction's bias for specific glaciers during multi-annual time intervals. This type of analysis is more limited than the cross-validation done to annual glacier-wide MB values in Bolibar et al. (2020c), as it only gives information about the bias of a sub-period of the reconstructions instead of the accuracy found via cross-validation. Our MB reconstructions are compared against ASTER geodetic MB from Davaze et al. (2020) for the 2000-2015 and 2003-2012 periods (Fig. 3.2 and 3.8) and against Pléiades geodetic MB from Berthier et al. (2014) for the 2003-2012 period (Fig. 3.8).

For certain glaciers, the ASTER and Pléiades geodetic MB give a less negative MB than the glaciological SMB used to train the deep learning SMB model. This fact might explain the slightly more negative trend of our reconstructions seen for the 2000-2015 and 2003-2012 periods, which experienced very negative MB after the well known summer 2003 heatwave. This is quite surprising, since both the GLACIOCLIM glaciological MB measurements and the annual glacier-wide MB data from Rabatel et al. (2016) have been calibrated with geodetic MB from photogrammetric DEMs, which have a very high spatial resolution. For some regions (i.e. Grandes Rousses), the independent geodetic MB are well within the uncertainty range of our model. However, large and steep glaciers in the Mont-Blanc massif and some other regions, such as Bossons, Talèfre and Tour display important differences. These glaciers have very large and high altitude accumulation areas, not seen in almost any glacier in our training dataset. On the other hand, several small glaciers present very important differences, with ASTER-derived MB being much less negative than our reconstructions. Data for small glaciers carry very large uncertainties, often of the same order of magnitude as the observations themselves. On top of that, flat or dome-type glaciers with large white areas with high reflectance present an important amount of noise, further increasing the associated uncertainty. This means that is quite hard to jump to conclusions from a direct comparison between these glaciers and our reconstructions. The differences and influence of geodetic MB on the calibration of MB series should be properly studied, as they are often not taken into account as an additional uncertainty source. This topic goes beyond the scope of this study, but glacier modelling studies could benefit from integrating this in the list of uncertainties.

3.6.2 Model differences between the updated version of Marzeion et al. (2015) and this study

In order to contrast the results from Sect. 3.4.4, three important different aspects between our approach and the one of M_{15U} need to be highlighted:

1. M_{15U}'s model works with simplified physics, with a temperature-index model calibrated on observations; in this study we used a fully statistical approach based on deep learning, where physics-based considerations only appear in the predictor selection.
2. M_{15U} calibrated their model with global MB observations, including 38 glaciers in the European Alps, most of them located in Switzerland for the 1901-2013 period; in this study we used observations of 32 glaciers, all located in the French Alps for the 1967-2015 period.
3. M_{15U} forced their updated model with CRU 6.0 (update of Harris et al., 2014), with 0.5° latitude/-longitude grid cells, which has a significantly lower spatial resolution and suitability to mountain areas than the SAFRAN reanalysis (Durand et al., 2009) used in this study, in which altitude bands

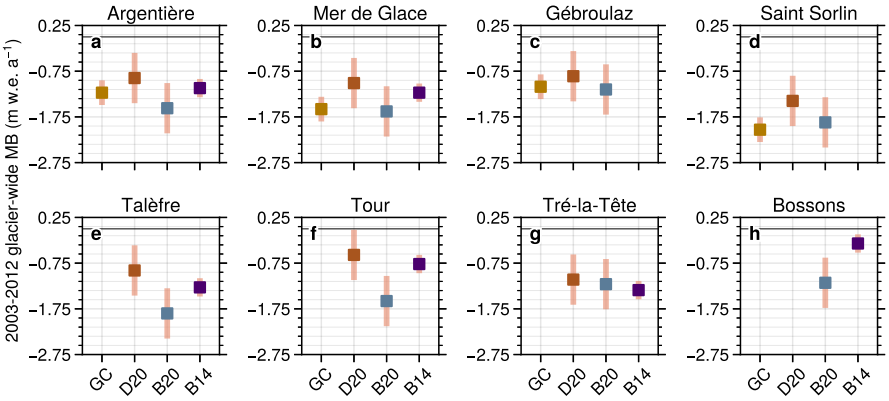

Figure 3.8: Comparison between glaciological observations from the GLACIOCLIM observatory (GC), ASTER geodetic mass balances from Davaze et al. (2020) (D20), the deep learning reconstructions from the present study (B20) and Pléiades geodetic mass balances from Berthier et al. (2014) (B14).

and aspects are considered for each massif, and meteorological observations from high-altitude stations are assimilated.

The cross-validations of both studies determined a performance with an average RMSE of 0.66 m.w.e. a^{-1} and an r^2 of 0.43 for M_{15U} for the European Alps, and an average RMSE of 0.49 m.w.e. a^{-1} and an r^2 of 0.79 for this study. However, due to the highly different methodologies and forcings of the two models, a direct comparison is not possible, so the following analysis is focused on the overall trends and sensitivities in the reconstructions and their potential sources.

3.6.3 Influence of area in glacier-wide MB signal and proof on non overfitting

Due to similarities between the averaged reconstructed glacier-wide MB and the observations during the 1984-2015 period, we decided to include an analysis to isolate the topographical influence in the glacier-wide MB signal, in order to verify that the model is not overfitting. Since the climate signal is the main common driver of annual variability of glacier-wide MB in the region, one needs to find a way to isolate the topographical signal. In Fig. 3.9, the median reconstructed annual glacier-wide MB of the 661 glaciers in the French Alps (i.e. the annual variability, hence a proxy of the climate signal) is subtracted to the mean annual values of the observations and of 4 subsets of glaciers divided by area classes. Therefore, one can observe the residual influence of glacier area on the glacier-wide MB signal. The influence of area on glaciers with observations is quite similar to glaciers with areas greater than 2 km^2, which is reasonable since glaciers with observations have an average of 4 km^2 (range: 0.3-31.8 km^2 in 2003). Moreover, one can see that even for a relatively short period of 30 years, the differences between the reconstructions for very small glaciers (< 0.5 km^2) and observations are quite important, accounting for an average cumulative loss of more than 5 m.w.e. As stated in Sect. 3.3, this does not necessarily mean that the model has fully captured the topographical influence in the glacier-wide MB signal in the region, but it does prove that the model is not overfitting since it exhibits consistent variations in MB when the topographical predictors move away from the training data. Moreover, this is coherent with the importance attributed to topographical predictors (Bolibar et al., 2020c).

The same analysis has been performed with the reconstructions from the updated version of Marzeion et al. (2015) (Fig. 3.10). The gradient with respect to glacier surface area appears to be similar, except for the behaviour of glaciers after 2007. Small and middle sized glaciers (0.1 - 2 km^2) switch to a positive influence, as opposite to large glaciers (> 2 km^2), which transition to a negative influence. Conversely, our results show a more continuous trend, without a change of behaviour in the last years of the analysed period.

3.6.4 Supplementary figures

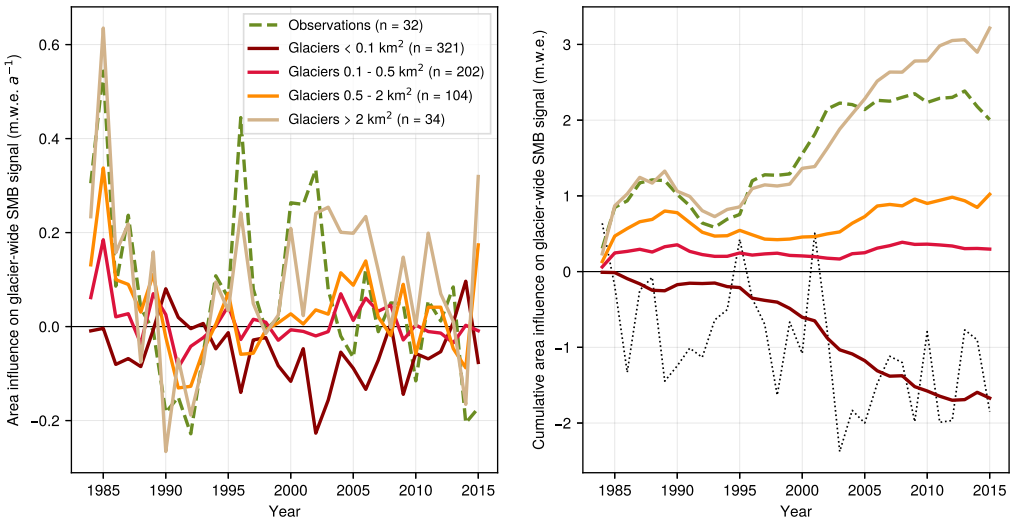

Figure 3.9: Influence of glacier area on the glacier-wide MB signal. The reconstructed median annual glacier-wide MB of the 661 glaciers in the French Alps can be seen as a proxy of the climate signal in the region. It is subtracted to the mean annual glacier-wide MB of the glaciers with observations and to four different subsets of reconstructions divided into glacier area size, showing only the annual differences based on glacier area classes. The dotted line depicts the subtracted signal (non cumulative) in order to give some context.

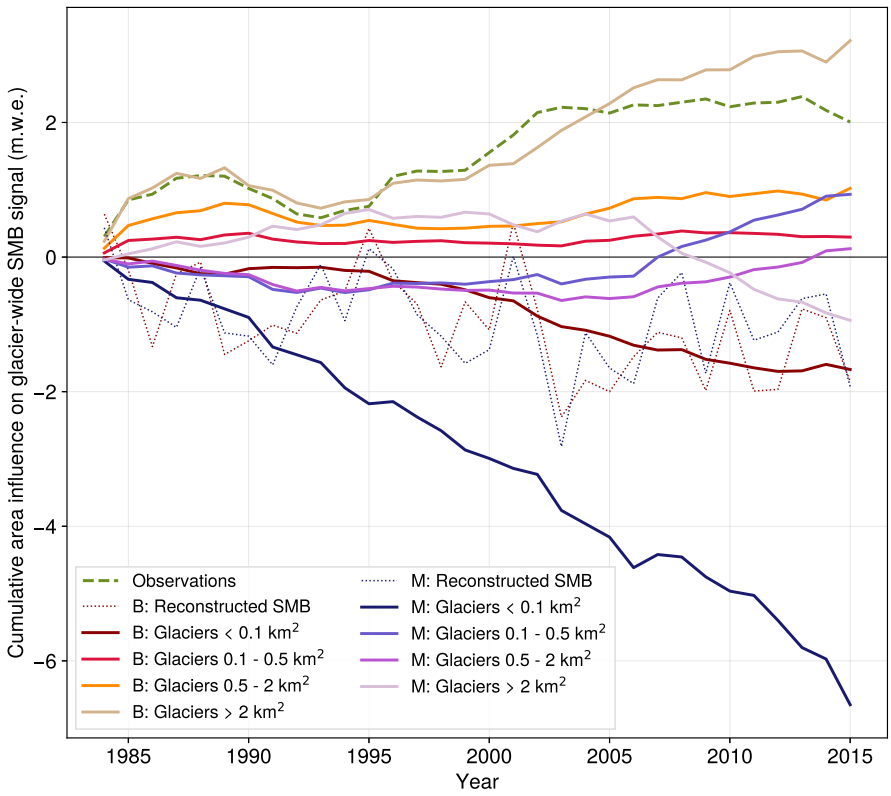

Figure 3.10: Same as S3 but comparing this study to the updated version of Marzeion et al. (2015). In the legend, "B" stands for Bolibar et al. (this study) and "M" for the update of Marzeion et al. (2015). Both models show a relatively similar gradient effect with respect to glacier area, with differences in the amplitude of the effects. The main differences appear from 2007, where small and middle sized glaciers (0.1 - 2 km^2) from the update of Marzeion et al. (2015) switch to a positive influence, as opposite to large glaciers (> 2 km^2), which transition to a negative influence. The reconstructed MB dotted lines are not cumulative and they are depicted in order to give some context of the subtracted climate signal.

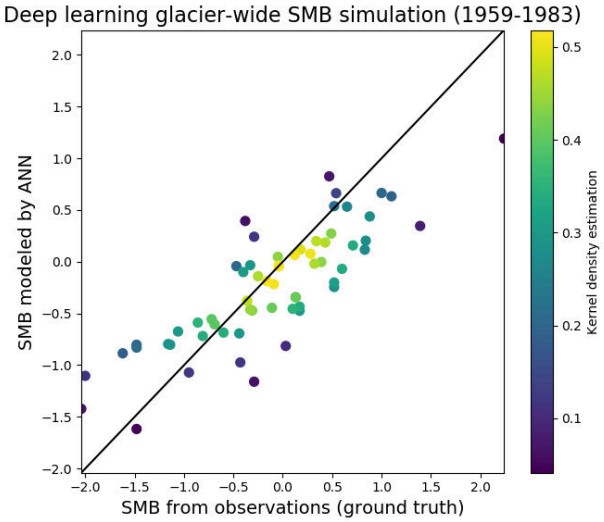

Figure 3.11: Cross-validation for annual glacier-wide MB values outside the main 1984-2014 training period. The black line indicates the one-to-one reference. Simulations have been done from 1959, the earliest date with observations to validate against the maximum number of values. This serves to confirm that the model is capable of reproducing glacier-wide MB outside the main observed period.

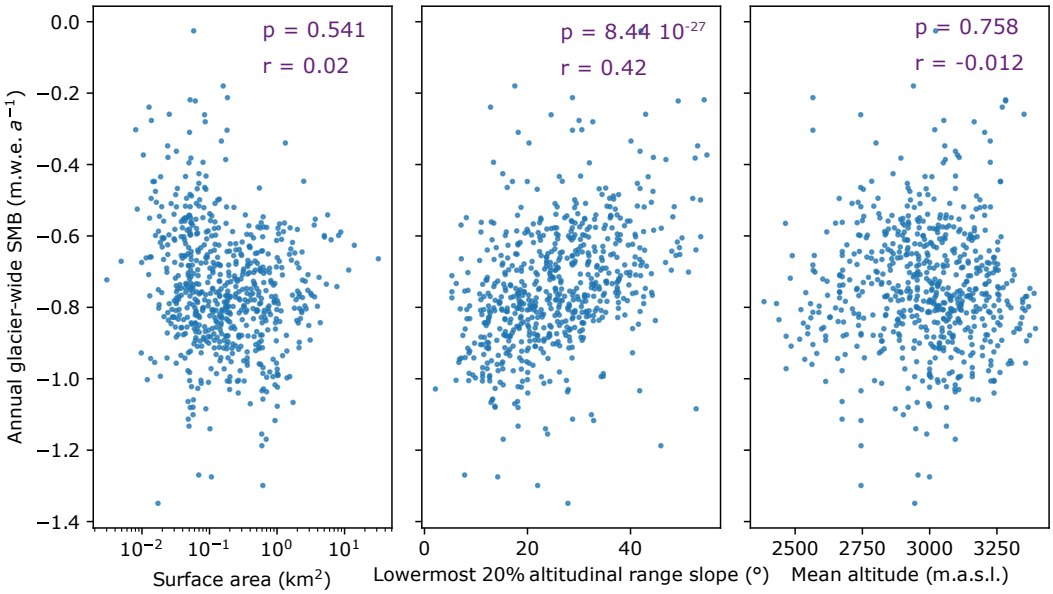

Figure 3.12: Average annual glacier-wide MB for each glacier over the entire study period with respect to (a) glacier surface area, (b) the lowermost 20% altitudinal range slope and (c) mean glacier altitude. p indicates the p-value and r the correlation between the topographical variables and the average glacier-wide MB.

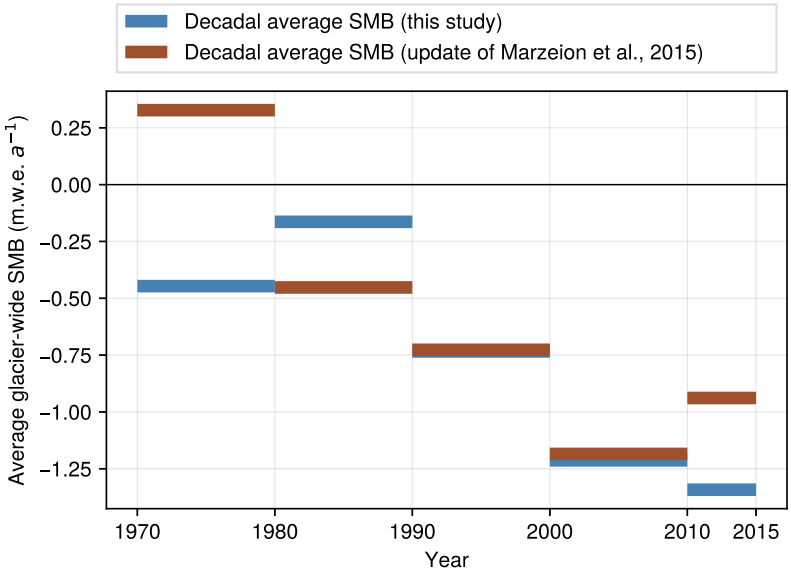

Figure 3.13: Comparison of area-weighted decadal glacier-wide MB simulations in the French Alps between this study and an update from Marzeion et al. (2015).

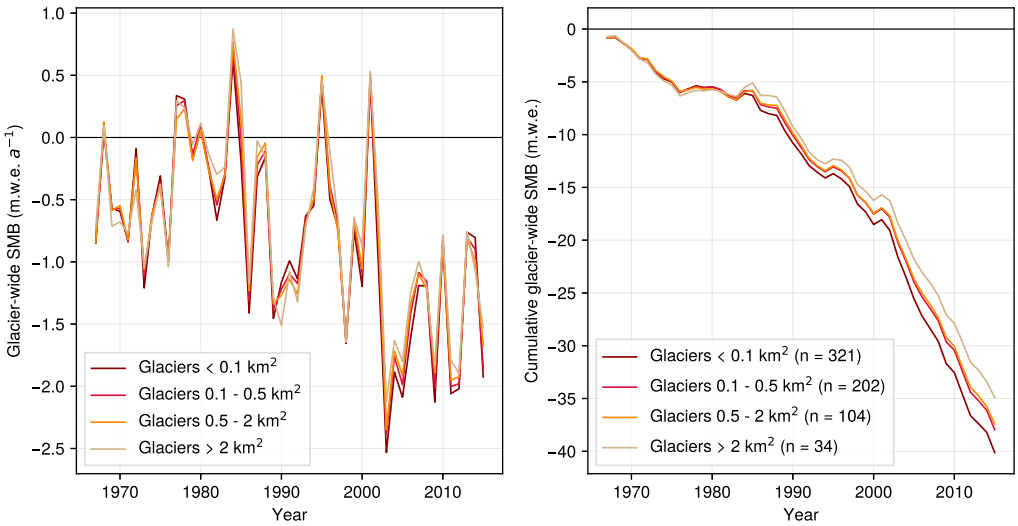

Figure 3.14: Average annual glacier-wide MB per glacier area classes

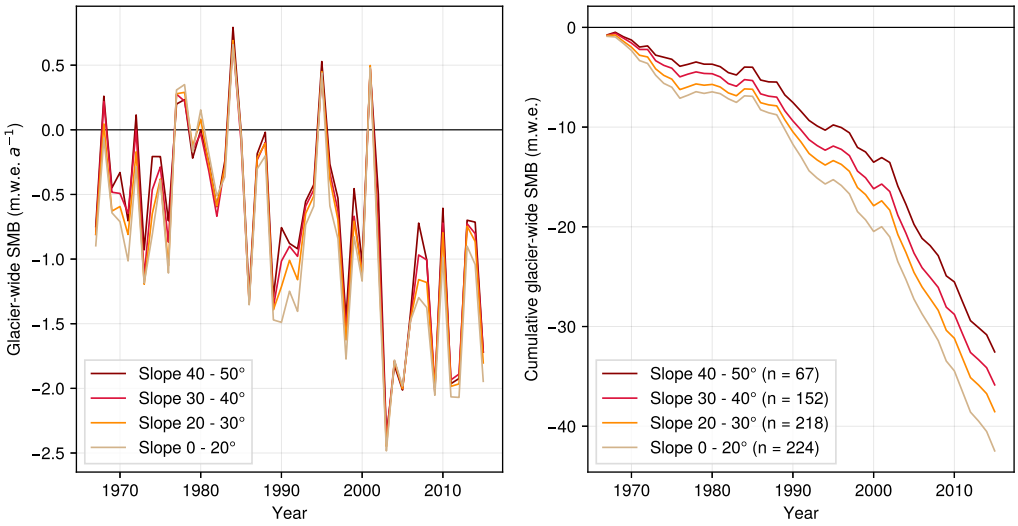

Figure 3.15: Average annual glacier-wide MB for classes of glacier slope of the lowermost 20% altitudinal range (i.e. a proxy of the glacier's tongue slope)

Chapter 4

Deep learning unveils nonlinear climate-glacier interactions through the 21^{st} century deglaciation of the French Alps

All situations in which the interrelationships between extremes are involved are the most interesting and instructive.
Wilhelm von Humboldt

Preface

After applying machine learning to model the evolution of French Alpine glaciers for the last half century, we can now look towards the future. This chapter is based on a draft written during the last months of my PhD. The original goal of this paper was to present the results of glacier evolution projections under multiple climate scenarios, in order to quantify and understand the fate of French Alpine glaciers through the 21^{st} century. Nonetheless, a parallel investigation on the effects of nonlinearities on mass balance models resulted in unexpectedly interesting results which progressively transformed the paper. In order to analyse and understand the effects of nonlinearities in climate forcings on glaciers, I performed a series of analyses in an attempt to unravel their causes and effects. This exploration implied a great deal of dead ends and problem reformulations, until reaching some common ground from multiple experiments. In this regard, this paper attempts to extract the nonlinear signals from climate and glacier data in order to determine some broader implications for other glacierized regions in the world. A month prior to submitting this PhD manuscript, I contacted Harry Zekollari in order to acquire some data from his 2019 study on the European Alps for a model comparison. A lengthy series of long e-mails loaded with figures quickly transformed into a fruitful collaboration which helped me acquire a better perspective on the subject. And eventually, as it has become the norm throughout my PhD, Clovis Galiez provided me with some last minute assistance with his invaluable expertise on machine learning, helping me finish my PhD with a little less suffering.

Based on Bolibar, J., Rabatel, A., Gouttevin, I., Zekollari, H., Galiez, C.: Deep learning unveils nonlinear

climate-glacier interactions through the 21st century deglaciation of the French Alps, in prep.

Abstract

The European Alps are experiencing some of the strongest glacier retreat in the world, challenging future regional water availability, hydropower generation, ecosystems and local-to-regional socioeconomic models. Predicting future glacier evolution requires a correct representation of nonlinear climate-glacier interactions, yet most glacier mass balance models are linear. Here, we perform the first glacier evolution projections ever based on deep learning by modelling glacier evolution in the French Alps through the 21st century. Our results predict a regional glacier volume loss between 75 and 88% by the end of the century depending on climate scenarios, with only high-altitude glaciers remaining in the Mont-Blanc and Pelvoux massifs. Deep learning captures important nonlinearities in air temperature and precipitation forcings on glaciers, highlighting how linear models compromise extreme positive and negative glacier mass balance rates, introducing long-term cumulative biases. These results suggest that current global glacier evolution projections based on linear mass balance models might be potentially underestimating the lower and higher bounds of future sea-level rise.

4.1 Introduction

Glaciers are experiencing important changes throughout the world as a consequence of anthropogenic climate change (IPCC, 2018). Despite marked differences among regions, the generalized retreat of glaciers is expected to have major environmental and social impacts (Huss et al., 2017; Zemp et al., 2019). Water resources provided by glaciers sustain around 10% of the world's population living near mountains and the contiguous plains (Immerzeel et al., 2020), depending on them for agriculture, hydropower generation (Farinotti et al., 2019b), industry or domestic use. Several aquatic and terrestrial ecosystems depend on these water resources as well, which ensure a base runoff during the warmest or driest months of the year (Cauvy-Fraunié and Dangles, 2019). Predicting future glacier evolution is of paramount importance in order to correctly anticipate and mitigate the resulting environmental and social impacts. During the last decade, several global glacier evolution models have provided the first estimates of future glacier evolution and sea-level rise (Hock et al., 2019a; Marzeion et al., 2020). All glacier models, independently from their approach, need to resolve the two main processes that determine glacier evolution: (1) glacier dynamics, characterized by the downwards movement of ice due to the effects of gravity in the form of deformation of ice and sliding; and (2) glacier mass balance, as the difference between the mass gained via accumulation (e.g. snowfall or avalanches) and the mass lost via different processes of ablation (e.g. melt of ice, firn and snow or calving) (Cuffey and Paterson, 2010). Simulating these processes at a large geographical scale is a challenging task, with models requiring several parametrizations and simplifications to operate. Recent efforts have been made in order to improve the representation of ice flow dynamics in these models, replacing empirical parametrizations with simplified physics (Maussion et al., 2019; Zekollari et al., 2019). Nonetheless, the vast majority of large-scale glacier evolution models rely on linear temperature-index models for glacier mass balance simulation. This type of models use a calibrated empirical linear relationship between positive degree days (PDD) and the melt of ice and snow (Hock, 2003). The main reason for their success comes from their suitability to large-scale studies with a low density of observations, often displaying an even better performance than more complex models (Réveillet et al., 2018). However, both the climate and glacier systems are known to be nonlinear (Steiner et al., 2005), implying

that these models can only offer a linearized approximation of climate-glacier relationships.

The French Alps, located in the westernmost part of the European Alps, are among the regions in the world with the strongest glacier retreat (Zemp et al., 2019; Bolibar et al., 2020b). Long-term historical interactions between French society and glaciers have developed a dependency of society on them for water resources, agriculture, tourism - particularly the ski business (Spandre et al., 2019) - and hydropower generation. This rapid glacier retreat is already having an environmental impact on natural hazards (Magnin et al., 2020), mountain ecosystems (Carlson et al., 2020) and biodiversity (Cauvy-Fraunié and Dangles, 2019). Without these cold water resources during the hottest months of the year, many aquatic and terrestrial ecosystems that depend on them will be impacted due to changes in runoff, water temperature or habitat humidity (Carlson et al., 2020; Robinson et al., 2014). Anticipating these environmental and social changes will be imperative for these territories to successfully adapt their socioeconomic models, requiring an accurate prediction of future glacier evolution. Glaciers in the European Alps have been monitored for several decades, resulting in the longest observational series in the world (Vincent et al., 2017; GLAMOS, 2019). This wealth of data provides a privileged environment for glaciological studies, creating an adequate testbed for innovative methods (Nanni et al., 2020). In this study, we investigate the future evolution of glaciers in the French Alps and their nonlinear response to multiple climate scenarios. We perform, to our knowledge, the first deep learning (i.e. deep artificial neural networks) glacier evolution projections ever by modelling the regional evolution of French alpine glaciers through the 21st century. We developed a state-of-the-art modelling framework based on a deep learning mass balance (MB) component, glacier-specific parametrizations of glacier dynamics and high-resolution climate ensemble projections from 29 combinations of global climate models (GCMs) and regional climate models (RCMs) adjusted and aggregated for mountain regions for three Representative Concentration Pathway (RCP) scenarios: 2.6, 4.5 and 8.5 (Verfaillie et al., 2017). The 29 GCM-RCM combinations available, hereafter named climate members, are representative of future climate trajectories with different concentration levels of greenhouse gases. 26 climate members cover intermediate scenarios (RCP 4.5) and worst-case scenarios (RCP 8.5), whereas scenarios with significant reductions of emissions (RCP 2.6) are only covered by three members (Table S1). With this study, we provide new state-of-the-art predictions of glacier evolution in a highly populated mountain region, while investigating nonlinearities in the response of glaciers to multiple future climate forcings.

4.2 Results

4.2.1 Glacier evolution through the 21st century

Our projections show a strong glacier mass decrease for all 29 climate members, with average ice volume losses by the end of the century of 75%, 80% and 88% under RCP 2.6 (±9%, n=3), RCP 4.5 (-17% +11%, n=13) and RCP 8.5 (-15% +11%, n=13) respectively (Fig. 4.1 and 4.7). Differences in projected glacier changes become more pronounced from the second half of the century, when about half of the initial 2015 ice volume has already been lost. Annual glacier-wide mass balance (MB) is estimated to remain stable throughout the whole century under RCP 4.5, with glacier retreat to higher elevations (positive effect on MB) compensating for the warmer climate (negative effect on MB). Conversely, for RCP 8.5 annual glacier-wide MB are estimated to become increasingly negative by the second half of the century, with average MB twice as negative as today's average values (Fig. 4.1A). MB rates only begin to approach equilibrium towards the end of the century under RCP 2.6, for which glaciers could potentially stabilize with the climate in the first decades of the 22nd century depending on their

response time (Fig. 4.7A). An analysis of the climate signal at the glaciers' mean altitude throughout the century reveals that air temperature, particularly in summer, is expected to be the main driver of glacier mass change in the region. Interestingly, the future warmer temperatures do not affect annual snowfall rates on glaciers due to higher precipitation rates (Fig. 4.2). This increase in future winter precipitation has already been documented (Smiatek et al., 2016), and it is complemented by glaciers shrinking to higher elevations as climate warms, where precipitation rates are higher as a result of orographic precipitation gradients (Roe, 2005). Therefore, solid precipitation is projected to remain almost constant independently from the future climate scenarios, with air temperature driving the future glacier-wide mass changes (Fig. 4.2A,D). These results are in agreement with the main known drivers of glacier mass change in the French Alps (Six and Vincent, 2014). Overall, glaciers are expected to undergo stable climate conditions under RCP 4.5, but increasingly higher temperatures and rainfall under RCP 8.5 (Fig. 4.2). These differences in the received climate signal are explained by the retreat of glaciers to higher altitudes, which keep up with the warming climate in RCP 4.5 but are outpaced by it under RCP 8.5.

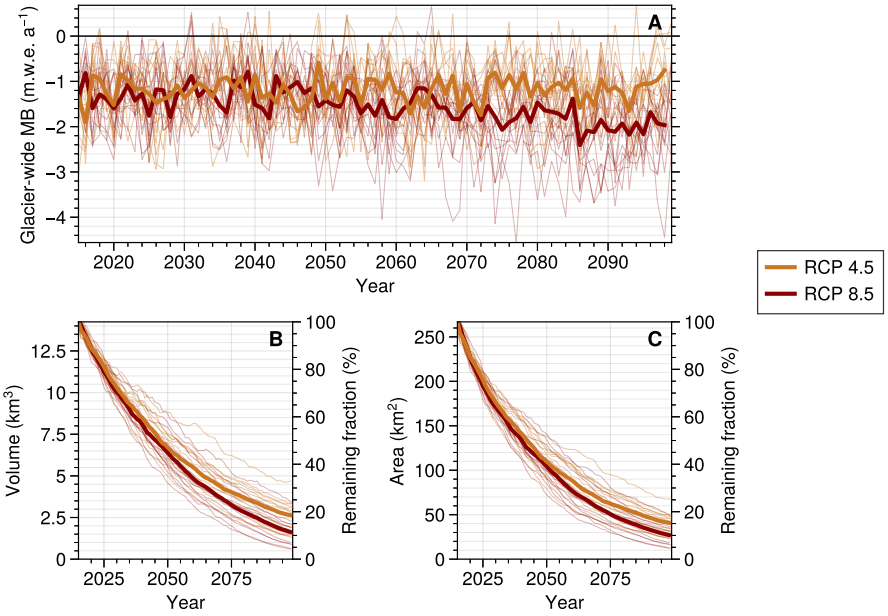

Figure 4.1: Glacier-wide MB, volume and area evolution of French Alpine glaciers through the 21st century. (A) Glacier-wide annual MB, (B) ce volume evolution, (C) Glacier area evolution. Thin lines represent each of the 29 individual member runs, while the thick lines represent the average for a given RCP.

The glacier ice volume distribution in the French Alps at the beginning of the 21st century is greatly uneven, with the Mont-Blanc massif amassing about 60% of the total ice volume in the year 2015 (7.06 out of 11.64 km^3, Fig. 4.3A). The vast majority of glaciers in the French Alps are very small glaciers (< 0.01 km^3), being remnants of the Little Ice Age with a strong imbalance with the current climate (Bolibar et al., 2020b). Our projections highlight the almost entire disappearance of all glaciers outside the Mont-Blanc and Pelvoux massifs under RCP 4.5 (Fig. 4.3) and 8.5 by the end of the century. By that time, considering RCP 4.5, these two high-altitude massifs are predicted to store on average 25% and 13.4% of their 2015 volume respectively, with most of the ice concentrated in a few large glaciers (Fig. 4.4). Glacier landscapes are expected to see important changes throughout the French Alps, with the average glacier altitude becoming 300 m (RCP 4.5) and 400 m (RCP 8.5) higher than nowadays (Fig. 4.3A and 4.9).

The Mont-Blanc and Écrins regions, with the latter being composed by the Pelvoux, Oisans and

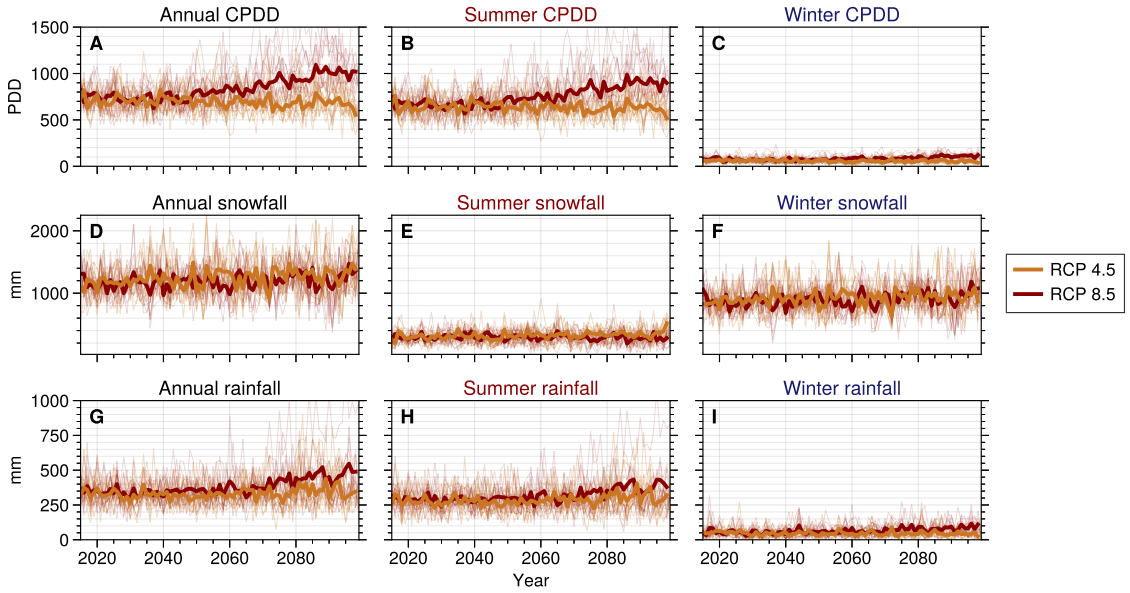

Figure 4.2: Climate signal over glaciers in the French Alps. The cumulative positive degree days (CPDD), snowfall and rainfall, computed at the glaciers' annually evolving centroids, display the climate forcing on glaciers taking into account glacier geometry change. Summer climate is computed between April 1st and September 30th and winter climate between October 1st and March 31st. Thin lines represent each one of the 29 individual member runs, while the thick lines represent the average for a given RCP.

Champsaur massifs, host the highest mountains in the French Alps. From a historical point of view, these two regions (Fig. 4.4) have played a very important role in the relationships between the French and European societies and mountains (Smit et al., 2019), being widely acknowledged as the birthplaces of alpinism and mountaineering (Mourey and Ravanel, 2017; Bourdeau, 2009). These mountains, and particularly their glaciers, have shaped the socioeconomic models of these regions, with well-developed tourism and hydropower industries (Bourdeau, 2009; Schut, 2013). Our results indicate an average projected loss of 58 and 49 km^2 of glacierized surface in the Mont-Blanc and Écrins regions respectively, and a total of 185 km^2 in the whole French Alps under RCP 4.5. The landscapes of these two emblematic mountain regions are expected to be greatly transformed (Fig. 4.4), with only a few high-altitude glaciers capable of sustaining the future warmer climate, such as the Bossons (4C) and Taconnaz (4D) glaciers around the Mont-Blanc summit (4810 m.a.s.l.) or the Glacier Blanc (4E) next to the Barre des Écrins (4102 m.a.s.l.). Highly touristic sites like the Mer de Glace (4B) and Argentière (4A) glaciers close to Chamonix, and the glaciers around la Meije summit next to La Grave will lose between 45 and 82% of their area under RCP 4.5. The case of Mer de Glace, the largest glacier in the French Alps (29 km^2 in 2015) is quite representative of this trend, with an expected loss of half of its surface area by the end of the century, losing the entirety of its emblematic tongue that gave its name (Fig. 4.4B).

4.2.2 Nonlinear climate-glacier interactions

Glacier mass changes are commonly modelled using empirical linear relationships between temperature and snow and ice melt (Huss and Hock, 2015; Maussion et al., 2019; Hock et al., 2019a; Marzeion et al., 2020). Since the climate and glacier systems are known to be nonlinear (Steiner et al., 2005), we investigated the benefits of using a nonlinear model to simulate annual glacier-wide MB at a regional scale. We compared model runs using a nonlinear deep learning MB model against a linear machine

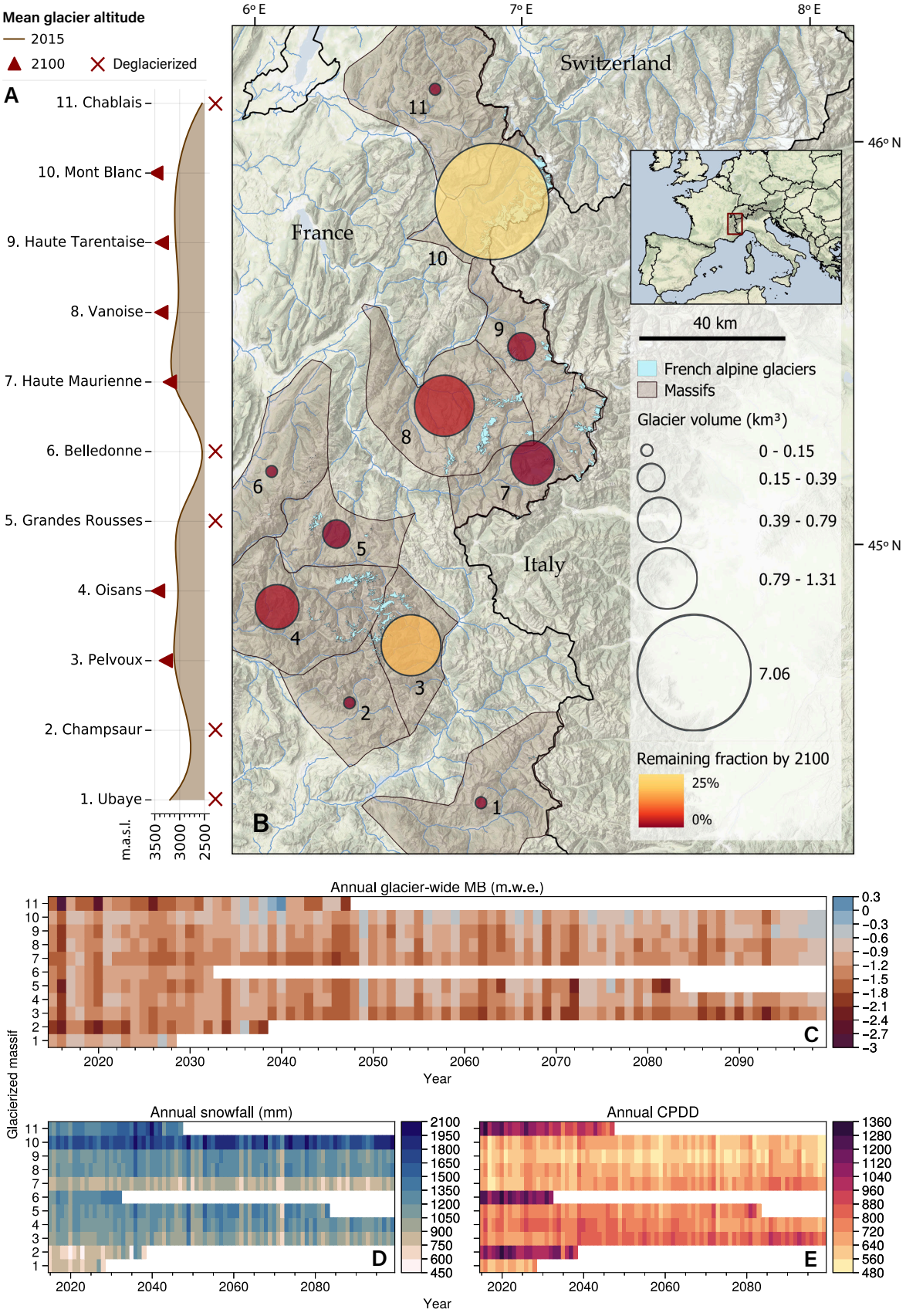

Figure 4.3: Average projected glacier and climate evolution per glacierized massif between 2015-2100 under RCP 4.5. (A) Projected mean glacier altitude evolution between 2015-2100. Massifs without glaciers by 2100 are marked with a cross, (B) Glacier ice volume distribution per massif, with its remaining fraction by 2100, (C) Annual glacier-wide MB per massif, (D) Annual snowfall per massif, (E) Annual cumulative positive degree days (CPDD) per massif. All values correspond to ensemble means under RCP4.5.

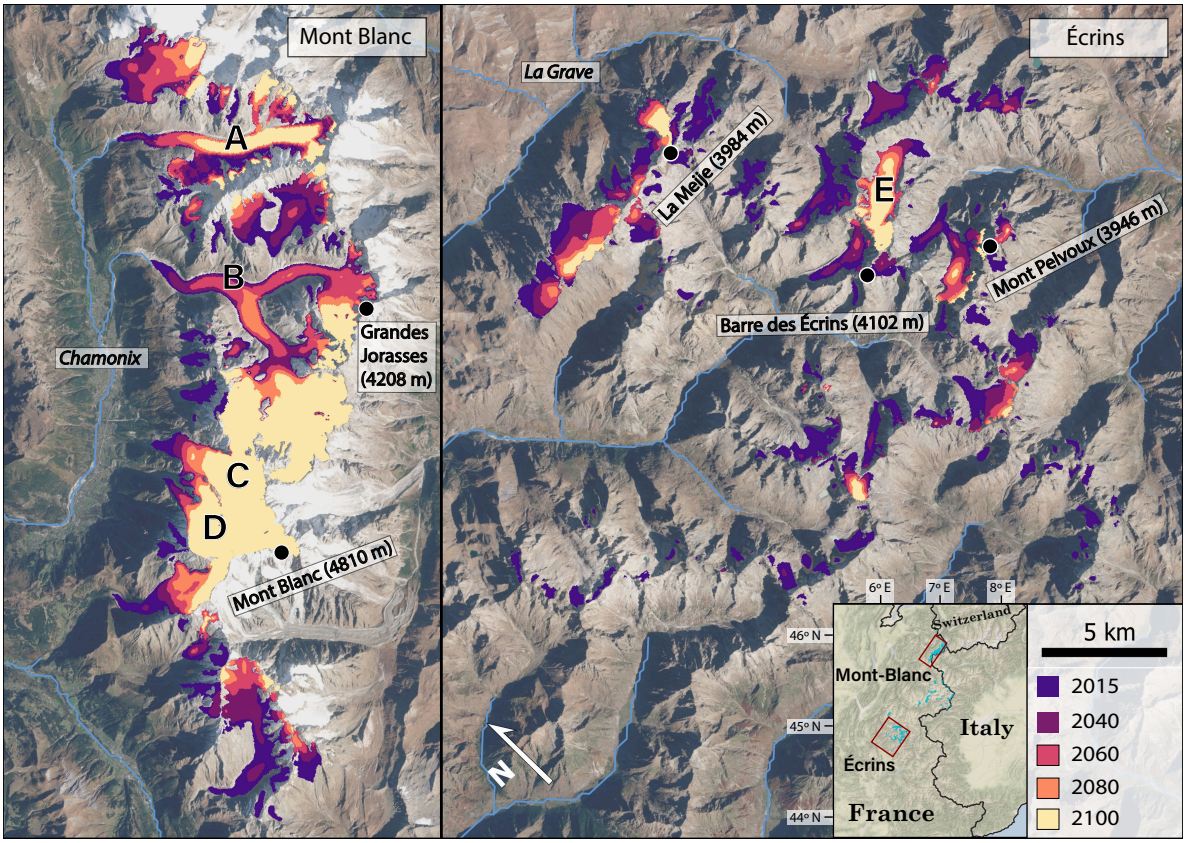

Figure 4.4: Projected glacier evolution in the Mont-Blanc and Écrins regions. Projections under CLMcom-CCLM4-8-17_CNRM-CERFACS-CNRM-CM5 RCP4.5, being the closest to the multi-model air temperature and precipitation mean. Specific glaciers (A) Mer de Glace, (B) Argentière, (C) Bossons, (D) Taconnaz and (E) Glacier Blanc are referenced in the main text.

learning MB model based on the Lasso (Tibshirani, 1996), i.e. regularized multilinear regression. Both models were trained with exactly the same data, and all other model components were kept the same in order to isolate the effects of the nonlinearities in the MB. Results show that important nonlinearities are captured by the deep learning MB model, whose nonlinearity and superior performance allow for a better representation of glacier mass changes, including significantly reduced biases for extreme values (see Materials and Methods). A sensitivity analysis of both MB models revealed nonlinear relationships between air temperature, winter and summer snowfall and glacier-wide MB, which the linear model was only able to approximate (Fig. 4.5). Regarding air temperature forcing, the linear Lasso model was found to underestimate negative MB rates and to overestimate positive MB rates under extreme positive and negative cumulative PDD (CPDD) anomalies respectively. Conversely, the linear MB model overestimated positive and negative MB rates under extreme positive and negative winter and summer snowfall anomalies respectively (Fig. 4.5). Since the Lasso is required to linearly approximate nonlinear responses to climate, it manages to correctly fit the main cluster of average values but performs poorly for extreme values (Bolibar et al., 2020c). This has the strongest impact under RCP 2.6 (Fig. 4.6), as the linear model tends to overestimate positive MB rates both from air temperature and snowfall (Fig. 4.5). The linear MB model manages to gain equilibrium with the climate in the last decades of the century, a situation that is never reached with the nonlinear MB model. Alternatively, the differences under RCP 8.5 are more moderate, since the nonlinear negative effects from air temperature and positive effects from snowfall compensate each other. Important differences only start to appear by the end of the 21st century (Fig. 4.6), when the temperatures rise enough

for the MB models to operate under extreme positive CPDD anomalies. Under these conditions the nonlinearities become significant enough to drive different behaviours between both MB models (Fig. 4.5). Our previous work has shown how linear MB models can be correctly calibrated for data around the mean temperature and precipitation values used during training, giving similar results and performance to deep learning. However, their accuracy drastically drops as soon as the input climate data moves away from the mean cluster of values used for training (Bolibar et al., 2020c). The lower explained variance of linear models is displayed during glacier evolution projections under radically different climate scenarios. Both models agree around the average values seen for training (i.e. -0.78 m.w.e. a^{-1}), but when conditions deviate from this mean training data centroid, the Lasso can only linearly approximate the extremes based on the linear trend set on the main cluster of average values (Fig. 4.6C, I).

We further assessed the effect of MB nonlinearities by comparing our simulated glacier changes with transiently modelled glacier evolution from the literature, which rely on linear temperature-index models for MB modelling. Previous studies on 21^{st} century large-scale glacier evolution projections have covered the French Alps (Marzeion et al., 2020). Here, we compare our results with those from a recent study that focused on the European Alps (Zekollari et al., 2019). Despite differences between the two modelling approaches (Table S2), both overall glacier volume projections present relatively similar results by the end of the century, with volume differences ranging between 14% for RCP 2.6 to less than 2% for RCP 4.5 (Fig. 4.10). Nonetheless, a close inspection of the annual glacier-wide MB rates from both models revealed interesting differences. A bias correction was applied to the MB series of the linear temperature-index model in order to enable a fair comparison between both models (see Materials and Methods). The comparison between our nonlinear deep learning MB model and the linear temperature-index MB model displayed similar patterns to those previously found between deep learning and Lasso (Fig. 4.11). Despite slightly different trends during the first half of the century, both linear models react similarly to the different future climate scenarios of the second half of the century, also resulting in more positive MB rates under RCP 2.6 and a transition towards less negative MB rates under RCP 8.5 (Fig. 4.11). As for the Lasso, the trends under RCP 8.5 are less clear, indicating the complex inter-

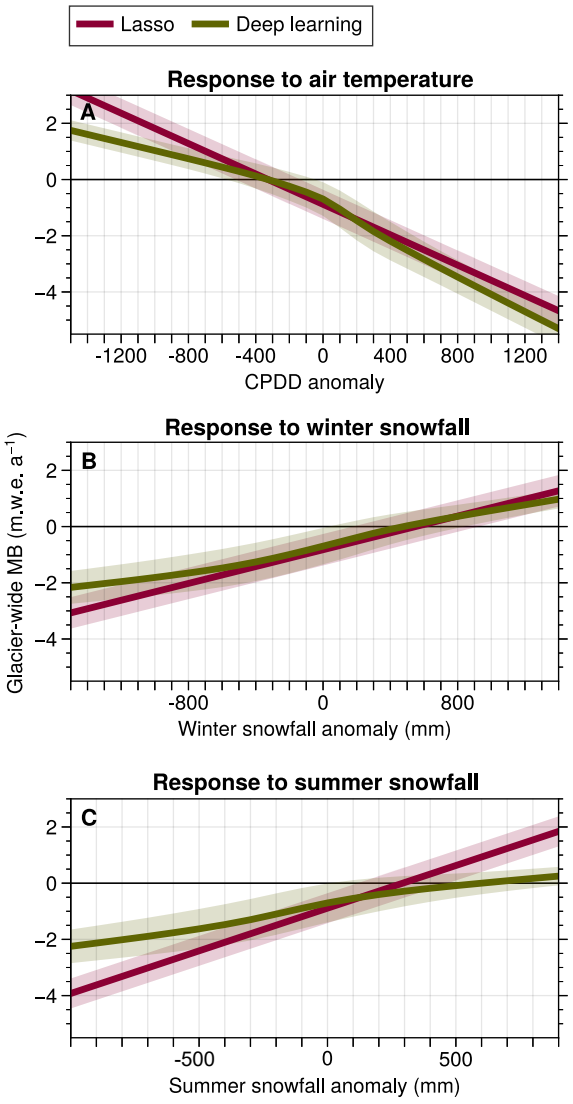

Figure 4.5: Nonlinear and linear response to climatic forcing of MB models. Nonlinear deep learning response and linear Lasso response to (A) Cumulative positive degree days (CPDD) anomalies, (B) winter snowfall and (C) summer snowfall. All climate anomalies are computed with respect to the 1967-2015 mean values. Envelopes indicate $\pm\sigma$ based on results for all 660 glaciers in the French Alps for the 1967-2015 period.

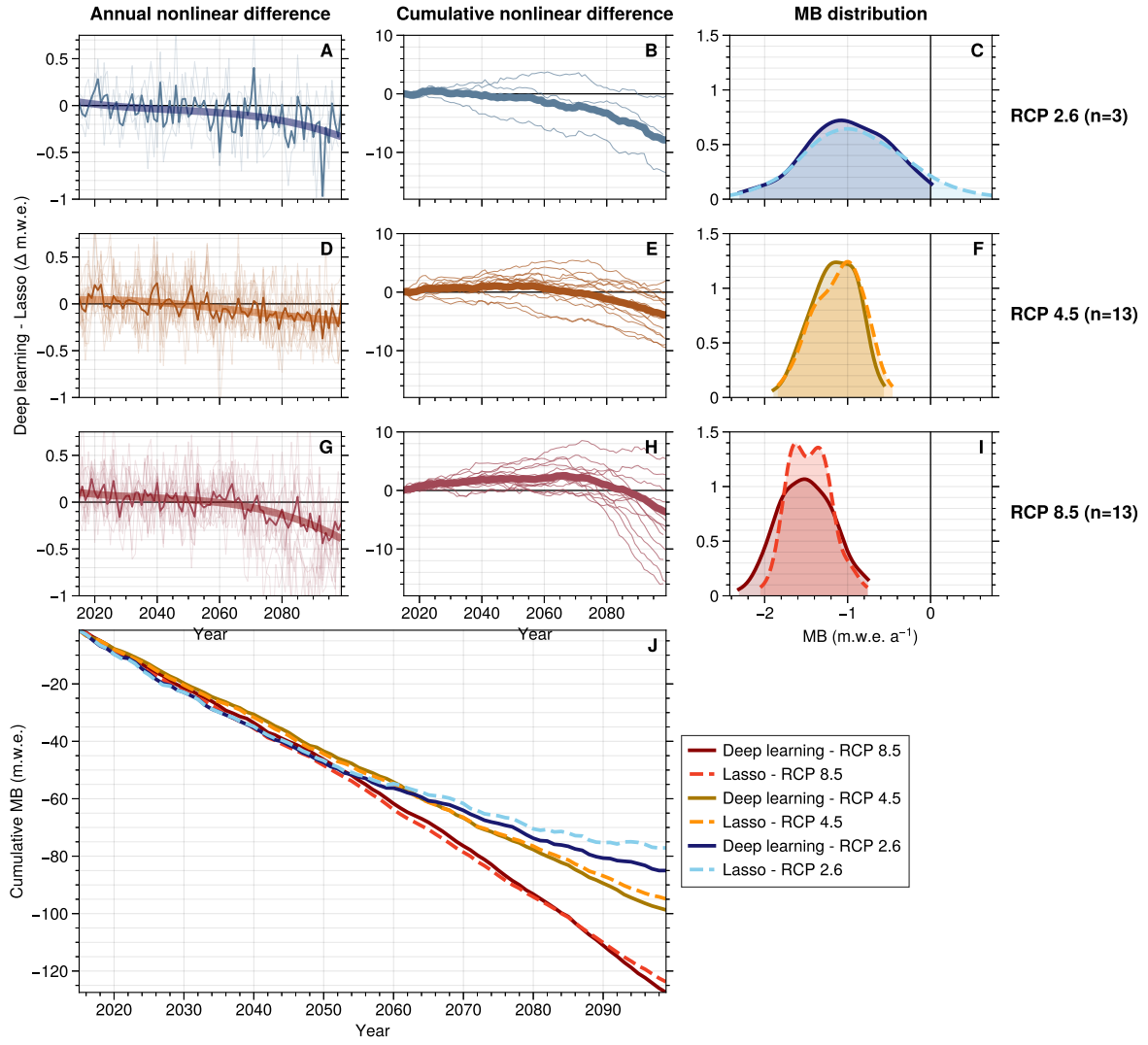

Figure 4.6: Effect of deep learning nonlinearities on glacier mass balance projections. Annual glacier-wide mass balance differences (A, D, G) and cumulative annual differences (B, E, H) between the nonlinear deep learning and the linear Lasso machine learning MB models. (C, F, I) Probability distribution functions of MB projections. (J) Cumulative MB for the different combinations of MB models and RCP scenarios. Thicker semi-transparent lines show a 3rd order polynomial fit on annual difference values.

play between the opposite effects of nonlinearities related to air temperature and snowfall. This similarity between patterns suggests that linear temperature-index models, which are widely used for regional-to-global MB modelling, might also potentially overestimate extreme positive annual glacier-wide MB rates. The trend for extreme negative MB rates is less clear, and it only seems to appear under extreme air temperature values found by the end of the 21st century under RCP 8.5. Both the linear machine learning and the temperature-index MB models rely on a linear relationship between PDDs, solid precipitation and MB. As we have shown, air temperature is the main driver of MB changes in the region, implying that these differences mainly come from a nonlinear response between PDDs, a proxy of air temperature, and glacier-wide MB (Fig. 4.5A).

Another important aspect of climate-glacier forcings is the role of glacier retreat. Glaciers are excellent climate proxies, fluctuating with climate variations. They advance or retreat in order to reach equilibrium with the present climate (Mackintosh et al., 2017). In order to study these climate-glacier interactions, we analyzed the consequences of glacier retreat on the climate signal received by glaciers.

Its effects on annual CPDDs, snowfall, rainfall and glacier-wide MB (Fig. 4.12), computed at the glaciers' mean altitude, were quantified by comparing model projections with an evolving glacier geometry against projections with a constant initial geometry. Results highlight how glaciers retreating to higher altitudes encounter greatly modified climatic conditions, experiencing reduced temperatures up to -350 PDDs a^{-1} for the highest greenhouse gases concentration scenario and consequently reduced melt (Fig. 4.12A). Precipitation-wise, glacier retreat induces an important reduction in rainfall (up to -100 mm a^{-1}) and an increase in snowfall (up to 220 mm a^{-1}), helping the glacier transition towards equilibrium (Fig. 4.11D,G). This change in climatic conditions has important consequences for glacier MB. The reduced melt and increased accumulation limit glacier mass loss, with annual differences up to 1.2 m.w.e. by the end of the century in the region. Despite this significant mitigation of glacier mass loss, our projections indicate that glacier retreat will not suffice to reach equilibrium with the future climate under any projected climate scenario in the French Alps (Fig. 4.7A and 4.11J).

Glacier retreat modulates the interplay between the two main factors that determine glacier MB: climate and topography. A statistical analysis of model results revealed that glacier maximum altitude, latitude and longitude are the most important factors for glacier survival in the French Alps, explaining 69% of the remaining glacierized fraction of glaciers by the end of the century (see Statistical Analysis). A high-altitude accumulation basin is the most decisive factor for a glacier to survive the future warmer climate (53% of importance, $p < 0.01$), ensuring great amounts of solid precipitation and a large cold area to retreat to. In a second term, glaciers in the northern massifs receive increased amounts of precipitation due to the more intense western fluxes and higher latitude (34% of importance, $p = 0.08$; e.g. Chablais and Mont-Blanc in Fig. 4.3D). The relationship with longitude is not statistically significant (13% of importance, $p = 0.57$), implying a minor role on modulating glacier change compared to latitude, likely explained by the relatively narrow range of longitudes covered by the French Alps. High amounts of snowfall do not suffice for glaciers to survive, as it can be seen for the Chablais massif. Its low altitudes translate into higher-than-average temperatures for glaciers (Fig. 4.3E), and prevent them from reaching an equilibrium with the climate at higher altitudes despite the high snowfall rates (Fig. 4.3D). Despite occupying a relatively small area (Fig. 4.3B), the French Alps display notorious differences in climatic conditions due to their particular geographical position, with an increasing precipitation gradient spanning from southeast to northwest (Fig. 4.3D) (Durand et al., 2009). On the one hand, the southern massifs (1-5 in Fig. 4.3) have a Mediterranean climate influence compared to the northern ranges (6, 8, 10, 11 in Fig. 4.3), which tend to receive increased precipitation from western Atlantic fluxes. Alternatively, eastern glaciers close to the Italian border (7 and 9 in Fig. 4.3) receive less precipitation, mainly from east returns. This type of precipitation events can have a very local extent, producing different amounts of accumulation between eastern and western glaciers (Vionnet et al., 2019). On the other hand, topography conditions glacier altitude, which modulates temperature and snowfall on glaciers. Massifs with vast high-altitude accumulation basins (e.g. the Mont-Blanc and Pelvoux massifs), provide areas with colder climates for glaciers to retreat to. Conversely, low-altitude massifs (e.g. Belledonne and Chablais) can no longer sustain glaciers with the present climate, with their small glaciers being remnants of the Little Ice Age. Such glaciers currently survive thanks to very specific topographical configurations, such as steep north-facing slopes or snow-feeding avalanche couloirs, that help to reduce the high ablation rates typical from these low altitudes. Glaciers in these massifs are projected to disappear within the next two to three decades (Fig. 4.3).

4.3 Discussion

We showed that by using a nonlinear glacier MB model based on deep learning, important nonlinearities in the response of glaciers to climate forcing are captured. A thorough cross-validation analysis indicated that deep learning models provide a more accurate representation of nonlinear glacier mass changes compared to linear models, with improvements up to +108% in explained variance (Bolibar et al., 2020c). These nonlinearities are ignored by linear MB models, whose linear approximations are only accurate for a certain range of MB rates, being specifically fitted for the main cluster of MB values used for training or calibration. As most MB distributions are Gaussian or Gumble-type (Thibert et al., 2018), this calibration is performed around the median values, where the highest concentration of data is found, thus reducing the loss function used for calibration (e.g. the root mean squared error, RMSE). Such a calibration produces a model that is accurate for the majority of MB rates, at the cost of sacrificing performance for extreme values. In the current context of strong glacier retreat, these median MB values are normally negative (Zemp et al., 2019), implying a drop in performance for extremely negative and neutral-to-positive MB rates (Fig. 4.13). Our analyses suggested that this particular behaviour of linear MB models is likely found in both machine learning (statistical) and temperature-index (empirical) models. A poor representation of extreme values is a core problem in modelling, even for nonlinear models. Nonetheless, this effect was found to be strongly reduced by deep learning models, due to their superior nonlinear explained variance. Our results also serve as a validation of the use of linear MB models for rather homogeneous climate conditions. In the absence of climate extremes, linear models successfully reproduce the trends of glacier MB rates, with a reduced bias similar to nonlinear models. However, their accuracy is still systematically lower than deep learning models, thus yielding unbiased but inaccurate predictions (Bolibar et al., 2020c).

As for many regions in the world, air temperature is the main driver of future glacier mass changes in our study. The most important nonlinearities were found in air temperature to MB forcings, whose differences are particularly notorious under extreme high and low CPDD anomalies. Combined with these air temperature forcing nonlinearities, the marked differences in MB response to solid precipitation between linear and nonlinear models can generate a wide range of MB responses to climate forcing (Fig. 4.5). All 29 climate members used for projections display rather similar conditions until 2050 due to the inertia of climate. Therefore, linear and nonlinear MB simulations for the first half of the century show a good agreement, since they operate close to the range of values seen during model calibration. This situation is sustained until the end of the century for RCP 4.5, displaying rather constant average MB rates, which result in very similar values between linear and nonlinear models (Fig. 4.6E and 4.115D). Alternatively, for the more extreme climate scenarios differences appear as models start to operate under extreme climates. For RCP 2.6, linear MB models tend to stabilize much faster than nonlinear models, showing a higher sensitivity to negative air temperature anomalies and positive snowfall anomalies (Fig. 4.6B, 4.10B). Conversely, under RCP 8.5 the nonlinear effects of air temperature and snowfall cancel each other out, acting similarly to linear models. Nonetheless, in the last decades of the century, as extreme air temperatures increase in frequency (Fig. 4.2A), the nonlinearities from air temperature forcing become greater, resulting in higher rates of mass loss for the deep learning model (Fig. 4.6G, 4.10E).

These different behaviours and resulting biases can potentially induce important consequences in long-term glacier evolution projections. Linear and nonlinear MB tend to agree for the common climate projections until the middle of the 21st century, displaying the capabilities of linear models to correctly operate within this range of values if enough data for calibration is available. Following these decades with a common climatic trend, nonlinearities start to come into play as the future climates

become more extreme. For the future scenarios with an important reduction of greenhouse gases emissions, as air temperatures will start to drop (e.g. Fig. 4.8A), many glaciers might find themselves in altitudes with an adequate climate for them to gain mass, potentially reaching equilibrium and neutral-to-positive MB rates. Conversely, for scenarios with uninterrupted greenhouse gases emissions, as air temperatures will increase unabated, glaciers will find themselves in a great imbalance with the present climate, resulting in strongly negative MB rates (e.g. Fig. 4.1A). In our case study we observed that linear MB models tend to overestimate the neutral-to-positive MB rates under RCP 2.6 (Fig. 4.6C) and tend to underestimate the extremely negative MB rates under RCP 8.5 (Fig. 4.1I). The cumulative MB differences for our study area were rather mitigated by the fact that half of the glacier volume is estimated to disappear by the middle of the century, a period for which linear and nonlinear models are forecasted to behave similarly (Fig. 4.6J). Even so, the nonlinear effects present in the last decades of the 21^{st} century are enough to introduce differences in cumulative MB up to 16% (Fig. 4.6H). It is important to bear in mind that these analyses were performed in a rather small glacierized region, with a very homogeneous climatic signal compared to many vast glacierized regions like High Mountain Asia or the Andes. The greater the climatic differences, the more complex the climate forcings on glacier MB, thus improving the chances of increased nonlinear responses. This implies that in large glacierized regions with highly heterogeneous topographical and climatic characteristics, glaciers are more likely to go through a higher variety of climate extremes, forcing MB models to operate more often outside the values observed during calibration. Therefore, the benefits of a nonlinear representation of glacier MB might be even greater than the ones found in this study area for many larger glacierized regions.

The main uncertainties in future glacier estimates proceed in a first term from future climate projections and levels of greenhouse gases emissions (differences between GCMs, RCMs and RCPs), whose relative importance progressively increases throughout the 21^{st} century. In a second term, glacier model uncertainty decreases over time, but it represents the greatest source of uncertainty until the middle of the century (Marzeion et al., 2020). Taking into account that for several regions in the world about half of the glacierized volume will be lost during this first half of the century, glacier models play a major role in the correct assessment of future glacier evolution. The two recent iterations of the Glacier Model Intercomparison Project (GlacierMIP Hock et al., 2019a; Marzeion et al., 2020) have proved a remarkable effort to aggregate, compare and understand global glacier evolution estimates and their associated uncertainties. Despite a wide variety of different approaches to simulate glacier dynamics, all glacier models in GlacierMIP rely on linear MB models. In this study, we have shown the effects of nonlinearities found in the relationships between air temperature (PDDs), solid precipitation and glacier MB used by most of these models. By unravelling nonlinear relationships between climate and glacier MB, we have demonstrated the limitations of linear MB models to represent extreme MB rates in long-term projections. Despite having focused this study on one single glacierized region, the French Alps, we argue that these behaviours observed in our data can potentially be transposed to many other glacierized regions in the world with even more enhanced consequences. Uncertainties on future projections of glacier evolution are already great for the second half of the 21^{st} century due to the effects of current greenhouse gases emissions on the future climate. Our results indicate that these uncertainties might be even greater than we previously thought, as linear models might introduce important biases under the extreme climates of the late 21^{st} century. This could therefore have remarkable implications on projections of future worldwide glacier evolution, suggesting that current global glacier models might be potentially giving estimates of future sea-level rise that are too low for climate scenarios with the highest and lowest greenhouse gases emissions.

4.4 Materials and methods

4.4.1 Glacier mass balance modelling

Glacier-wide MB is simulated annually for individual glaciers using deep learning (i.e. deep artificial neural networks) or the Lasso (regularized multilinear regression) (Tibshirani, 1996). This modelling approach was described in detail in a previous publication dedicated to the methods, where the ALpine Parameterized Glacier Model (ALPGM) was presented (Bolibar et al., 2020c). A dataset of 32 glaciers with direct annual glacier-wide MB observations and remote sensing estimates was used to train the models. For these 32 glaciers, a total of 1048 annual glacier-wide MB values are available, covering the 1967-2015 period with some gaps. In order to simulate annual glacier-wide MB values, (a) topographical and (b) climate data for those glaciers and years were compiled for each of the 1048 glacier-year values. (a) Topographical predictors were computed based on the glaciers' annually updated digital elevation model (DEM). These predictors are composed of: the mean glacier altitude, maximum glacier altitude, slope of the lowermost 20% altitudinal range of the glacier, glacier surface area, latitude, longitude and aspect. (b) Climate predictors are based on climatic anomalies computed at the glaciers' mean altitude with respect to the 1967-2015 reference period mean values. Models were trained using the SAFRAN reanalysis dataset (Durand et al., 2009), including observations of mountain regions in France for the 1950-2015 period. This reanalysis is specifically designed to represent climate over complex mountain terrain, being divided by mountain massif, aspect and altitudinal bands of 300 m. Winter climate data are computed between October 1 and March 31, and summer data between April 1 and September 30. Climate predictors consist of: the annual CPDD, winter snowfall, summer snowfall, monthly temperature and monthly snowfall. This creates a total of 34 input predictors for each year (7 topographical, 3 seasonal climate and 24 monthly climate predictors).

In order to avoid overfitting, models were thoroughly cross-validated using all data for the 1967-2015 period in order to ensure a correct out-of-sample performance. Three different types of cross validation were performed: a Leave-One-Glacier-Out (LOGO), a Leave-One-Year-Out (LOYO) and a Leave-Some-Years-and-Glaciers-Out (LSYGO). Each one of these cross-validations served to evaluate the model performance for the spatial, temporal and both dimensions respectively. When working with spatiotemporal data, it is imperative to respect spatial and temporal data structures during cross-validation in order to correctly assess an accurate model performance (Roberts et al., 2017). With this cross-validation we determined a deep learning MB model RMSE of 0.59 m.w.e. a^{-1} and a r2 of 0.69, explaining 69% of the total MB variance. Alternatively, the Lasso MB model displayed an RMSE of 0.85 m.w.e. a^{-1} and an r2 of 0.35 (Bolibar et al., 2020c). Simulations for projections in this study were made by generating an ensemble of 60 cross-validated models based on LSYGO. Each one of these models was created by training a deep learning model with the full dataset except all data from a random glacier and year, and evaluating the performance on these hidden values. This ensures that the model is capable of reproducing MB rates for unseen glaciers and years. Simulations were then performed by averaging the outputs of each one of the 60 ensemble members. This approach is known as a cross-validation ensemble (Hastie et al., 2009). Future projections of glacier-wide MB evolution were then performed using climate projections from ADAMONT (Verfaillie et al., 2017). This dataset applies the same statistical adjustment specific to mountain regions from the SAFRAN dataset to EURO-CORDEX (Smiatek et al., 2016) GCM-RCM-RCP members, covering a total of 29 different future climate scenarios for the 2005-2100 period. This represents a major improvement over most climate data used to force regional and glacier models. The high spatial resolution enables a detailed representation of mountain weather patterns, which are often undermined by coarser resolution climate datasets.

4.4.2 Glacier geometry evolution

A well established parametrization based on empirical functions (Huss et al., 2010) was used in order to redistribute the annually simulated glacier-wide mass changes over each glacier. This parametrization reproduces in an empirical manner the ice dynamics of glaciers. As for the MB modelling approach, a detailed explanation on this method can be found in a previous dedicated paper on the methods (Bolibar et al., 2020c). In our model, we specifically computed this parameterized function for each individual glacier larger than 0.5 km^2, representing 80% of the total glacierized area in 2015, using two DEMs covering the whole French Alps: a photogrammetric one in 1979 and a SPOT-5 one in 2011. We previously demonstrated that this period is long enough to represent the secular trend of glacier dynamics in the region. Both DEMs were resampled and aligned at a common spatial resolution of 25 m. For each glacier, an individual parameterized function was computed representing the differences in glacier surface elevation with respect to the glacier's altitude between the 1979-2011 period. This method has the advantage of including glacier-specific dynamics in the model, encompassing a wide range of different glacier behaviours. Glaciers smaller than 0.5 km^2 often display a high climate imbalance, with their equilibrium line being higher than the glacier's maximum altitude. Such glaciers are often remnants of the Little Ice Age, and mainly lose mass via non-dynamic downwasting (Paul et al., 2004). For such cases, we assumed that ice dynamics no longer play an important role, and the mass changes were applied equally throughout the glacier. With this, the glacier-specific ice thickness (Farinotti et al., 2019a) and the DEM are updated every year, adjusting the 3D geometry of each glacier. This enables the recalculation of every topographical predictor used for the MB model, thus changing the mean glacier altitude at which climate data for each glacier is retrieved. This annual geometry adjustment accounts for the effects of glacier retreat on the climate signal received by glaciers.

The performance of this parametrization was validated in a previous study, indicating a correct agreement with observations (Bolibar et al., 2020c). The dataset of initial glacier ice thickness, available for the year 2003, determines the starting point of our simulations. We performed a validation simulation for the 2003-2015 period by running our model through this period and comparing the simulated glacier surface area of each of the 32 glaciers with MB to observations from the 2015 glacier inventory (Gardent et al., 2014). Then, we ran multiple simulations for this same period by altering the initial ice thickness by ±30% and the glacier geometry update parametrizations by ±10%, according to the estimated uncertainties of each of the two methods. These results revealed that the main uncertainties on glacier simulations arise from the initial ice thickness used to initialize the model. This is well in agreement with the known uncertainties of glacier evolution models, with glacier ice thickness being the second largest uncertainty after the future GCM-RCM-RCP climate members used to force the model (Huss and Hock, 2015). Glacier ice thickness observations are available for four different glaciers in the regions, which were compared to the estimates used in this model. Ice thickness accuracy varied significantly, with an overall correct representation of the ice distribution but with local biases reaching up to 100%. The ice thickness data for two of the largest glaciers in the French Alps were modified in order to improve data quality. Ice thickness data for Argentière glacier (12.27 km^2 in 2015) was taken from a combination of field observations including seismic, ground-penetrating radar or how-water drilling (Rabatel et al., 2018), and simulations (Farinotti et al., 2019a). The estimated ice thickness for Mer de Glace (28.87 km^2 in 2015) was increased by 25% in order to correct the bias with respect to field observations (Bolibar et al., 2020c). Since these two glaciers are expected to be some of the few large glaciers that will survive the 21^{st} century climate, an accurate representation of their initial ice thickness has an important effect on the estimates of remaining ice.

4.4.3 Model comparison and extraction of nonlinearities

The nonlinearities present in the simulated annual glacier-wide MB values were captured by running two different glacier simulations with two different MB models. The advantage of this method is that by only changing the MB model, we can keep the rest of the model components and parameters the same in order to have a controlled environment for our experiment. Therefore, we were capable of isolating the different behaviours of the nonlinear deep learning model and a linear machine learning model based on the Lasso. Both machine learning MB models were trained with exactly the same data coming from the 1048 annual glacier-wide MB values, and both were cross-validated using LSYGO. Additionally, the specific responses of the deep learning and Lasso MB models to air temperature and snowfall were computed by performing a sensitivity analysis. A dataset of predictors covering all the glaciers in the French Alps for the 1967-2015 period was modified (Bolibar et al., 2020b), creating multiple copies of this dataset with specific CPDD and winter and summer snowfall anomalies for all glaciers. For each one of these copies, a specific CPDD anomaly ranging from -1500 PDD and +1500 PDD in steps of 100 PDD was prescribed to all glaciers. Since both MB models also include monthly temperature data, this PDD anomaly was distributed evenly between the ablation season (April 1 - September 30), following the expected increase of mostly summer temperatures instead of winter temperatures in the future (Fig. 4.1). Tests were performed distributing the PDD anomalies equally among all months of the year with very similar results. The same was done with winter snowfall anomalies, ranging between -1500 mm and +1500 mm in steps of 100 mm, and summer snowfall anomalies, ranging between -1000 mm and +1000 mm in steps of 100 mm. The anomaly in snowfall was evenly distributed for every month in the accumulation (October 1 - April 31) and ablation seasons respectively. This experiment enabled the exploration of the response to specific climate forcings of a wide range of glaciers of different topographical characteristics in a wide range of different climatic setups, determined by all meteorological conditions from the years 1967-2015.

Alternatively, the comparisons against an independent large-scale glacier evolution model were less straightforward to achieve. GloGEMflow (Zekollari et al., 2019) is a state-of-the-art global glacier evolution model used in a wide range of studies, including the two first phases of GlacierMIP (Hock et al., 2019a; Marzeion et al., 2020). Several differences are present between ALPGM, the model used in this study, and GloGEMflow (Table S2), that hinder a direct meaningful comparison between both. In order to overcome these differences, some adaptations were performed to GloGEMflow, accompanied with some hypotheses to ensure a realistic comparison. The first main difference is related to the climate data used to force the models. GloGEMflow relies on EURO-CORDEX ensembles (Smiatek et al., 2016), whereas ALPGM uses ADAMONT (Verfaillie et al., 2017), an adjusted version of EURO-CORDEX specifically designed for mountain regions. This implies that specific climatic differences between massifs can be better captured by ALPGM than GloGEMflow. Nonetheless, since the main GCM-RCM climate signal is the same, the main large-scale long-term trends are quite similar. We reduced these differences by running simulations with GloGEMflow using exactly the same 29 climate members used by ALPGM in this study (Table S1). The initial glacier ice thickness data for the year 2003 also differs slightly between both models. The original estimates of the methods used by both models are different (Huss and Farinotti, 2012; Farinotti et al., 2019a), and we performed some additional modifications to the two largest glaciers in the French Alps in order to improve the accuracy of the data based on field observations. Despite these differences, we do not expect them to drive important differences between models, since the average altitude difference between both models is generally never greater than 50 m (Fig. 4.14). Only during the last decade of the 21st century under RCP 8.5 this differences approach 90 m, as glaciers in GloGEMflow almost completely disappear. Since in ALPGM the climate forc-

ing of glaciers is taken at the mean glacier altitude, the observed MB differences between both models mostly arise from different model responses rather than different climate forcings. Another source of discrepancy between both models comes from the different MB data used to calibrate or train the MB models. GloGEMflow has been previously applied in a study over the whole European Alps, and its temperature-index model was mainly calibrated with MB data from the Swiss Alps. Swiss glaciers have displayed less negative MB rates than French glaciers during the last decades, thus likely introducing a cold bias in simulations specific to the French Alps. In order to improve the comparability between both models, a MB bias correction was applied to GloGEMflow's simulated MB, based on the average annual MB difference between both models for the 2003-2015 period (0.4 m.w.e. a^{-1}). Finally, there are differences as well in the glacier dynamics of both models, with ALPGM using a glacier-specific parameterized approach and GloGEMflow explicitly reproducing the ice flow dynamics. Nonetheless, these differences have been shown to be rather small, having a lower impact on results than climate forcings or the initial glacier ice thickness (Zekollari et al., 2019).

4.4.4 Statistical analysis

The statistical analysis on the main factors determining glacier survival in the French Alps was performed via a classic least-squares linear regression with the Statsmodels Python library (Seabold and Perktold, 2010). A linear model was fitted based on the main topographical characteristics of glaciers, including the maximum glacier altitude, the average glacier slope throughout the century, and latitude and longitude. These predictors were fitted to predict the ice volume fraction by 2100 for each glacier, computed as the ice volume in 2100 divided by the ice volume in 2015. Results were determined by extracting the coefficients given to each of the predictors, enabling the computation of the importance and contribution of each one of them. P values served to determine if predictors were significant or not, providing the degree of trust in the results.

4.5 Supplementary material

4.5.1 Supplementary figures

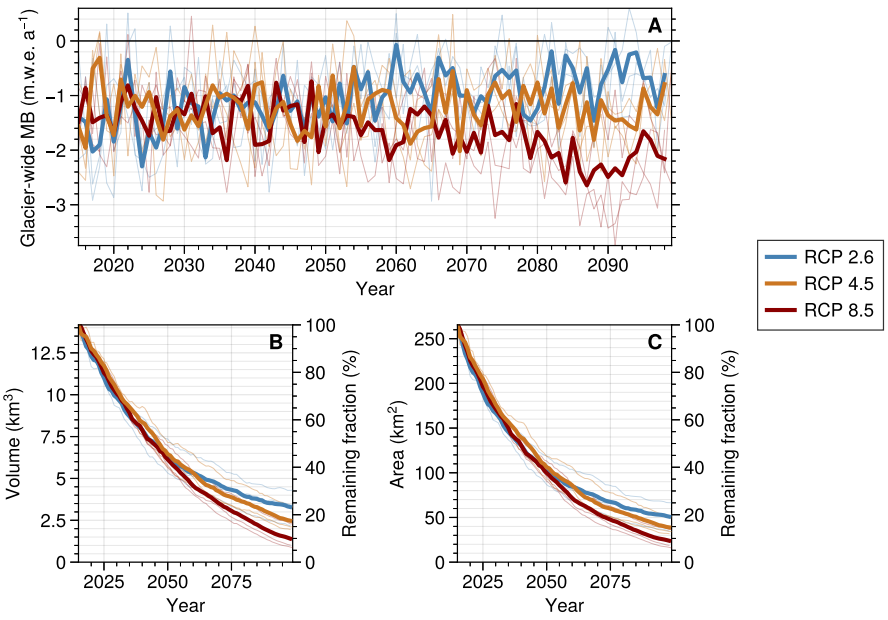

Figure 4.7: Glacier-wide MB, volume and area evolution of French Alpine glaciers through the 21st century for climate members including RCP 2.6. Glacier-wide MB (A), ice volume (B) and surface area (C) projections under RCP 2.6, 4.5 and 8.5

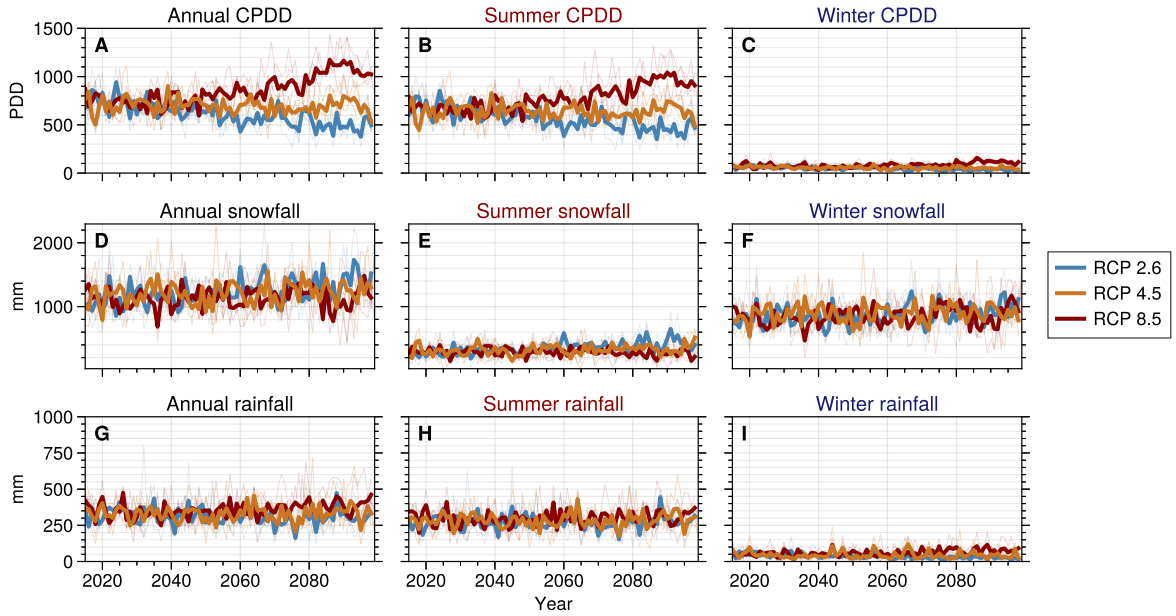

Figure 4.8: Climate signal over glaciers in the French Alps for climate members including RCP 2.6. The average climate signal, computed at the glacier's annually evolving centroid, displays the average climate forcing on glaciers taking into account glacier geometry change. Summer climate is computed between April 1st and September 30th and winter climate between October 1st and March 31st.

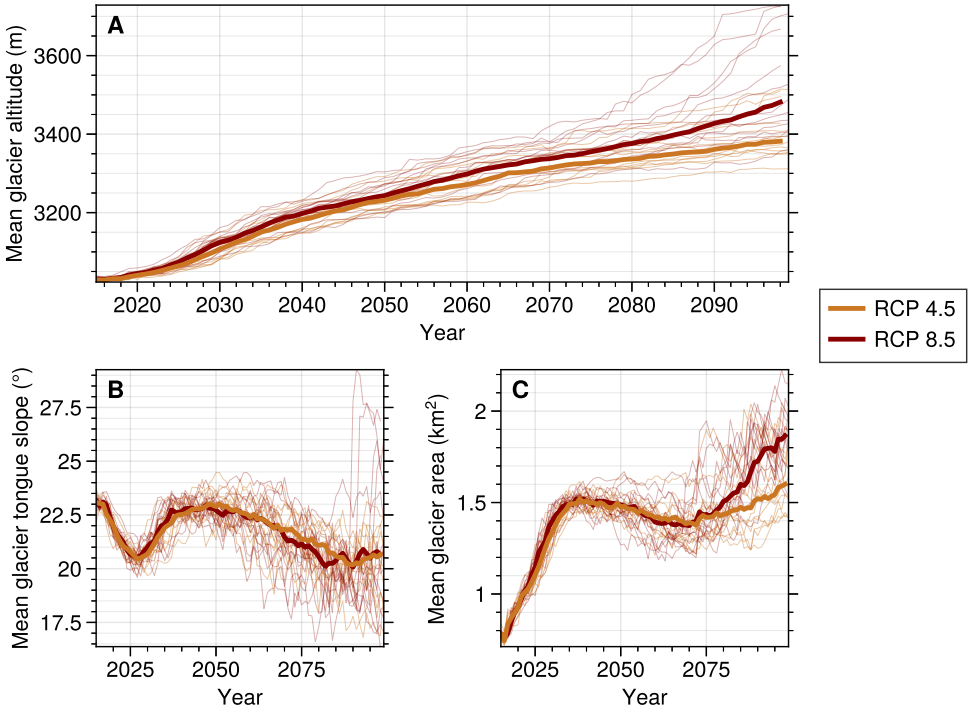

Figure 4.9: Projections of glacier topographical characteristics. (A) Mean glacier altitude projections, (B) Mean slope of the lowermost 20% altitudinal range of glaciers, as a proxy of the glacier's tongue slope, (C) Mean glacier surface area projections.

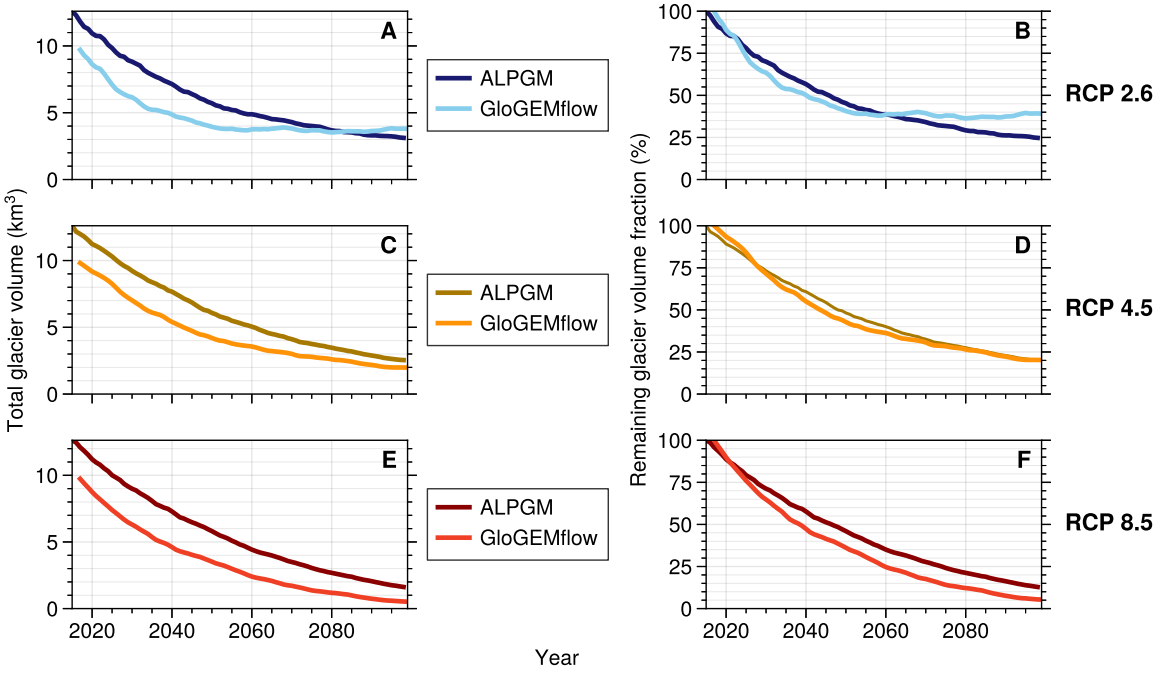

Figure 4.10: Comparison of total ice volume projections between nonlinear and linear models. Comparison of the total ice volume projections (A, C, E) and remaining total ice volume fraction (B, D, F) between the ALPGM (nonlinear, this study) and GloGEMflow (linear) glacier evolution models in the French Alps.

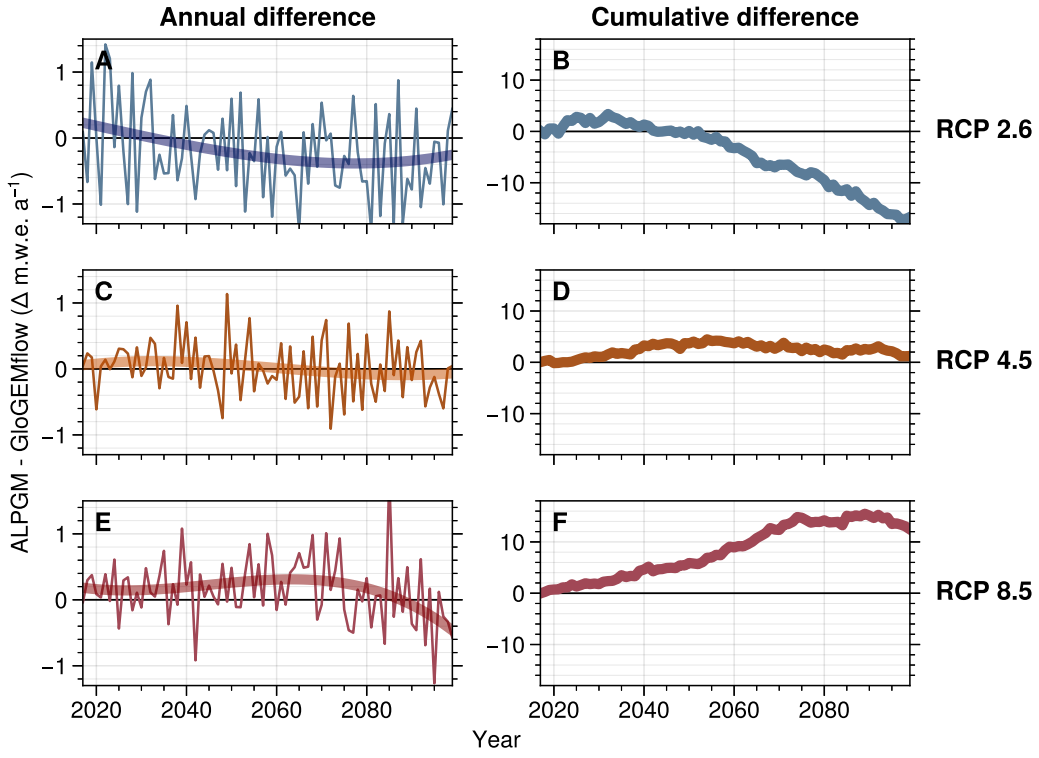

Figure 4.11: Effects of deep learning nonlinearities compared to another linear glacier model. Difference in average annual glacier-wide MB between the ALPGM (nonlinear, this study) and GloGEMflow (linear) glacier evolution models. MB data from GloGEMflow have been corrected by adding a bias computed between ALPGM and GloGEMflow for the 2003-2015 period to improve comparability.

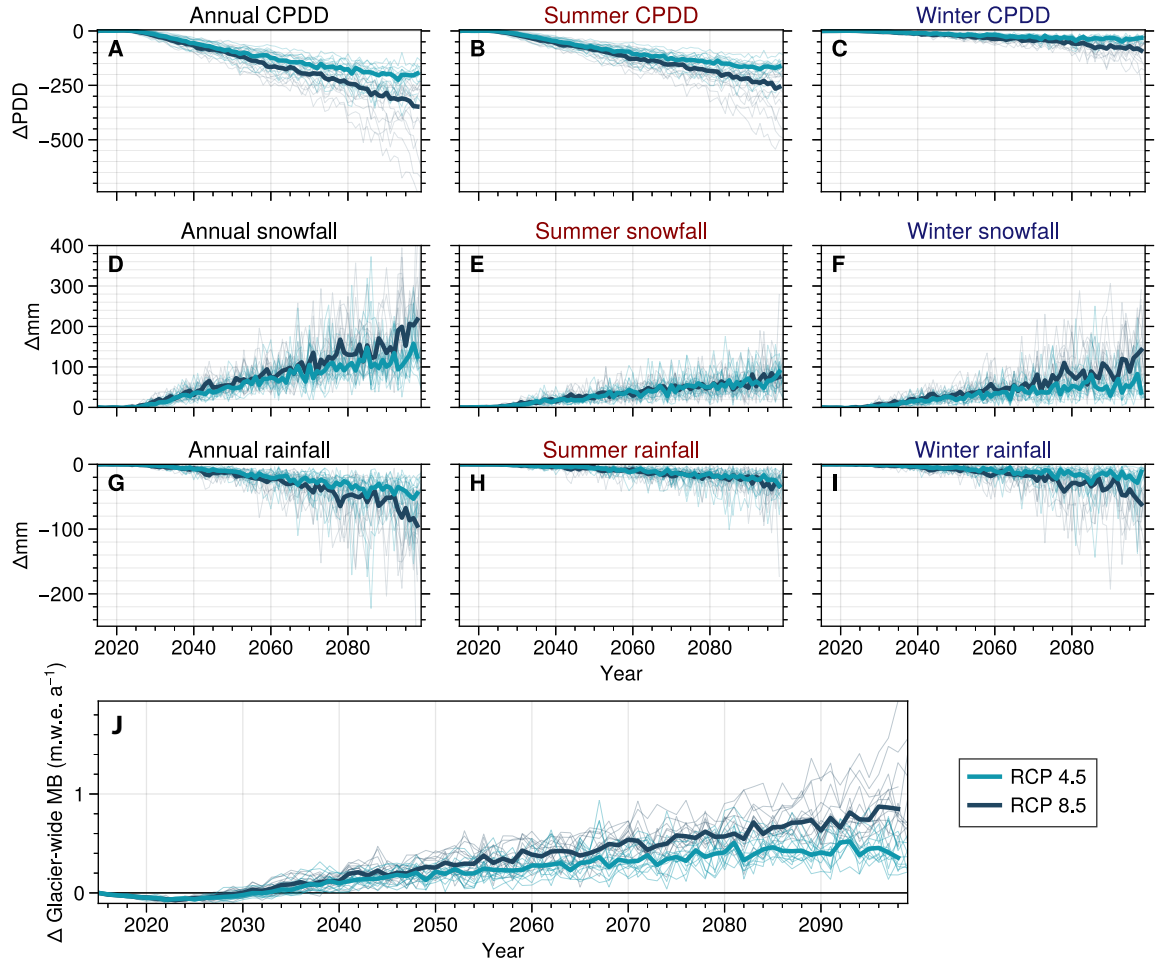

Figure 4.12: Glacier retreat effects on the climate signal of glaciers. Computed as the difference between model runs with glacier dynamics and model runs without glacier dynamics (i.e. static glaciers). Glaciers adjusting their geometry by shrinking to higher altitudes modify their received climate signal (A-I). These changes in the received climate help mitigate their mass losses, in an effort to reach equilibrium with the present climate (J).

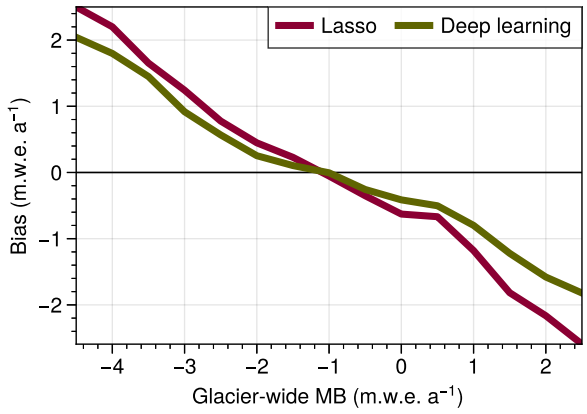

Figure 4.13: Glacier-wide MB bias for the Lasso and deep learning models. Average annual glacier-wide MB bias for the Lasso and deep learning MB models. Values computed using LSYGO cross-validation, based on data for the 1967-2015 period.

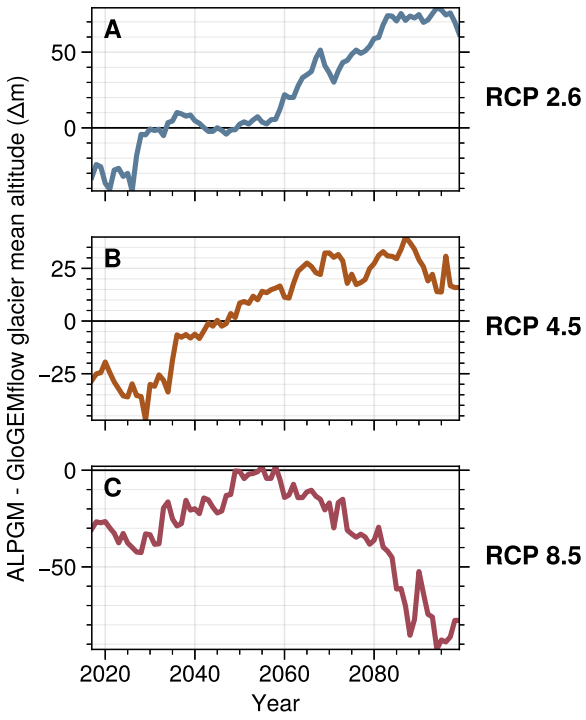

Figure 4.14: Mean glacier altitude difference between ALPGM and GloGEMflow. Mean annual glacier altitude difference between ALPGM (this study) and GloGEMflow for (A) RCP 2.6, (B) RCP 4.5 and (C) RCP 8.5.

4.5.2 Supplementary tables

ADAMONT climate projections member	Available RCPs
CLMcom-CCLM4-8-17_CNRM-CERFACS-CNRM-CM5	RCP 4.5 / RCP 8.5
CLMcom-CCLM4-8-17_ICHEC-EC-EARTH	RCP 4.5 / RCP 8.5
CLMcom-CCLM4-8-17_MOHC-HadGEM2-ES	RCP 4.5 / RCP 8.5
CLMcom-CCLM4-8-17_MPI-M-MPI-ESM-LR	RCP 4.5 / RCP 8.5
DMI-HIRHAM5_NCC-NorESM1-MR	RCP 4.5 / RCP 8.5
IPSL-INERIS-WRF331F_IPSL-IPSL-CM5A-MR	RCP 4.5 / RCP 8.5
KNMI-RACMO22E_MOHC-HadGEM2-ES	RCP 2.6 / RCP 4.5 / RCP 8.5
MPI-CSC-REMO2009_MPI-M-MPI-ESM-LR	RCP 2.6 / RCP 4.5 / RCP 8.5
SMHI-RCA4_CNRM-CERFACS-CNRM-CM5	RCP 4.5 / RCP 8.5
SMHI-RCA4_ICHEC-EC-EARTH	RCP 2.6 / RCP 4.5 / RCP 8.5
SMHI-RCA4_IPSL-IPSL-CM5A-MR	RCP 4.5 / RCP 8.5
SMHI-RCA4_MOHC-HadGEM2-ES	RCP 4.5 / RCP 8.5
SMHI-RCA4_MPI-M-MPI-ESM-LR	RCP 4.5 / RCP 8.5

Table 4.1: List of the 29 climate members used to force the glacier evolution model. Climate members are composed by a combination of GCM-RCM-RCP. Since only three members include RCP 2.6, separate analyses have been performed using only these members in order to have comparable climate variabilities.

	This study	**Zekollari et al. (2020)**
MB component	Deep learning	Accumulation and temperature-index melt model
Glacier dynamics component	Glacier-specific parametrizations for glaciers > 0.5 km^2 (h method). Equal loss distributed over all glacier altitudes for glaciers < 0.5 km^2, representing non-dynamic downwasting.	Ice flow dynamics based on shallow ice approximation along the flowline (for glaciers > 1 km) and three generalized retreat parameterizations based on h method (for glaciers < 1 km)
MB calibration data	1048 values of annual glacier-wide MB from glaciological observations and remote sensing estimates for the French Alps	Calibration based on geodetic mass balances, covering 38% of all glaciers in the European Alps (mainly in Switzerland), correspond to about 60% of the total glacier area.
Climate projection forcings	High-resolution (300 m altitude bands divided by massifs) mountain-adjusted climate forcings with 13 GCM-RCM member combinations	EURO-CORDEX ensemble at 0.11° resolution
Glacie ice thickness	Farinotti et al. (2019) + field measurements	Huss and Farinotti (2012)

Table 4.2: Comparison of glacier evolution models characteristics. Differences between the glacier model used in this study (ALPGM) vs the glacier model used in Zekollari et al., 2019 (GloGEMflow).

Part II

Glacierized mountain catchments

Chapter 5

Glacio-hydrological modelling of glacierized mountain catchments

Water is the driver of nature.
Leonardo da Vinci

Preface

This second part of the manuscript is driven by the BERGER project, in which my PhD project is integrated, combining the glacio-hydrological modelling efforts presented here with an ecological study on the impacts of glacier retreat on aquatic communities and their adaptation in the French Alps. An unexpected shift in the initial objectives of this PhD project resulted in a lengthy investigation of machine learning methods applied to glacier evolution modelling, which impacted the initial plans for glacio-hydrological modelling. Efforts for this part of the PhD work have been focused on the technical implementation and validation of a novel glacier component for a hydrological model: J2K (Krause, 2002). With this implementation, we are providing a proof-of-concept of hydrological modelling with dynamic glacier surfaces in J2K over a well-documented, high-altitude alpine catchment, and the technical means for an application on glacio-hydrological studies at a regional scale in the French Alps. This work has been done with the help of Sven Kralisch from the University of Jena (Germany). His expertise on the hydrological model used in this study has greatly helped to accelerate the development of the updated glacier module in the last months of this project.

5.1 Introduction

Glaciers supply water that supports ecosystems and human communities both nearby and far away from glaciers (IPCC, 2018). The strong climatic diversity of glacierized alpine catchments enables the storage of precipitation in the form of snow and ice at high altitudes. In the European Alps, this water storage is progressively released throughout the year during the warmest months, providing a baseflow that cannot be encountered in non-glacierized catchments. At the beginning of the melt season, snow provides important water resources downstream. Once most of the snow has melted, leaving bare glacier ice exposed, glaciers continue providing freshwater resources, ensuring an uninterrupted runoff throughout the melt season (Huss et al., 2017). In one of the few existing glacio-hydrological

studies in the French Alps, Lafaysse et al. (2011) estimated that melt water from glaciers contributed to 20% of the August discharge of the Durance at Serre Ponçon catchment (3500 km^2). According to Huss (2011) in a study using a simple routing of glacier discharge, glaciers contributed to 25% of the summer low flow of the Rhone river (about 100000 km^2 in catchment size), with an even enhanced contribution during the 2003 drought. This role of glaciers as late summer buffers is currently being challenged by anthropogenic climate change. Glacier retreat in the European Alps is progressively transforming the hydrological regime of high-mountain catchments, with potential environmental and social impacts (Zekollari et al., 2019). In the French Alps, the local population have a strong dependency on water resources, using them for agriculture, hydropower generation and domestic use. The regional socioeconomic model of many alpine valleys is built around mountain tourism, with a strong dependency on the cryosphere, both as a tourism attraction (Schut, 2013; Spandre et al., 2019) and as an electricity generation source (Schaefli et al., 2019). Moreover, late summer runoff from glaciers provides reliable water resources for domestic use, industries and agriculture. The decrease in glacier freshwater contributions has ecological impacts as well, affecting biodiversity in glacier-fed rivers (Cauvy-Fraunié and Dangles, 2019) and in humid areas that no longer receive runoff during the warmest period of the year (Carlson et al., 2020). Glaciers provide cold water resources that help regulate the temperature, flow regimes, sediment concentration and nutrient supply of mountain streams (Huss et al., 2017). These cold waters are essential to some specialized species, whose survival will be challenged by glacier retreat (Lencioni, 2018; Cauvy-Fraunié and Dangles, 2019). Alternatively, these changing streams can be quickly colonized by aquatic communities adapted to higher water temperatures, increasing competition between species (Robinson et al., 2014). Anticipating these future hydrological changes is of paramount importance in order to correctly adapt and manage future water social and environmental needs.

Hydrological models can provide answers to these questions, predicting the hydrological evolution under different future climate scenarios. In France, multiple hydrological models are being developed and used for research and operational purposes. At one end of the spectrum of model complexity, the lumped GR rainfall-runoff models, with the CemaNeige snow component (Coron et al., 2017), use a simplified modelling approach with catchment-scale representations of the transformation of precipitation into discharge. They rely on the calibration of 1 to 6 parameters (depending on the model variant and time-step), and do not include a glacier component. This limits their usability in high-altitude, upstream catchments where observational data for calibration is scarce and glaciers may play an important role. At the other end of the complexity spectrum, the physics-based SIM (SAFRAN-ISBA-MODCOU) model combines a meteorological analysis system (SAFRAN), with a land surface model (ISBA) and a hydrogeological model (MODCOU) developed by the Mines de Paris (Habets et al., 2008). For research purposes, it has been adapted to alpine areas by incorporating elevation bands, aspect classes, and glacier melt and retention of underground water (Lafaysse et al., 2011). However its adaptation and deployment over the entire French alpine region, including glacierized areas, is highly demanding (e.g. Lecourt, 2018) and has not been considered yet. For more operational applications, the reservoir-based MORDOR model (Paquet, 2004), developed by Électricité de France (EDF), has a more intermediate complexity. It is actively used to forecast runoff in mountain catchments in France and to anticipate changes in hydropower production, both for short and long term periods. However this model is not open to applications outside the scope of EDF operational and research objectives. Finally, The GSM-Socont model (Schaefli et al., 2005), a Swiss semi-distributed glacio-hydrological model, has been recently applied to perform projections of the Arve watershed in the Mont-Blanc massif through the $21st$ century (Laurent et al., 2020). Out of all these models, only the GSM-Socont model includes a dynamic representation of glaciers, and Laurent et al. (2020) is the

first study of this kind in a French glacierized catchment. The vast majority of hydrological models deployed in France have none, or a very simplified representation of glaciers, including them as static ice reservoirs. Some models do have such glacier modules, but they are not activated due to a lack of data to calibrate and validate them. Such a representation is problematic in the current context of glacier retreat, neglecting future changes in hydrological regimes driven by glaciers.

This static representation of glaciers is also found in the J2K hydrological model (Krause, 2002), developed at the University of Jena (Germany). J2K is a distributed open-source model, based on Hydrological Response Units (HRUs), homogeneous spatial units in terms of hydrological processes. It allows the representation of multiple physical processes, land use covers, pedology, geology and topography. Moreover, the representation of multiple anthropogenic water uses, such as agriculture irrigation or reservoir management dams can be taken into account in the model. J2K is being used by a large community of hydrologists, both in France and internationally, for a wide variety of geographical configurations (Krause, 2002; Nepal et al., 2014; Braud et al., 2017). J2K has already been applied to glacierized catchments in the Himalayas (Nepal et al., 2014), but simulations have only been performed for past periods, keeping the glacier surface area constant in time. In this chapter, I present an updated glacier module for J2K, including a dynamic representation of glaciers. We introduce and validate this new implementation in a partially-glacierized (4.5 % in 2003) alpine catchment in the French Alps: the Arvan catchment in the Grandes Rousses massif. By introducing glacier evolution in a distributed hydrological model, we aim at improving hydrological simulations and discharge projections out of glacierized catchments, in support of diverse applications but primarily to assess the impacts of changes in glacier discharge on aquatic communities living in glacier-fed streams. Such an application requires a distributed hydrological model able to provide discharge information on upstream sub-catchments.

5.2 Methods

5.2.1 Study area

The Arvan catchment (58.8 km^2, Fig. 5.1) is a partially glacierized alpine catchment, located in the Grandes Rousses massif, between 1368 and 3373 m a.s.l. It includes the Saint-Sorlin Glacier (2.069 km^2 in 2015, 3.5% of glacial coverage at catchment scale), being the glacier with the second longest mass balance observation series in France (1957-present). Two villages are located within the catchment: Saint-Sorlin-d'Arves and Saint-Jean-d'Arves, with the latter including water flow measurements for the 2000-2016 period. This study site has been chosen due to its wealth of glaciological, meteorological and hydro-biological data, providing an adequate testbed to validate the modelling approach within the context of the BERGER project.

5.2.2 Data

This work has been implemented in a version of J2K dedicated to the Rhône river catchment, situated in France and Switzerland. Therefore, most of the datasets used (except the climate data which only cover France) have a full coverage of this geographical region.

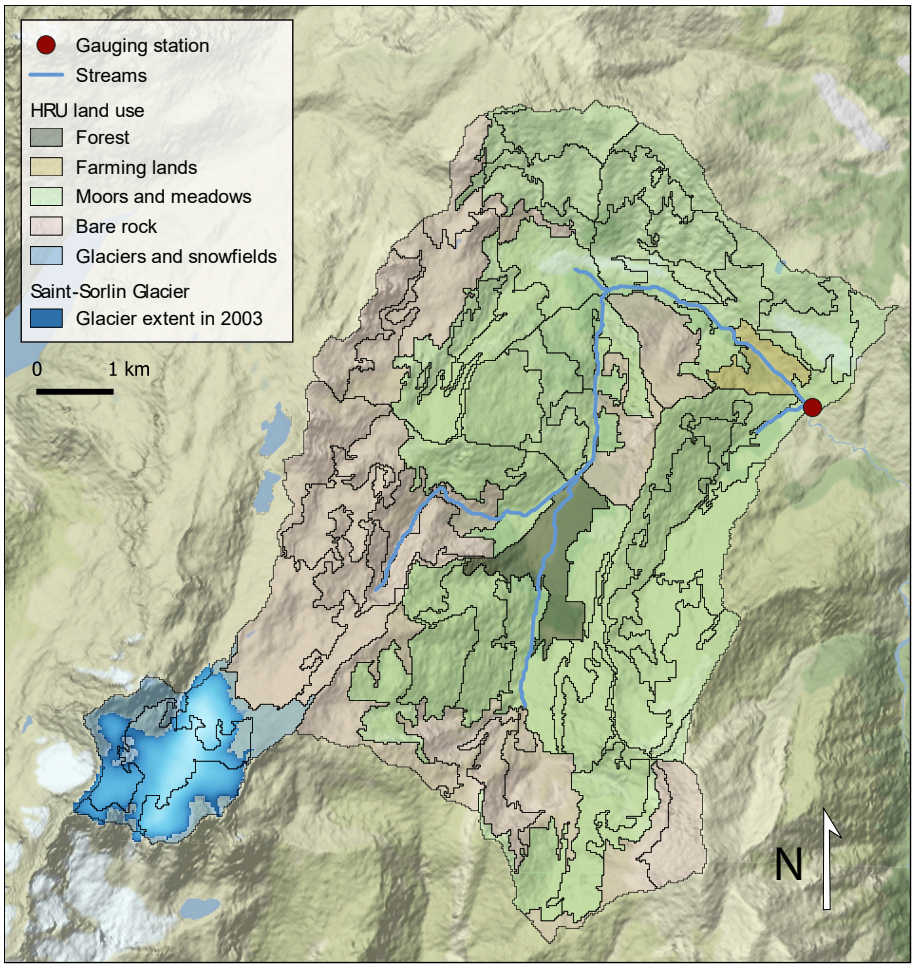

Figure 5.1: The Arvan catchment at Saint-Jean d'Arves, with its division into HRUs and their main land use.

Climate

The J2K hydrological model is forced with climate data coming from SPAZM (Gottardi et al., 2012). SPAZM is a statistical method to interpolate meteorological data, particularly precipitation, in mountain areas. This interpolation has been applied on French mountainous regions, based on an observational network, taking into account the local orography and the main atmospheric patterns bringing precipitation. With a resolution of 1 km^2, this dataset is well adapted to representing the complex meteorological conditions of a glacierized alpine catchment. Temperature and precipitation are available from the year 1953 until the end of the year 2012, which suit the needs of J2K.

Land cover

Land cover use is determined by the Corine Land Cover 2006 (CLC2006) European database. It has a minimum vectorial detail of 25 ha and it takes into account a maximum of 44 different land cover uses. Land use data is used to determine certain variables in different hydrological processes, such as the surface albedo or the leaf area index.

Pedology

Pedology information is used to estimate the size of the superficial soil reservoirs in the model. The following databases have been used to describe pedology: The Soil European Database, providing soil

thickness data; and the ECOCLIMAP database, with a 1 km resolution, describing soil texture. The representation of these superficial soil reservoirs is based on Sauquet et al. (2014), adapted for mountain territories.

Geology

Geology data is taken from the Bureau des Recherches Géologiques et Minières (BRGM) dataset, grouped in eight different classes, five of which are dominant in the French Alps: fluvioglacial deposits, shale and metamorphic rocks, detrital rocks, limestone and marls. In J2K, geology is used to determine the size and time to empty the deep ground reservoirs.

Hydrology

Hydrological observations at the Saint-Jean-d'Arves station (Fig. 5.1), are available with a daily frequency for the 2000-2016 period. This data is compiled as part of DREAL Rhône-Alpes's database of hydrological observations (Brigode et al., 2020). This station measured an average interannual flow of 1.8 m^3/s, with 10% of temporal gaps for this period and a low reliability of winter measurements. During winter, ice forms in the river, altering the measured water altitude, and in autumn strong rains can often carry large rocks which alter the measured river section. This introduces time gaps or artefacts in the observations, reducing their reliability for certain periods.

Glaciology

Several different datasets are available for the Saint-Sorlin Glacier. Seasonal (winter and summer) point MB data from the GLACIOCLIM French national observatory are available at 30 different points since 1995. Glacier-wide MB observations, performed every year in September, cover the 1957-2019 period. Seasonal glacier-wide MB data were computed specifically for the 2000-2010 period (Davaze et al., 2018). Glacierized surface areas for this glacier proceed from the results of model simulations using the ALPGM model, introduced in Chapter 2.

5.2.3 The J2K hydrological model

J2K is an open-source hydrological model coded in Java. It is structured in Hydrological Response Units (HRUs), irregular spatial divisions representing homogeneous conditions from a hydrological point of view. HRUs are determined by a combination of different spatial data, such as the surface slope, altitudes from a DEM, vegetation cover, geology and the distribution of sub-catchments. For the J2K model version used in our study, HRUs are determined by taking into account the sub-catchments with control gauging stations from the hydrological network of observations. These control points are used for model calibration and validation, enabling a comparison of model simulations with observations. The automatic generation of HRUs is performed with a special tool named HRU-delin, providing the modelling structure for any given catchment with the required data. The physical characteristics of each HRU are stored in specific files, which are used by the model to simulate different hydrological processes.

Simulations are performed in two nested loops, a first one iterating every timestep (days in most cases), and another one iterating in space (HRUs). Total precipitation can be partially intercepted by vegetation, whose remaining fraction that reaches the ground will be further divided into infiltrated and surface runoff (RD1) fractions. Infiltrated water will first fill a Large Pore Space (LPS) reservoir,

which can then be transferred towards a Medium Pore Space (MPS) reservoir (Fig. 5.2). Evapotranspiration (ET) is mainly retrieved from water intercepted by vegetation and water available in the MPS reservoir. It is computed on vegetation following the Penman-Monteith reference potential evapotranspiration (Howell and Evett, 2004). J2K allows ground water to form subsurface runoff (RD2) if the surface slope is steep enough or the substrate has low infiltration. The remaining fraction is assumed to percolate towards a deep reservoir (RG1). The simulated total water flow within an HRU is equivalent to the sum of the runoff, the subsurface flow and a slow flow from the deep reservoir. Water flow is routed among HRUs via streams if the HRU is located on a valley bed. Conversely, HRUs not containing a water stream route their water flow towards neighbouring HRUs using a simplified kinematic wave method (Chen, 1970). Every type of water storage (e.g. RD1, RD2) from each HRU is routed separately until reaching the catchment's outlet.

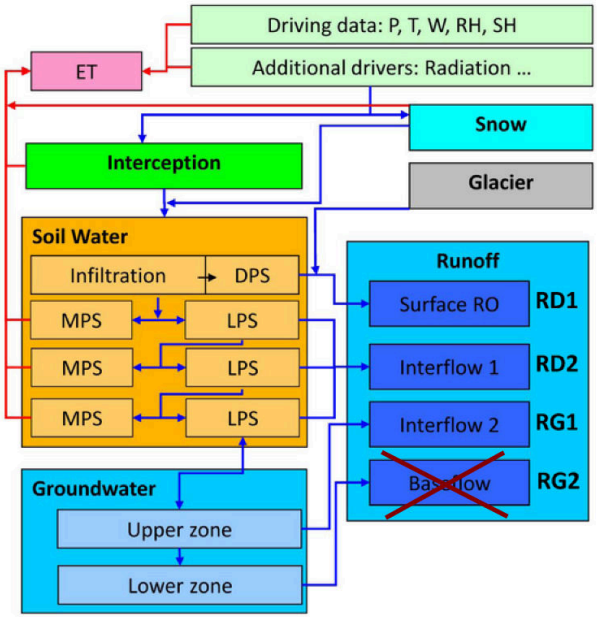

Figure 5.2: Workflow of the J2K hydrological model. *Taken from the J2K documentation.*

J2K establishes a simulation workflow using temporal (HRU-Loop) and spatial (Time-Loop) contexts, which iterate and perform simulations for each HRU and day of a given catchment and time period. These contexts are implemented in the Jena Adaptable Modelling System (JAMS) platform, in which J2K is integrated. The simulation of specific hydrological processes are performed in components, being separate entities taking a given set of input parameters, processing them and returning multiple output parameters. J2K includes a great number of these components, which are often independently developed by researchers from different groups. In this chapter we will only explain and detail the components that have been directly updated for this work.

5.2.4 Existing glacier module

The previously existing glacier module developed for the Himalayas is based on a snow processing component and a glacier MB component. In our case study, we used the snow processing component from the Rhône version of J2K (also used over the ice-free parts of the catchement), combined with the glacier MB component from the Himalayas version of the model (Nepal et al., 2014).

In order to compute the glacier MB and the resulting runoff, the snowpack on the glacier is first

processed with the snow component, determining the characteristics of snow on the glacier. This component simulates the accumulation and melt of the snowpack caused by air temperature or rain. The thermal characteristics of the snowpack are also taken into account by means of a cold content. Here, we show only the most relevant equations, as these processes were already available in J2K prior to this PhD work.

Accumulation and melt are computed based on the following temperature (Eq. 5.1).

$$T_{acc} = T_{melt} = \frac{T_{min} + T_{max}}{2} \tag{5.1}$$

If T_{melt} exceeds a certain threshold value (here chosen to be 0°C) the snowpack transitions from accumulation phase to melt. The amount of energy available for melt is computed with a daily timestep via a degree-day approach (with α_{snow} as daily degree-day factor), where the advected energy from the rain is also accounted for. The sum of these two components gives the potential snow melt rate (M_p, in mm), defined by equation 5.2.

$$M_p = \alpha_{snow} \cdot T_{melt} + r_{factor} \cdot rain \cdot T_{melt} \tag{5.2}$$

In this equation r_{factor} can be calculated based on heat capacity and latent heat of fusion , under the hypothesis that rain water is at air temperature prior to warming and melting the snowpack, resulting in an $r_{factor} = 0.0125$ °C^{-1}.

Density and snow height are diagnosed from the snow water equivalent (SWE) based on initial snow density (taken as 300 kg/m^3) and accounting for melt and settlement processes due to rain-on-snow, according to Bertle (1966). The snowpack can store liquid water in its pores up to a certain critical density. When a certain amount of liquid water is reached with respect to the total SWE (about 40-45%), rendering the density higher than a critical value $d_{crit} = 700$ kg m^{-3}, all liquid water in excess is immediately released. In addition, liquid water within a wet snowpack is also released as runoff at a slower pace, depending on the snowpack saturation degree. The water released from the snowpack (q_{snow}), in mm m^{-2}, is computed as the sum of these two contributions (Eq. 2.3).

$$q_{snow} = H \cdot max(d - d_{crit}, 0) + WC \cdot (1 - e^{(1-(d_{crit}/d)^4)}) \tag{5.3}$$

where d is the snowpack density, H the snow height and WC the snowpack liquid water content.

If no snow is present in a given glacierized HRU, ice melt can occur. This is computed using a temperature-index melt model (Hock, 2003), following equation 5.4.

$$q_{ice} = \alpha_{ice} \cdot (T_{melt} - T_{base}) \tag{5.4}$$

where α_{ice} is the melt factor specific for ice and T_{base} is a user-defined temperature beyond which melt is triggered, in our case 0°C.

This previously existing glacier module implemented in the Himalayas also takes into account the effects of debris cover, which will not be described here since they have not been used in this work.

Finally, rain runoff, snow melt and ice melt over the glacier are further adapted taking into account a storage and release time within the snowpack and glacier, respectively. This inertia is accounted

for by three calibration coefficients, k_{rain}, k_{snow} and k_{ice}. Here, we relied on calibration from previous studies to infer the value of these coefficients (k_{rain}=5, k_{snow}=5, k_{ice}=10). These updated runoff values are computed following equations 5.5, 5.6 and 5.7.

$$Q_{rain} = q_{rain(t-1)} \cdot (1 - e^{-(1/k_{rain})}) + q_{rain(t)} \cdot e^{-(1/k_{rain})} \tag{5.5}$$

$$Q_{snow} = q_{snow(t-1)} \cdot (1 - e^{-(1/k_{snow})}) + q_{snow(t)} \cdot e^{-(1/k_{snow})} \tag{5.6}$$

$$Q_{ice} = q_{ice(t-1)} \cdot (1 - e^{-(1/k_{ice})}) + q_{ice(t)} \cdot e^{-(1/k_{ice})} \tag{5.7}$$

where $q_{rain(t-1)}$ is the rain runoff from the previous timestep, $q_{snow(t-1)}$ is the snow water release from the previous timestep, $q_{ice(t-1)}$ the ice runoff from the previous timestep.

5.2.5 An updated glacier module

We updated the already existing glacier module from the J2K model version used in the Himalayas (Nepal et al., 2014), creating a new module named *GlacierModuleAlps*. Several components of J2K have been adapted in order to take into account these changes in glacier surface area.

Glacier dynamics

A Python package named *Glaciers-to-J2K* has been created, which automatically computes the glacierized fraction of each HRU based on polygons with the extension and surface type of each HRU and annual glacier boundaries. Glacier boundaries can proceed from any glacier model providing annual gridded glacier extents. *Glaciers-to-J2K* computes the glacierized and non-glacierized fraction of each HRU by overlapping HRU outlines with annual glacier extents. Then, these fractions are interpolated with a daily timestep throughout a given ablation sub-period, with a default period between June 1^{st} to September 30^{th}. This enables a daily representation of glacier area evolution, necessary for hydrological simulations with J2K. These time series are stored in a *.dat* file.

In J2K, the generation of HRUs for a certain catchment can only be done prior to model simulations. The extent and content of HRUs is static in time, preventing the model from making them evolve throughout a simulation. This specificity of J2K makes it difficult for the model to include a dynamic representation of glaciers, explaining why all simulations for glacierized catchments have so far been performed with static glacierized areas (Gao et al., 2012; Nepal et al., 2014). In order to overcome this limitation, we have developed an approach allowing the introduction of glacier evolution through time, based on prescribed glacier surface areas fed to the model at a regular timestep (e.g. daily in this study).

Two new components named *GlacierFractionReader* and *GlacierFractionAssigner* have been added, responsible for reading the daily glacierized fractions for each HRU and assigning them to the right HRU during the temporal (Time-Loop) and spatial (HRU-Loop) iterations.

Glacier mass balance and runoff

Within the HRU loop of the model, if the glacierized fraction of a given HRU is different than zero, a glacier is detected and the simulation of glacier runoff is triggered. The snow and ice runoff are

computed following the equations 5.5, 5.6 and 5.7. The resulting daily glacier MB for each HRU is calculated from the input liquid and solid precipitation and the output ice (Q_{ice}), snow (Q_{snow}) and rain (Q_{rain}) runoff (Eq. 5.8).

$$MB = (rain + snow - Q_{ice} - Q_{snow} - Q_{rain}) \tag{5.8}$$

The main novelty from this updated module is the fact that we are scaling the precipitation falling on glaciers with the prescribed glacierized fractions ($g_{fraction}$). Precipitation in J2K is divided into rain and snow in varying fractions, with a transition range of temperatures determined by the user (between 0-2°C in our case). For HRUs containing a glacier, the input precipitation is split between the glacierized and non-glacierized fractions. These fractions evolve with a daily timestep, enabling the correct representation of glacier evolution through time in J2K. The glacierized area for each HRU is also updated with a daily timestep by multiplying the HRU area by the glacierized fraction.

Mass balance calibration

The updated glacier module computes glacier MB with a daily timestep using a temperature-index model (Hock, 2003). This type of model relies on an empirical relationship between air temperature and melt, which is clearly observed in the French Alps despite presenting a high spatial variability. Temperature is known to correlate well with melt energy, mainly through short-wave radiation (Sicart et al., 2008). In order to correctly calibrate glacier MB, three parameters can be tuned: a precipitation rate factor specific for the glacier, a snow melt factor (α_{snow}) and an ice melt factor (α_{ice}). Precipitation is known to be underestimated at high altitudes (> 3000 m a.s.l.) in meteorological reanalysis datasets due to the lack of in-situ observations. This has been highlighted for SAFRAN (Vionnet et al., 2019) and is also likely to be the same case for the SPAZM dataset, even though it integrates more observations for high altitude areas. This means that increasing precipitation via a multiplicative correction factor is often needed in order to correctly reproduce accumulation rates on glaciers.

In order to calibrate the snow and ice melt factors and the precipitation multiplicative corrective factor in J2K for the Saint-Sorlin Glacier (Eq. 5.3 and 5.4), we used seasonal (winter and summer) glacier-wide MB direct observations from the GLACIOCLIM glacier observatory. The precipitation correction factor was calibrated based on winter MB data, and the ice and snow melt factors on summer MB data. Due to time constraints, this calibration was performed manually. J2K includes a parameter optimization module, but the recalculation of glacier MB from a daily to seasonal frequency was performed outside J2K, in the *Glaciers-to-J2K* Python package, in order to accelerate the development. In the future, this recalculation should be moved inside J2K to enable the automatic calibration of the precipitation correction factor and melt factors for ice and snow for large catchments.

Non-glacierized fraction

Glacierized HRUs might contain a non-glacierized fraction as well. The precipitation outside the glacier, within the previously existing workflow in J2K, is multiplied by the non-glacierized HRU fraction ($1 - g_{fraction}$). This enables an accurate separation between glacierized and non-glacierized runoff contributions for each HRU. As for the glacierized HRUs, the non-glacierized area is computed daily by multiplying the HRU total area by the non-glacierized fraction.

5.3 Results

This updated glacier module for the J2K hydrological model has been implemented and validated in the Arvan glacierized catchment at Saint-Jean d'Arves in the French Alps (Fig. 5.1). In this catchment configuration, the Saint-Sorlin Glacier occupies four different HRUs, whose glacierized fraction and surface area have been computed for every year between 2003 and 2012 using glacier extensions simulated with ALPGM (Bolibar, 2020).

5.3.1 Glacier dynamics

The evolution of glaciers in the updated glacier module of J2K is represented with prescribed annual glacier extents taken from an independent glacier evolution model. For this case study, ALPGM provided annual glacier ice thickness data from the year 2003, where initial glacier ice thickness data are available from Farinotti et al. (2019a). The 1985-2003 period was used as a spin-up period for the model, in order to correctly initialize the water reservoirs and snow pack. During the spin-up period, since no glacier ice thickness data is available, the extent of the glacier was kept the same as the year 2003. We consider this approximation to be acceptable, taking into account that this simulated period is only used as spin-up. The match between the initial glacier ice extent and the catchment HRUs was not perfect, with small parts of the glacier exceeding the HRUs extent (Fig. 5.1). The prescribed glacier surface areas by the ALPGM glacier model also carry uncertainties, particularly from the initial glacier ice thickness (Bolibar et al., 2020c). Simulated glacier MB data for this period have a very small error (Fig. 3.7), and the parameterization used to update the glacier geometry was specifically calibrated for this glacier. These uncertainties resulted in the simulated glacier geometry only evolving in thickness but not extent between 2004 and 2006. This can be seen in the prescribed glacier surface area changes, which do not evolve until early 2006 (Fig. 5.3). As soon as the prescribed glacier surface area evolves, J2K captures a realistic glacier area evolution during the ablation season. Hence, the overall glacier surface area in J2K is correctly represented, despite the slight mismatches in glacier and HRU data. The Saint-Sorlin Glacier displayed a total surface area of 2.79 km^2 in the year 2003 (Gardent et al., 2014), close to the 2.66 km^2 obtained in J2K (Fig. 5.3).

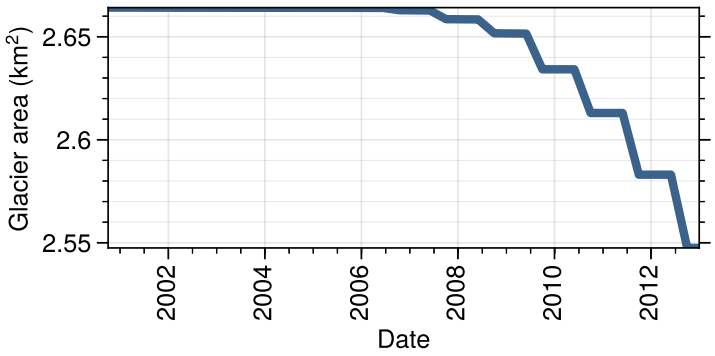

Figure 5.3: Daily evolution of the glacierized surface area of Saint-Sorlin Glacier in J2K. Glacier retreat during the ablation season is well captured in the model, following the prescribed interpolated area evolution. The glacier area is only updated from October 2003 onwards, after the first year with available glacier ice thickness data.

5.3.2 Glacier mass balance

This manual MB calibration enabled a correct representation of the MB of Saint-Sorlin Glacier, but the interannual variability is still not well captured, particularly for the 2005-2008 period (Fig. 5.4). An automatic calibration, testing a wide range of parameter configurations, would certainly yield a much better representation. The best results (annual RMSE = 2.20^9 L) were obtained by increasing precipitation on the glacier by 70%, with a melt factor for ice of 4 mm/°C, lower than the values of 5.2 mm/°C found in the literature (Réveillet et al., 2017), and a melt factor for snow of 2.66 mm/°C, also inferior than values indicated in the literature (4.2 mm/°C). The melt factor for snow we calibrated ended up being the same as the one previously used for the whole catchment with outlet at Saint-Jean d'Arves. The resulting simulated winter MB estimates were less accurate (RMSE winter = 1.56^9 L) than summer estimates (RMSE summer = 1.11^9 L), which are very well captured by the model (Fig. 5.4b and 5.4c).

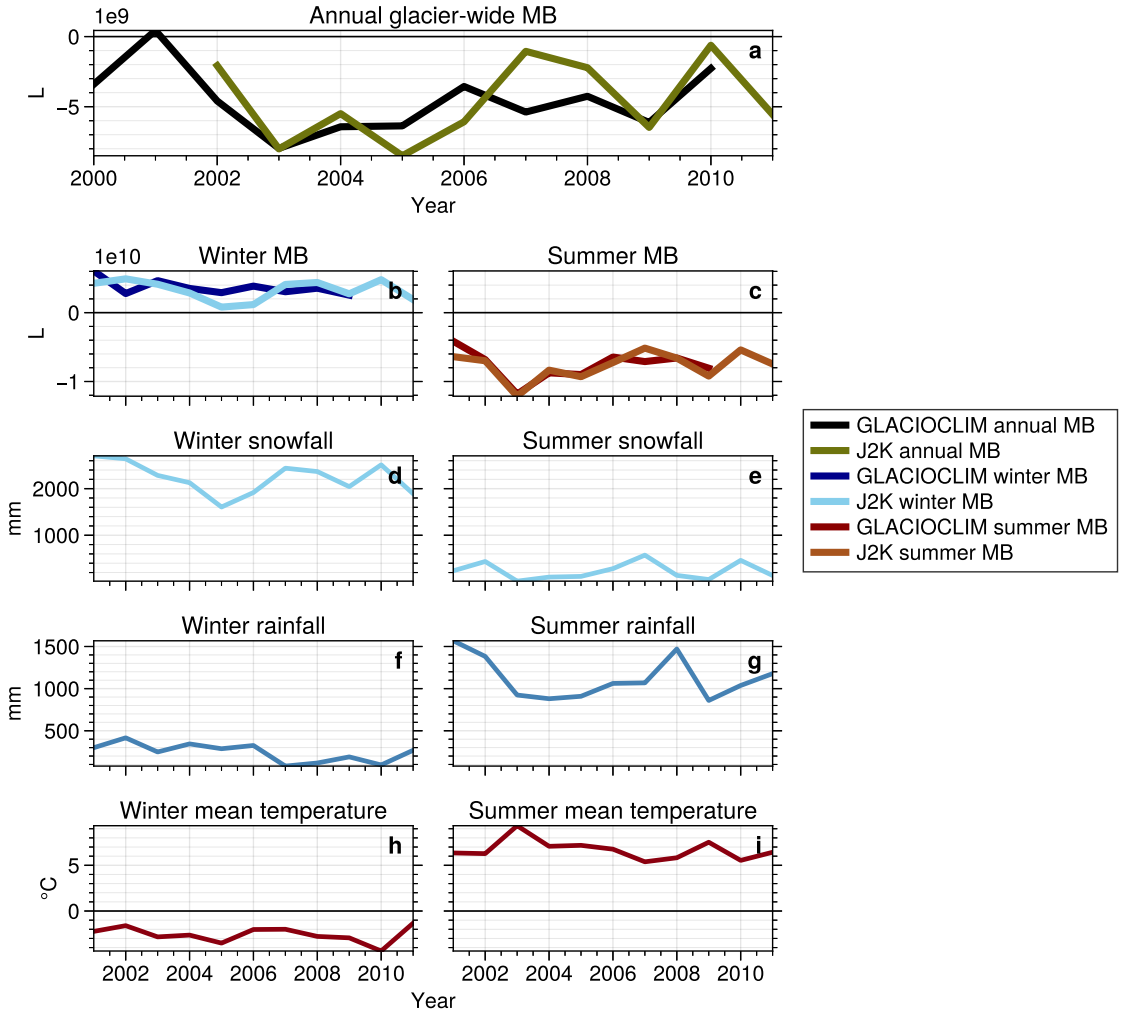

Figure 5.4: Glacier-wide annual (a), seasonal winter (October-April) (b) and summer (May-September) (c) MB for Saint-Sorlin Glacier, with glaciological observations from the GLACIOCLIM observatory and simulated MB from J2K. Winter snowfall (d) and temperature (h), and summer snowfall (g) and temperature (i) are computed as an average of the four HRUs of the glacier. They are shown in order to give context on the meteorological conditions for those years.

5.3.3 Glacier runoff

Runoff values in J2K are extracted at Saint-Jean d'Arves, where observations from the gauging station are available (Fig. 5.1). A comparison between the observed and the simulated average monthly discharges reveals a correct agreement between both (Fig. 5.5), displaying a Kling-Gupta Efficiency (KGE) of 0.69 and a Nash-Sutcliffe Efficiency (NSE) of 0.41. The addition of the glacier module improves the average monthly runoff distribution, allowing a better representation of the tail of late summer and early autumn glacier discharge contributions (Fig. 5.5). When looking specifically at the snow (March-June) and ice (July-October) melt seasons, the updated glacier module also manages to improve the performance of the simulated discharge, especially for the ice melt season (Table 5.1).

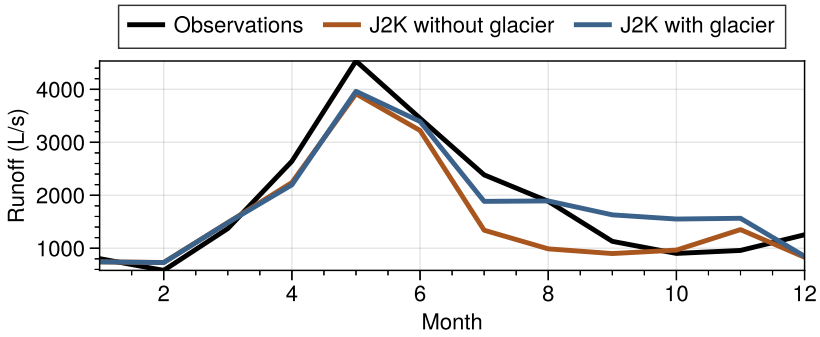

Figure 5.5: Average monthly runoff from the gauging station at Saint-Jean-d'Arves La Villette and from J2K simulations with and without the glacier.

The total runoff contribution of the Saint-Sorlin Glacier is found to be quite important during the summer and autumn period, with peak monthly contributions ranging between 40-80% and annual contributions between 17-35%. By separating the net glacier contributions (only ice melt) from the total glacier contributions, we can observe how the ice melt contributions greatly vary between years depending on the late spring and summer snowpack characteristics (Fig. 5.6). The highest glacier contributions are found to have occured in the years 2003, with its famous summer heatwave, and the year 2009.

	J2K with glacier	**J2K without glacier**
KGE	0.69	0.66
KGE snow melt	0.71	0.69
KGE ice melt	0.55	0.45
NSE	0.41	0.36
NSE snow melt	0.41	0.37
NSE ice melt	0.11	-0.15

Table 5.1: Performance of J2K discharge simulations at Saint-Jean d'Arves with and without the updated glacier module. The snow melt period is computed as the runoff between March-June and the ice melt period as the runoff between July-October.

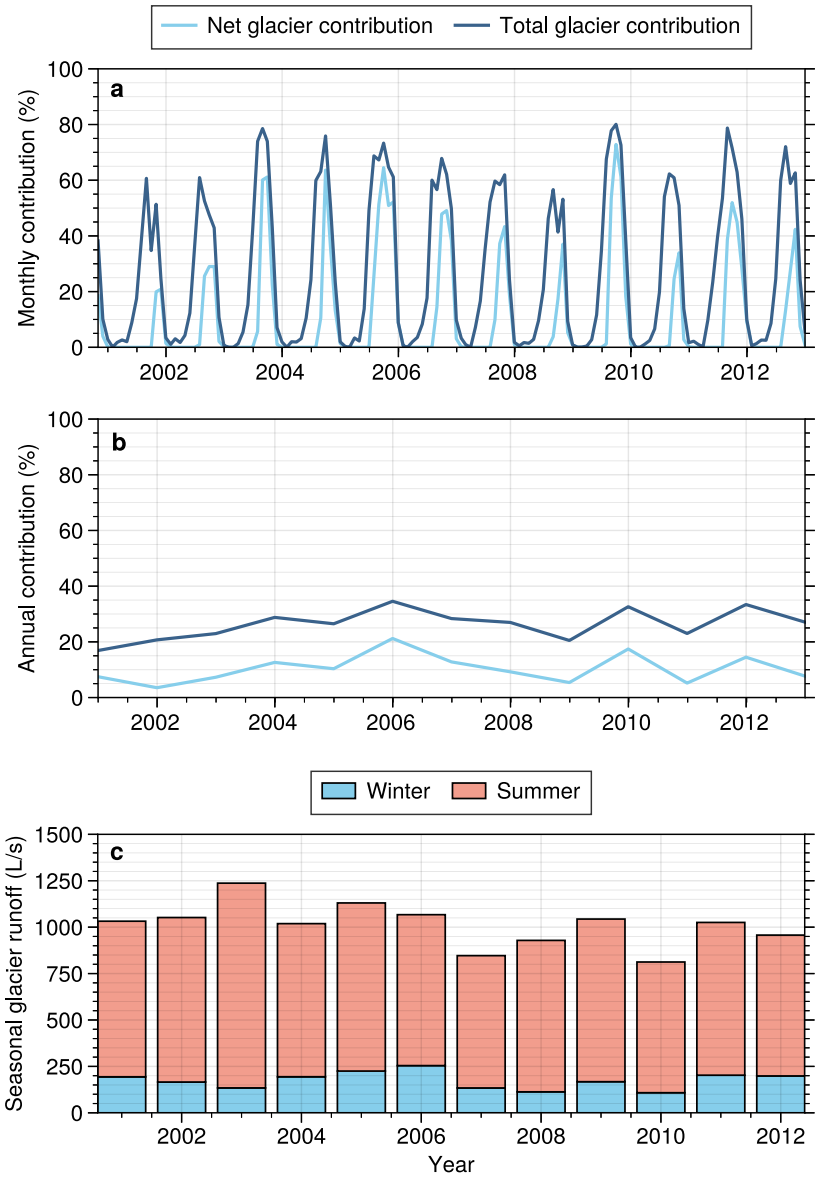

Figure 5.6: (a) Monthly total and net (only ice melt) glacier contributions to the total catchment discharge, (b) annual total and net glacier contributions and (c) seasonal glacier runoff.

5.4 Discussion and conclusions

We introduced an updated glacier module for the J2K distributed process-based hydrological model, allowing a representation of glacier dynamics. This updated glacier module was applied to the Arvan glacierized catchment in the French Alps as a case study, in order to (a) demonstrate the capability of including glacier dynamics in the J2K model based on ALPGM outputs and (b) highlight the added value of the representation of glaciers within a hydrological model operating in high-altitude, partially glacierized alpine catchments. The addition of glacier dynamics can benefit hydrological models in their current representation of the hydrological regimes of glacierized catchments, but it is especially expected to be of great importance to future hydrological projections, when glacier shrinkage will drive significant changes at catchment scale (Hock et al., 2019b). Physical realism of hydrological models has been long sought as an important asset to improve their performance and predictive power (Hrachowitz et al., 2013), notably with an aim of ensuring the reliability of simulations in future pro-

jections (e.g. Gao et al., 2020). Despite the small changes in glacier area in this case study (Fig. 5.3), we showed that the updated glacier module enabled an improved representation of both monthly runoff distribution (Fig. 5.5) and daily discharge rates, with an improved KGE and NSE (Table 5.1). The most important differences were related to the glacier discharge contributions between late summer and autumn, when the net glacier runoff contributions are the highest. The discharge contributions from these months will also be the most severely affected by glacier retreat, indicating the progressive transition from a glacio-nival regime to a nival regime (Hock et al., 2019b). The here presented developments are necessary to carry on realistic simulations of the Arvan and most high altitude partially glacierized catchments for the coming decades.

We leveraged the seasonal GLACIOCLIM MB data to perform a stepwise calibration of the glacier specific parameters: the precipitation corrective factor (based on winter MB only) and the ice melt factor (based on summer MB only). As found in previous studies (Schaefli and Huss, 2011), this resulted in a realistic simulation of both MB components, while the agreement with the annual MB observations only led to some equifinality between these parameters and precluded the selection of a physically sound solution. For the present study we re-used a snow melt factor that had been adjusted through automatic calibration based on river discharge at the catchment outlet in previous simulations without the updated glacier module. A recalibration of this parameter could have been performed in the stepwise framework, based on river discharge during the snow melt period (March to late June). Nonetheless, we were obliged to shorten the calibration phase due to time constrains. For the vast majority of French Alpine glaciers no seasonal MB observations are available. In order to overcome this limitation, a potential strategy would be to use MB reconstructions from ALPGM produced during this PhD work (Bolibar et al., 2020b), in order to calibrate the parameters from the MB model (Stahl et al., 2008), implying a revision of the calibration strategy for J2K. Following Konz and Seibert (2010), we hypothesize that the ice melt factor could be calibrated based on late summer and early autumn discharge at the catchment outlet, a period when glacier contribution to the flow is essential, provided that the glacierized fraction of the catchment is not negligible. Indeed, these authors found that only three days of discharge measurements from the melt period can already help calibrate the parameters of a glacio-hydrological model. Then, the precipitation multiplication factor could be calibrated to ensure that the annual glacier-wide MB is respected. The possibilities and limitations of this strategy should be first evaluated on glaciers and catchments with seasonal MB estimates, such as the Arvan case study. Another current limitation that should be overcome for future simulations is the transformation from snow to ice. This is in fact rather straightforward from a technical point of view, since there is already a variable tracking the snow age which could be easily used to gradually transition old snow into firn and ice. This would be essential in order to correctly take into account years with positive MB rates in long-term simulations.

The implemented approach presented here could be easily extended to all glaciers in the French Alps, as well as to glacierized catchments with multiple glaciers. J2K has already been deployed, adjusted and evaluated at the scale of the whole Rhone river basin which encompasses all glaciers from the French Alps (Braud et al., 2017). Similarly, ALPGM provides a regional glacier reconstruction and projection tool for the French Alps, so that the combination of both models enables glacio-hydrological simulations and projections at this scale. Every HRU in J2K has an ID which can be matched to any Randolph Glacier Inventory (RGI) ID, allowing a specific calibration of melt and precipitation factors for each individual glacier. In catchments with small glaciers located close together, these might end up sharing an HRU. For these cases, the optimization of the melt model would have to be shared among all the glaciers present in that HRU. Alternatively, the size of the HRU separation can be reduced, improving the spatial representation of the catchment. Nonetheless, this has an important computa-

tional cost. We believe this updated modelling framework has enough flexibility to enable an accurate calibration of different melt factors and precipitation lapse rates in mountainous regions. The modelling framework of J2K includes a large array of components representing different processes related to snow and ice. This level of detail, together with the code execution efficiency of Java allow a detailed representation of the many processes involved in the high-altitude water cycle at large geographical scales.

We expect this updated glacier module to become a key component for J2K to correctly assess the impacts of future glacier retreat of glacierized catchments. For the case of the French Alps and the BERGER project, it will be applied at a regional scale in order to simulate the future hydrological changes of all glacierized catchments in the French Alps. Unlike the recent study by Laurent et al. (2020) in the Mont-Blanc massif, the choice of a process-based, distributed hydrological model opens the way to diverse applications that require knowledge of the different runoff components, including glacier contributions in diverse, mostly ungauged, locations of the catchment. The future regional ALPGM-J2K simulation results will enable biologists to assess the potential impacts of climate change and glacier retreat on aquatic biodiversity. The expected decrease of late summer and autumn runoff, the increase in summer water temperature and changes in sediment loads will alter the habitat of many aquatic species, making it possible for new species to move in and increase competition with already vulnerable ones (Robinson et al., 2014). Moreover, since many studies have already used J2K in glacierized regions, particularly in the Himalayas (Gao et al., 2012; Nepal et al., 2014, 2020), this updated glacier module can be easily reused by other experienced scientists. By contributing to an open-source hydrological model with such a broad international community, we increase the impact and transferability of this work, following the principles that have guided the preceding chapters.

5.5 Code availability

The source code of the Python package *Glaciers-to-J2K* is available in the following GitHub repository: https://github.com/JordiBolibar/Glaciers-to-J2K

Part III

Outlook

Chapter 6

Conclusions and perspectives

In the study of nature, as in the practice of art, it is not given to man to achieve the goal without leaving a trail of dead ends he had pursued.

Baron Louis Bernard Guyton de Morveau

6.1 Summary of the results

The initial objective of this PhD work was to study the evolution of all glaciers in the French Alps from the last decades of the 20^{th} century until the end of the 21^{st} century, and to explore the impact of their retreat in the hydrological budget of the Rhône river catchment. However, this initial objective was adapted following the exploration of machine learning methods for glacier mass balance simulation at the end of the first year of the project. My strong interest in these rather unexploited methods in glaciology led to important changes in the results, largely expanding the efforts dedicated on methods, and reducing the amount of results on glacio-hydrological modelling. Consequently, the resulting scientific questions that were addressed during these three years also evolved. In this section, I will address each one of these questions, giving an overview of the results and determining the accomplished objectives as well as the remaining challenges.

Question 1 - Can deep learning be applied to model annual glacier mass balance changes at a regional scale? What are the benefits of using nonlinear deep learning models compared to linear machine learning?

In Chapter 2, based on a paper published in *The Cryosphere* journal, we introduced, to our knowledge, the first effort ever to apply deep learning to simulate glacier evolution. A new open-source regional glacier evolution model (ALPGM) was developed, whose main novelty was a mass balance component based on machine learning. Our work showed promising results, proving that deep learning can be successfully used to simulate glacier mass balance. A detailed comparison between linear machine learning methods and deep learning highlighted how important nonlinearities are captured by deep learning. Since both the climate and glacier systems are known to be nonlinear (e.g., the glacier mass balance response to temperature), this resulted in an improved performance from deep learning models, with an improved accuracy (RMSE) of up to +58% and an improved explained variance (r^2) of up to +108%. Moreover, despite using a rather small dataset of annual mass balance data, we proved that by rigorously cross-validating the models, deep learning can still learn from "small data"

without overfitting. Spatiotemporal data demands that the independence of both dimensions have to be respected during cross-validation. We devised different types of cross-validation which allowed an accurate evaluation of the performance of models in the spatial and temporal dimensions, while fully utilizing the whole dataset to train the models.

Question 2 - What are the annual glacier changes of all glaciers in the French Alps for the last half century?

In Chapter 3, based on a paper published in the *Earth System Science Data* journal, we applied the deep learning methods developed in Chapter 2 to the reconstruction of annual glacier-wide MB series of all glaciers in the French Alps (N=661) between 1967 and 2015. Our results showed that French alpine glaciers went through slightly negative MB rates from the late 1960s and during the 1970s (-0.44 m w.e. a^{-1}). Then, during the 1980s their MB was almost stable (-0.16 m.w.e. a^{-1}, with several positive years), before becoming more negative from the 1990s (-0.71 m.w.e. a^{-1}). Their MB rates became remarkably more negative from the 2000s (-1.18 m.w.e. a^{-1}), especially after the famous heatwave from the year 2003. This year established an inflection point, from which MB became increasingly negative up to -1.26 m.w.e. a^{-1} for the first half of the 2010s. Important differences were found between massifs, with the Mont-Blanc massif showing the least negative MB, and the Chablais massif presenting the highest losses. We showed how this method correctly captured the interannual variability of the glacier-wide MB signal of glaciers in the French Alps, mostly driven by climate, and how it also captured differences between glaciers with various topographical characteristics.

Question 3 - How will French alpine glaciers evolve during the 21st century? How does glacier retreat affect the climate signal on glaciers? What are the main factors that determine glacier survival in the French Alps? What are the benefits of using a nonlinear mass balance model for future glacier projections?

In Chapter 4, we presented the results of glacier evolution projections for all glaciers in the French Alps through the 21^{st} century under different climate scenarios. We estimate that French Alpine glaciers will experience ice volume losses by the end of the century of 75%, 80% and 88% under RCP 2.6, 4.5 and 8.5 respectively. Half of the initial 2015 ice volume is expected to be lost by 2050, independently from future climate scenarios. This severe glacier retreat will have a strong impact on most glacierized massifs in the French Alps, with only significant glaciers remaining in the high-altitude Mont-Blanc and Pelvoux massifs by the end of the century. An analysis on the effects of glacier retreat indicated that glaciers greatly modify their received climate signal when retreating to higher altitudes in an attempt to regain equilibrium with the present climate. By doing so, they move to higher areas with a colder climate, experiencing reduced temperatures up to -350 PDD a^{-1}, reduced rainfall up to -100 mm a^{-1} and increased snowfall up to +220 mm a^{-1}. Despite this strong adaptation, glaciers in the French Alps are not expected to regain equilibrium with the climate under any future climate scenario. Moreover, we performed a statistical analysis on model results, showing that the main factors determining glacier survival in the French Alps are a high-altitude accumulation basin, ensuring abundant accumulation during winter, and in a second term a higher latitude, hinting at the increased precipitation rates received by the northernmost massifs. At last, we performed a thorough analysis on the nonlinearities present in the climatic forcings of glaciers in the French Alps. Our results revealed that linear MB models successfully approximate average MB rates seen in the past during calibration, but tend to overestimate and underestimate positive and negative extreme MB values respectively, for which nonlinearities are stronger. This can have potential consequences in long-term MB projections, as

biases linked to extreme MB rates accumulate over decades. We argue that despite not showing large cumulative differences in the French Alps due to the rather homogeneous climate signal in the region, these differences can potentially drive important long-term biases in larger glacierized areas with more heterogeneous topographical and climatic characteristics. Therefore, we suggest that current global glacier evolution projections based on linear MB models might be potentially underestimating the lower and higher bounds of future sea-level rise.

Question 4 - What are the current limitations in the representation of glaciers in hydrological models in France? How can we improve this?

Current hydrological models used in France by territorial stakeholders or hydro-power managers generally suffer from a simplified representation of glaciers as static ice reservoirs. This is highly problematic in the current context of rapid glacier retreat in the French Alps. Glacio-hydrological models need to accurately represent glacier evolution in order to take into account the progressive changes induced by the evolution of glacier runoff on hydrological regimes, both in terms of seasonality and total amount of discharge. These changes can drive important social and environmental impacts in the French Alps, which demand adequate tools to perform accurate glacio-hydrological projections. In this work, we introduced an updated glacier module for the well-established J2K hydrological model (Krause, 2002), capable of representing the daily evolution of glaciers. This approach is based on prescribed annual glacier extents, that can proceed from any glacier evolution model. We validated this method in the Arvan partially glacierized catchment, located in the Grandes Rousses massif, for which we also assessed the effects of glacier retreat on the recent past. With this new enhanced representation of glaciers in the J2K hydrological model, we have set the means for future glacio-hydrological studies in the Rhône river catchment to assess the hydro-ecological impacts of glacier retreat. Moreover, the glacier evolution data generated by ALPGM can potentially be used as input to other hydrological models (e.g. MORDOR, GR), in order to introduce glacier evolution as it has been done for J2K.

6.2 Perspectives on future research venues

This PhD work served to bring attention to the benefits of using deep learning for regression problems in glacier evolution modelling. At the beginning of this PhD, to my knowledge, there were no papers published using deep learning on glaciers. For the AGU Fall Meeting 2019, a new session on machine learning, artificial intelligence (AI) and remote sensing on the cryosphere was created for the first time. This session served to catalyse all the current research in this sub-field, with many papers published around that period. For the first time, researchers working on these topics were able to exchange, discuss and even collaborate in bringing new methods to different applications in glaciology. This experience was followed by another session on machine learning and AI for glaciology at the EGU General Meeting 2020, which despite the virtual format due to the global COVID-19 crisis, further displayed the huge potential of these applications from a wide range of glaciological problems. Machine learning and data science in glaciology are still a very novel field, but many promising applications are being presented by the day (e.g. Leong and Horgan, 2020; Brinkerhoff et al., 2020), showing multiple directions for the sub-field to evolve towards.

So far, as it was shown in these two previous sessions at AGU and EGU, the great majority of efforts have been focused on classification problems. New satellite imagery, with ever improving spatial and temporal resolution, is being successfully exploited by deep learning methods to automatically extract

glacier fronts in Greenland and Antarctica (e.g. Lea, 2018; Baumhoer et al., 2019; Mohajerani et al., 2019; Zhang et al., 2019) and supraglacial lakes (e.g. Yuan et al., 2020). The validation of these approaches is more straightforward than for regression problems, mainly demanding the manual delineation or classification of geometric features in satellite imagery. Moreover, in such applications where interpretability is not a concern, the full predictive power of convolutional neural networks (NNs) can be unleashed. Conversely, regression problems in glaciology remain highly unexplored, due to the inherent complexity of correctly representing physical processes with NNs. This brings us to the last scientific question of this PhD work.

Question 5 - What are the caveats of the deep learning modelling approach used in this work? What improvements are needed to overcome these limitations for glaciological studies?

The work of this PhD showed how deep learning models can be extremely challenging to interpret. We attempted to partially do so by training a parallel linear machine learning model (Lasso) with the same dataset, and by thoroughly cross-validating it respecting spatiotemporal structures in data. Nonetheless, these represented just approximations of what the true underlying NN model actually is, and raised many questions on how to address this interpretability issue.

Fortunately, in the last years enormous progress has been made towards interpretable machine learning and particularly interpretable NNs. NNs are universal function approximators, meaning that any sufficiently large NN can approximate any nonlinear function with a finite set of parameters (Winkler and Le, 2017). This remarkable predicting power comes at the cost of very low interpretability, requiring deep changes in the way we design NNs. In order to represent a partially known physical process with a NN, two main approaches are being proposed nowadays: (1) NNs are optimized following a certain loss function, which determines how they learn and update the weights of the different connections between neurons. By consciously modifying a NN's architecture, one can constrain the way NNs learn based on prior knowledge. The most prominent way so far has been to encode prior knowledge, in the form of differential equations (DEs), as the loss function of a NN. By doing so, the learning of NNs is constrained following currently known equations (Raissi et al., 2017; Karpatne et al., 2018). Additionally, by using specific architectures that suit the specificities of a given physical process, the learning can be further constrained, limiting or enhancing the interactions between certain input predictors (Karpatne et al., 2017). Such an approach enables an equation-guided learning, but does not fully deal with the "black box" consequences on interpretability. (2) Another way of looking at this problem is that, instead of trying to constrain the learning of NNs, NNs can be reduced to the smallest possible entities, in order to decrease their complexity to the point they can be interpreted. This radically different approach is currently showing very exciting results. The beauty of this approach resides on the fact that it manages to create hybrid models, mixing a classical physical approach based on DEs with the phenomenal predictive power of NNs to optimize unknown parameters (Rackauckas et al., 2020). The main structure of such a model remains a DE, which is augmented with NNs that replace the unknowns parameters. New methods enable the optimization of DEs combined with NNs, allowing the NNs to produce nonlinear functions that optimize the unknowns following an equation determined by the DE (Raissi et al., 2017; Rackauckas et al., 2020; Bradbury et al., 2020). Since these "small" NNs are based on just one or two input predictors, their output values can be sampled using Monte Carlo methods at their input. By applying a sparse regression on these outputs, one can obtain a mathematical representation of the nonlinear function learnt by the NN (Brunton et al., 2016). This mathematical representation of NNs can be used to interpret them, while suggesting reformulations in the currently known equations used in the model (Rackauckas et al., 2020).

The sub-field of glacier machine learning and data science is ripe for progress, and many innovative studies are offering new perspectives on how to improve our understanding of glacier processes with models. Not all solutions go through NNs, as a study by Werder et al. (2019) recently showed. They applied a Bayesian inference inverse model to estimate glacier ice thickness. By reusing an already established model by Huss and Farinotti (2012) describing the ice thickness distribution of glaciers, they were able to improve the assimilation of observations for the optimization of model parameters, while performing a detailed assessment of their uncertainties and errors. Rounce et al. (2020) followed a similar approach with a regional glacier evolution modelling study of MB in High Mountain Asia. The use of Bayesian inference provided new insights on the main sources of model uncertainty, further highlighting the benefits of transitioning from deterministic to probabilistic modelling. More recently, a study by Brinkerhoff et al. (2020) took this approach to another level by applying it to a surrogate model based on deep learning. Bayesian inference can be computationally expensive, and its application to highly complex models involving several parameters, such as a 3D spatially-explicit hydrological model coupled with ice dynamics, is not feasible for now. In this study, they bypassed this limitation by substituting this model with a "black box" NN, producing an equivalent solution at a fraction of the computational cost. This surrogate model allowed the use of Bayesian inference in order to correctly estimate parameter uncertainties and errors. Such diverse approaches display new ways of tackling glaciological modelling, that can provide major changes in our understanding of glacier processes and their drivers.

These new methods offer great perspectives to overcome the main limitations of our current glacier evolution modelling approach. By reusing currently known equations of glacier processes, such as the Shallow Ice Approximation (Hutter, 1983) or enhanced temperature-index or surface energy balance models, we can aim at building new methods on top of the most reliable theoretical bases in our field. This offers the possibility to optimize and potentially reformulate these equations, in order to exploit data using NNs in an interpretable manner, creating knowledge that can be reused by the whole glaciological community. During the last year of my PhD, I have been thinking about and developing these ideas, gathering them in the form of a postdoc proposal. With it, I propose to use hybrid models composed by differential equations and NNs to simulate glacier evolution at a large scale. Such an approach can potentially enable a detailed interpretation of specific glacier processes (e.g. ice dynamics or glacier sliding) from parameters optimized by NNs, which could be taken into account by reformulating currently known equations. I hope to be able to continue investigating this line of research, as I keep learning from these two fascinating research fields that are glaciology and machine learning.

Bibliography

Baumhoer, C. A., Dietz, A. J., Kneisel, C., and Kuenzer, C.: Automated Extraction of Antarctic Glacier and Ice Shelf Fronts from Sentinel-1 Imagery Using Deep Learning, Remote Sensing, 11, 2529, doi: 10.3390/rs11212529, URL https://www.mdpi.com/2072-4292/11/21/2529, 2019.

Beniston, M., Farinotti, D., Stoffel, M., Andreassen, L. M., Coppola, E., Eckert, N., Fantini, A., Giacona, F., Hauck, C., Huss, M., Huwald, H., Lehning, M., López-Moreno, J.-I., Magnusson, J., Marty, C., Morán-Tejéda, E., Morin, S., Naaim, M., Provenzale, A., Rabatel, A., Six, D., Stötter, J., Strasser, U., Terzago, S., and Vincent, C.: The European mountain cryosphere: a review of its current state, trends, and future challenges, The Cryosphere, 12, 759–794, doi: 10.5194/tc-12-759-2018, URL https://www.the-cryosphere.net/12/759/2018/, 2018.

Benn, D. I. and Evans, D. J. A.: Glaciers & glaciation, Routledge, New York, NY, USA, 2nd edn., URL http://www.imperial.eblib.com/EBLWeb/patron/?target=patron&extendedid=P_615876_0, oCLC: 878863282, 2014.

Berthier, E., Vincent, C., Magnússon, E., Gunnlaugsson, , Pitte, P., Le Meur, E., Masiokas, M., Ruiz, L., Pálsson, F., Belart, J. M. C., and Wagnon, P.: Glacier topography and elevation changes derived from Pléiades sub-meter stereo images, The Cryosphere, 8, 2275–2291, doi: 10.5194/tc-8-2275-2014, URL https://www.the-cryosphere.net/8/2275/2014/, 2014.

Berthier, E., Cabot, V., Vincent, C., and Six, D.: Decadal Region-Wide and Glacier-Wide Mass Balances Derived from Multi-Temporal ASTER Satellite Digital Elevation Models. Validation over the Mont-Blanc Area, Frontiers in Earth Science, 4, doi: 10.3389/feart.2016.00063, URL http://journal.frontiersin.org/Article/10.3389/feart.2016.00063/abstract, 2016.

Bertle, F. A.: Effect of snow compaction on runoff from rain on snow, 35, US Department of the Interior, Bureau of Reclamation, 1966.

Bolibar, J.: ALPGM (ALpine Parameterized Glacier Model) v1.1, doi: 10.5281/zenodo.3609136, URL https://doi.org/10.5281/zenodo.3609136, 2020.

Bolibar, J., Rabatel, A., Gouttevin, I., and Galiez, C.: A deep learning reconstruction of mass balance series for all glaciers in the French Alps: 1967-2015, Zenodo, doi: 10.5281/zenodo.3663630, URL https://doi.org/10.5281/zenodo.3663630, [Dataset], 2020a.

Bolibar, J., Rabatel, A., Gouttevin, I., and Galiez, C.: A deep learning reconstruction of mass balance series for all glaciers in the French Alps: 1967–2015, Earth System Science Data, 12, 1973–1983, doi: 10.5194/essd-12-1973-2020, URL https://essd.copernicus.org/articles/12/1973/2020/, 2020b.

Bolibar, J., Rabatel, A., Gouttevin, I., Galiez, C., Condom, T., and Sauquet, E.: Deep learning applied to glacier evolution modelling, The Cryosphere, 14, 565–584, doi: 10.5194/tc-14-565-2020, URL https://www.the-cryosphere.net/14/565/2020/, 2020c.

Bourdeau, P.: Examining innovation in the Alps at the local scale: A region on the move, the "Pays des Ecrins", Revue de géographie alpine, doi: 10.4000/rga.797, URL http://journals.openedition.org/rga/797, 2009.

Bradbury, J., Frostig, R., Hawkins, P., Johnson, M. J., Leary, C., Maclaurin, D., and Wanderman-Milne, S.: JAX: composable transformations of Python+ NumPy programs, 2018, URL http://github. com/google/jax, p. 18, 2020.

Branger, F., Kermadi, S., Krause, P., Labbas, M., Jacqueminet, C., Michel, K., Braud, I., and Kralisch, S.: Investigating the impact of two decades of urbanization on the water balance of the Yzeron peri-urban catchment, France., 2012.

Bratko, I.: Machine Learning: Between Accuracy and Interpretability, in: Learning, Networks and Statistics, edited by Riccia, G., Lenz, H.-J., and Kruse, R., pp. 163–177, Springer Vienna, Vienna, doi: 10.1007/978-3-7091-2668-4_10, URL http://link.springer.com/10.1007/978-3-7091-2668-4_10, 1997.

Braud, I., Branger, F., Gouttevin, I., Sauquet, E., Tilmant, F., and Montginoul, M.: J2000-Rhône: a distributed hydrological model including water-use modelling to assess sustainability of the water resource, URL https://hal.inrae.fr/hal-02606805, published: 10th HyMeX workshop, 2017.

Brigode, P., Génot, B., Lobligeois, F., and Delaigue, O.: Summary sheets of watershed-scale hydroclimatic observed data for France, doi: 10.15454/UV01P1, URL https://data.inra.fr/citation?persistentId=doi:10.15454/UV01P1, type: dataset, 2020.

Brinkerhoff, D., Aschwanden, A., and Fahnestock, M.: Constraining subglacial processes from surface velocity observations using surrogate-based Bayesian inference, arXiv:2006.12422 [physics], URL http://arxiv.org/abs/2006.12422, arXiv: 2006.12422, 2020.

Brun, F., Berthier, E., Wagnon, P., Kääb, A., and Treichler, D.: A spatially resolved estimate of High Mountain Asia glacier mass balances from 2000 to 2016, Nature Geoscience, 10, 668–673, doi: 10.1038/ngeo2999, URL http://www.nature.com/doifinder/10.1038/ngeo2999, 2017.

Brunner, M. I., Farinotti, D., Zekollari, H., Huss, M., and Zappa, M.: Future shifts in extreme flow regimes in Alpine regions, Hydrology and Earth System Sciences, 23, 4471–4489, doi: 10.5194/hess-23-4471-2019, URL https://hess.copernicus.org/articles/23/4471/2019/, 2019.

Brunton, S. L., Proctor, J. L., and Kutz, J. N.: Discovering governing equations from data by sparse identification of nonlinear dynamical systems, Proceedings of the National Academy of Sciences, 113, 3932–3937, doi: 10.1073/pnas.1517384113, URL http://www.pnas.org/lookup/doi/10.1073/pnas.1517384113, 2016.

Carlson, B. Z., Georges, D., Rabatel, A., Randin, C. F., Renaud, J., Delestrade, A., Zimmermann, N. E., Choler, P., and Thuiller, W.: Accounting for tree line shift, glacier retreat and primary succession in mountain plant distribution models, Diversity and Distributions, 20, 1379–1391, doi: 10.1111/ddi.12238, URL http://doi.wiley.com/10.1111/ddi.12238, 2014.

Carlson, B. Z., Hébert, M., Van Reeth, C., Bison, M., Laigle, I., and Delestrade, A.: Monitoring the Seasonal Hydrology of Alpine Wetlands in Response to Snow Cover Dynamics and Summer Climate: A Novel Approach with Sentinel-2, Remote Sensing, 12, 1959, doi: 10.3390/rs12121959, URL https://www.mdpi.com/2072-4292/12/12/1959, 2020.

Cauvy-Fraunié, S. and Dangles, O.: A global synthesis of biodiversity responses to glacier retreat, Nature Ecology & Evolution, 3, 1675–1685, doi: 10.1038/s41559-019-1042-8, URL http://www.nature.com/articles/s41559-019-1042-8, 2019.

Chen, C.-l.: Surface irrigation using kinematic-wave method, Journal of the Irrigation and Drainage Division, 96, 39–46, publisher: ASCE, 1970.

Chollet, F.: Keras, URL https://keras.io, 2015.

Consortium, R. G. I.: Randolph Glacier Inventory 6.0, doi: 10.7265/N5-RGI-60, URL http://www.glims.org/RGI/randolph60.html, type: dataset, 2017.

Coppola, E., Raffaele, F., and Giorgi, F.: Impact of climate change on snow melt driven runoff timing over the Alpine region, Climate Dynamics, 51, 1259–1273, doi: 10.1007/s00382-016-3331-0, URL http://link.springer.com/10.1007/s00382-016-3331-0, 2018.

Coron, L., Thirel, G., Delaigue, O., Perrin, C., and Andréassian, V.: The suite of lumped GR hydrological models in an R package, Environmental Modelling & Software, 94, 166–171, doi: 10.1016/j.envsoft.2017.05.002, URL https://linkinghub.elsevier.com/retrieve/pii/S1364815217300208, 2017.

Cuffey, K. and Paterson, W. S. B.: The physics of glaciers, Butterworth-Heinemann/Elsevier, Burlington, MA, 4th ed edn., oCLC: ocn488732494, 2010.

Davaze, L., Rabatel, A., Arnaud, Y., Sirguey, P., Six, D., Letreguilly, A., and Dumont, M.: Monitoring glacier albedo as a proxy to derive summer and annual surface mass balances from optical remote-sensing data, The Cryosphere, 12, 271–286, doi: 10.5194/tc-12-271-2018, URL https://tc.copernicus.org/articles/12/271/2018/, 2018.

Davaze, L., Rabatel, A., Dufour, A., Arnaud, Y., and Hugonnet, R.: Region-wide annual glacier surface mass balance for the European Alps from 2000 to 2016, Frontiers in Earth Science, 8, 149, publisher: Frontiers, 2020.

de Bezenac, E., Pajot, A., and Gallinari, P.: Deep Learning for Physical Processes: Incorporating Prior Scientific Knowledge, arXiv:1711.07970 [cs, stat], URL http://arxiv.org/abs/1711.07970, arXiv: 1711.07970, 2018.

Dong, Y., Su, H., Zhu, J., and Zhang, B.: Improving Interpretability of Deep Neural Networks With Semantic Information, in: Proceedings of the IEEE Conference on Computer Vision and Pattern Recognition (CVPR), 2017.

Ducournau, A. and Fablet, R.: Deep learning for ocean remote sensing: an application of convolutional neural networks for super-resolution on satellite-derived SST data, in: 2016 9th IAPR Workshop on Pattern Recogniton in Remote Sensing (PRRS), pp. 1–6, IEEE, Cancun, Mexico, doi: 10.1109/PRRS.2016.7867019, URL http://ieeexplore.ieee.org/document/7867019/, 2016.

Durand, Y., Laternser, M., Giraud, G., Etchevers, P., Lesaffre, B., and Mérindol, L.: Reanalysis of 44 Yr of Climate in the French Alps (1958–2002): Methodology, Model Validation, Climatology, and Trends for Air Temperature and Precipitation, Journal of Applied Meteorology and Climatology, 48, 429–449, doi: 10.1175/2008JAMC1808.1, URL http://journals.ametsoc.org/doi/abs/10.1175/2008JAMC1808.1, 2009.

Dussaillant, I., Berthier, E., Brun, F., Masiokas, M., Hugonnet, R., Favier, V., Rabatel, A., Pitte, P., and Ruiz, L.: Two decades of glacier mass loss along the Andes, Nature Geoscience, 12, 802–808, doi: 10.1038/s41561-019-0432-5, URL http://www.nature.com/articles/s41561-019-0432-5, 2019.

Farinotti, D., Huss, M., Fürst, J. J., Landmann, J., Machguth, H., Maussion, F., and Pandit, A.: A consensus estimate for the ice thickness distribution of all glaciers on Earth, Nature Geoscience, 12, 168–173, doi: 10.1038/s41561-019-0300-3, URL http://www.nature.com/articles/s41561-019-0300-3, 2019a.

Farinotti, D., Round, V., Huss, M., Compagno, L., and Zekollari, H.: Large hydropower and water-storage potential in future glacier-free basins, Nature, 575, 341–344, doi: 10.1038/s41586-019-1740-z, URL http://www.nature.com/articles/s41586-019-1740-z, 2019b.

Fausett, L. V.: Fundamentals of neural networks: architectures, algorithms, and applications, Prentice Hall, Englewood Cliffs, N.J., oCLC: 28215780, 1994.

Fischer, M., Huss, M., and Hoelzle, M.: Surface elevation and mass changes of all Swiss glaciers 1980–2010, The Cryosphere, 9, 525–540, doi: 10.5194/tc-9-525-2015, URL https://www.the-cryosphere.net/9/525/2015/, 2015.

Gagliardini, O., Zwinger, T., Gillet-Chaulet, F., Durand, G., Favier, L., de Fleurian, B., Greve, R., Malinen, M., Martín, C., Råback, P., Ruokolainen, J., Sacchettini, M., Schäfer, M., Seddik, H., and Thies, J.: Capabilities and performance of Elmer/Ice, a new-generation ice sheet model, Geoscientific Model Development, 6, 1299–1318, doi: 10.5194/gmd-6-1299-2013, URL https://www.geosci-model-dev.net/6/1299/2013/, 2013.

Gao, T., Kang, S., Krause, P., Cuo, L., and Nepal, S.: A test of J2000 model in a glacierized catchment in the central Tibetan Plateau, Environmental Earth Sciences, 65, 1651–1659, doi: 10.1007/s12665-011-1142-5, URL http://link.springer.com/10.1007/s12665-011-1142-5, 2012.

Gao, Y., Chen, J., Luo, H., and Wang, H.: Prediction of hydrological responses to land use change, Science of The Total Environment, 708, 134 998, doi: 10.1016/j.scitotenv.2019.134998, URL https://linkinghub.elsevier.com/retrieve/pii/S0048969719349903, 2020.

Gardent, M., Rabatel, A., Dedieu, J.-P., and Deline, P.: Multitemporal glacier inventory of the French Alps from the late 1960s to the late 2000s, Global and Planetary Change, 120, 24–37, doi: 10.1016/j.gloplacha.2014.05.004, URL https://linkinghub.elsevier.com/retrieve/pii/S092181811400099X, 2014.

Gerbaux, M., Genthon, C., Etchevers, P., Vincent, C., and Dedieu, J.: Surface mass balance of glaciers in the French Alps: distributed modeling and sensitivity to climate change, Journal of Glaciology, 51, 561–572, doi: 10.3189/172756505781829133, URL https://www.cambridge.org/core/product/identifier/S0022143000210769/type/journal_article, 2005.

GLAMOS: Swiss Glacier Mass Balance (release 2019), doi: 10.18750/MASSBALANCE.2019.R2019, URL https://doi.glamos.ch/data/massbalance/massbalance_2019_r2019.html, medium: .csv type: dataset, 2019.

Gottardi, F., Obled, C., Gailhard, J., and Paquet, E.: Statistical reanalysis of precipitation fields based on ground network data and weather patterns: Application over French mountains, Journal of Hydrology, 432-433, 154–167, doi: 10.1016/j.jhydrol.2012.02.014, URL http://linkinghub.elsevier.com/retrieve/pii/S002216941200114X, 2012.

Habets, F., Boone, A., Champeaux, J. L., Etchevers, P., Franchistéguy, L., Leblois, E., Ledoux, E., Le Moigne, P., Martin, E., Morel, S., Noilhan, J., Quintana Seguí, P., Rousset-Regimbeau, F., and Viennot, P.: The SAFRAN-ISBA-MODCOU hydrometeorological model applied over France, Journal of Geophysical Research, 113, D06 113, doi: 10.1029/2007JD008548, URL http://doi.wiley.com/10.1029/2007JD008548, 2008.

Ham, Y.-G., Kim, J.-H., and Luo, J.-J.: Deep learning for multi-year ENSO forecasts, Nature, 573, 568–572, doi: 10.1038/s41586-019-1559-7, URL http://www.nature.com/articles/s41586-019-1559-7, 2019.

Hanzer, F., Förster, K., Nemec, J., and Strasser, U.: Projected cryospheric and hydrological impacts of 21st century climate change in the Ötztal Alps (Austria) simulated using a physically based approach, Hydrology and Earth System Sciences, 22, 1593–1614, doi: 10.5194/hess-22-1593-2018, URL https://www.hydrol-earth-syst-sci.net/22/1593/2018/, 2018.

Harris, I., Jones, P., Osborn, T., and Lister, D.: Updated high-resolution grids of monthly climatic observations - the CRU TS3.10 Dataset: UPDATED HIGH-RESOLUTION GRIDS OF MONTHLY CLIMATIC OBSERVATIONS, International Journal of Climatology, 34, 623–642, doi: 10.1002/joc.3711, URL http://doi.wiley.com/10.1002/joc.3711, 2014.

Hastie, T., Tibshirani, R., and Friedman, J.: The Elements of Statistical Learning, Springer Series in Statistics, Springer New York, New York, NY, doi: 10.1007/978-0-387-84858-7, URL http://link.springer.com/10.1007/978-0-387-84858-7, 2009.

Hawkins, D. M.: The Problem of Overfitting, Journal of Chemical Information and Computer Sciences, 44, 1–12, doi: 10.1021/ci0342472, URL http://pubs.acs.org/doi/abs/10.1021/ci0342472, 2004.

He, K., Zhang, X., Ren, S., and Sun, J.: Delving Deep into Rectifiers: Surpassing Human-Level Performance on ImageNet Classification, 2015 IEEE International Conference on Computer Vision (ICCV), doi: 10.1109/iccv.2015.123, URL http://dx.doi.org/10.1109/ICCV.2015.123, 2015.

Hock, R.: Temperature index melt modelling in mountain areas, Journal of Hydrology, 282, 104–115, doi: 10.1016/S0022-1694(03)00257-9, URL http://linkinghub.elsevier.com/retrieve/pii/S0022169403002579, 2003.

Hock, R., Bliss, A., Marzeion, B., Giesen, R. H., Hirabayashi, Y., Huss, M., Radić, V., and Slangen, A. B. A.: GlacierMIP – A model intercomparison of global-scale glacier mass-balance models and projections, Journal of Glaciology, 65, 453–467, doi: 10.1017/jog.2019.22, URL https://www.cambridge.org/core/product/identifier/S0022143019000224/type/journal_article, 2019a.

Hock, R., Rasul, G., Adler, C., Cáceres, B., Gruber, S., Hirabayashi, Y., Jackson, M., Kääb, A., Kang, S., Kutuzov, S., and others: High mountain areas, publisher: The Intergovernmental Panel on Climate Change (IPCC), 2019b.

Hoelzle, M., Haeberli, W., Dischl, M., and Peschke, W.: Secular glacier mass balances derived from cumulative glacier length changes, Global and Planetary Change, 36, 295–306, doi: 10.1016/S0921-8181(02)00223-0, URL https://linkinghub.elsevier.com/retrieve/pii/S0921818102002230, 2003.

Hoerl, A. E. and Kennard, R. W.: Ridge Regression: Biased Estimation for Nonorthogonal Problems, Technometrics, 12, 55–67, doi: 10.1080/00401706.1970.10488634, URL http://www.tandfonline.com/doi/abs/10.1080/00401706.1970.10488634, 1970.

Hoinkes, H. C.: Glacier Variation and Weather, Journal of Glaciology, 7, 3–18, doi: 10.3189/S0022143000020384, URL https://www.cambridge.org/core/product/identifier/S0022143000020384/type/journal_article, 1968.

Horner, I., Branger, F., McMillan, H., Vannier, O., and Braud, I.: Information content of snow hydrological signatures based on streamflow, precipitation and air temperature, Hydrological Processes, 34, 2763–2779, doi: 10.1002/hyp.13762, URL https://onlinelibrary.wiley.com/doi/abs/10.1002/hyp.13762, 2020.

Houghton, J. T., Ding, Y., Griggs, D. J., Noguer, M., van der Linden, P. J., Dai, X., Maskell, K., and Johnson, C.: Climate change 2001: the scientific basis, The Press Syndicate of the University of Cambridge, 2001.

Howell, T. A. and Evett, S.: The Penman-Monteith Method, Evapotranspiration: Determination of Consumptive Use in Water Rights Proceedings, Continuing Legal Education in Colorado, Inc. Denver, Colorado, 2004.

Hrachowitz, M., Savenije, H., Blöschl, G., McDonnell, J., Sivapalan, M., Pomeroy, J., Arheimer, B., Blume, T., Clark, M., Ehret, U., Fenicia, F., Freer, J., Gelfan, A., Gupta, H., Hughes, D., Hut, R., Montanari, A., Pande, S., Tetzlaff, D., Troch, P., Uhlenbrook, S., Wagener, T., Winsemius, H., Woods, R., Zehe, E., and Cudennec, C.: A decade of Predictions in Ungauged Basins (PUB)—a review, Hydrological Sciences Journal, 58, 1198–1255, doi: 10.1080/02626667.2013.803183, URL https://www.tandfonline.com/doi/full/10.1080/02626667.2013.803183, 2013.

Huss, M.: Present and future contribution of glacier storage change to runoff from macroscale drainage basins in Europe: GLACIER CONTRIBUTION TO CONTINENTAL-SCALE RUNOFF, Water Resources Research, 47, doi: 10.1029/2010WR010299, URL http://doi.wiley.com/10.1029/2010WR010299, 2011.

Huss, M.: Extrapolating glacier mass balance to the mountain-range scale: the European Alps 1900–2100, The Cryosphere, 6, 713–727, doi: 10.5194/tc-6-713-2012, URL https://www.the-cryosphere.net/6/713/2012/, 2012.

Huss, M. and Farinotti, D.: Distributed ice thickness and volume of all glaciers around the globe: GLOBAL GLACIER ICE THICKNESS AND VOLUME, Journal of Geophysical Research: Earth Surface, 117, n/a–n/a, doi: 10.1029/2012JF002523, URL http://doi.wiley.com/10.1029/2012JF002523, 2012.

Huss, M. and Fischer, M.: Sensitivity of Very Small Glaciers in the Swiss Alps to Future Climate Change, Frontiers in Earth Science, 4, doi: 10.3389/feart.2016.00034, URL http://journal.frontiersin.org/Article/10.3389/feart.2016.00034/abstract, 2016.

Huss, M. and Hock, R.: A new model for global glacier change and sea-level rise, Frontiers in Earth Science, 3, doi: 10.3389/feart.2015.00054, URL http://journal.frontiersin.org/Article/10.3389/feart.2015.00054/abstract, 2015.

Huss, M. and Hock, R.: Global-scale hydrological response to future glacier mass loss, Nature Climate Change, 8, 135–140, doi: 10.1038/s41558-017-0049-x, URL http://www.nature.com/articles/s41558-017-0049-x, 2018.

Huss, M., Farinotti, D., Bauder, A., and Funk, M.: Modelling runoff from highly glacierized alpine drainage basins in a changing climate, Hydrological Processes, 22, 3888–3902, doi: 10.1002/hyp.7055, URL http://doi.wiley.com/10.1002/hyp.7055, 2008.

Huss, M., Jouvet, G., Farinotti, D., and Bauder, A.: Future high-mountain hydrology: a new parameterization of glacier retreat, Hydrology and Earth System Sciences, 14, 815–829, doi: 10.5194/hess-14-815-2010, URL http://www.hydrol-earth-syst-sci.net/14/815/2010/, 2010.

Huss, M., Hock, R., Bauder, A., and Funk, M.: Conventional versus reference-surface mass balance, Journal of Glaciology, 58, 278–286, doi: 10.3189/2012JoG11J216, URL https://www.cambridge.org/core/product/identifier/S0022143000212021/type/journal_article, 2012.

Huss, M., Dhulst, L., and Bauder, A.: New long-term mass-balance series for the Swiss Alps, Journal of Glaciology, 61, 551–562, doi: 10.3189/2015JoG15J015, URL https://www.cambridge.org/core/product/identifier/S0022143000204036/type/journal_article, 2015.

Huss, M., Bookhagen, B., Huggel, C., Jacobsen, D., Bradley, R., Clague, J., Vuille, M., Buytaert, W., Cayan, D., Greenwood, G., Mark, B., Milner, A., Weingartner, R., and Winder, M.: Toward mountains without permanent snow and ice: MOUNTAINS WITHOUT PERMANENT SNOW AND ICE, Earth's Future, 5, 418–435, doi: 10.1002/2016EF000514, URL http://doi.wiley.com/10.1002/2016EF000514, 2017.

Hutter, K.: Theoretical Glaciology, Springer Netherlands, Dordrecht, doi: 10.1007/978-94-015-1167-4, URL http://link.springer.com/10.1007/978-94-015-1167-4, 1983.

Immerzeel, W. W., Lutz, A. F., Andrade, M., Bahl, A., Biemans, H., Bolch, T., Hyde, S., Brumby, S., Davies, B. J., Elmore, A. C., Emmer, A., Feng, M., Fernández, A., Haritashya, U., Kargel, J. S., Koppes, M., Kraaijenbrink, P. D. A., Kulkarni, A. V., Mayewski, P. A., Nepal, S., Pacheco, P., Painter, T. H., Pellicciotti, F., Rajaram, H., Rupper, S., Sinisalo, A., Shrestha, A. B., Viviroli, D., Wada, Y., Xiao, C., Yao, T., and Baillie, J. E. M.: Importance and vulnerability of the world's water towers, Nature, 577, 364–369, doi: 10.1038/s41586-019-1822-y, URL http://www.nature.com/articles/s41586-019-1822-y, 2020.

Ingrassia, S. and Morlini, I.: Neural Network Modeling for Small Datasets, Technometrics, 47, 297–311, doi: 10.1198/004017005000000058, URL http://www.tandfonline.com/doi/abs/10.1198/004017005000000058, 2005.

Ioffe, S. and Szegedy, C.: Batch Normalization: Accelerating Deep Network Training by Reducing Internal Covariate Shift, 2015.

IPCC: Climate Change 2013: The Physical Science Basis. Contribution of Working Group I to the Fifth Assessment Report of the Intergovernmental Panel on Climate Change, 2018.

Jiang, G.-Q., Xu, J., and Wei, J.: A Deep Learning Algorithm of Neural Network for the Parameterization of Typhoon-Ocean Feedback in Typhoon Forecast Models, Geophysical Research Letters, 45, 3706–3716, doi: 10.1002/2018GL077004, URL http://doi.wiley.com/10.1002/2018GL077004, 2018.

Jouvet, G., Huss, M., Blatter, H., Picasso, M., and Rappaz, J.: Numerical simulation of Rhonegletscher from 1874 to 2100, Journal of Computational Physics, 228, 6426–6439, doi: 10.1016/j.jcp.2009.05.033, URL https://linkinghub.elsevier.com/retrieve/pii/S002199910900285X, 2009.

Jóhannesson, T., Raymond, C., and Waddington, E.: Time–Scale for Adjustment of Glaciers to Changes in Mass Balance, Journal of Glaciology, 35, 355–369, doi: 10.3189/S002214300000928X, URL https://www.cambridge.org/core/product/identifier/S002214300000928X/type/journal_article, 1989.

Karpatne, A., Atluri, G., Faghmous, J. H., Steinbach, M., Banerjee, A., Ganguly, A., Shekhar, S., Samatova, N., and Kumar, V.: Theory-Guided Data Science: A New Paradigm for Scientific Discovery from Data, IEEE Transactions on Knowledge and Data Engineering, 29, 2318–2331, doi: 10.1109/TKDE.2017.2720168, URL http://ieeexplore.ieee.org/document/7959606/, 2017.

Karpatne, A., Watkins, W., Read, J., and Kumar, V.: Physics-guided Neural Networks (PGNN): An Application in Lake Temperature Modeling, arXiv:1710.11431 [physics, stat], URL http://arxiv.org/abs/1710.11431, arXiv: 1710.11431, 2018.

Konz, M. and Seibert, J.: On the value of glacier mass balances for hydrological model calibration, Journal of hydrology, 385, 238–246, 2010.

Krause, P.: Quantifying the impact of land use changes on the water balance of large catchments using the J2000 model, Physics and Chemistry of the Earth, Parts A/B/C, 27, 663–673, doi: 10.1016/S1474-7065(02)00051-7, URL http://linkinghub.elsevier.com/retrieve/pii/S1474706502000517, 2002.

Krogh, A. and Vedelsby, J.: Neural network ensembles, cross validation, and active learning, in: Advances in neural information processing systems, pp. 231–238, 1995.

Kääb, A., Berthier, E., Nuth, C., Gardelle, J., and Arnaud, Y.: Contrasting patterns of early twenty-first-century glacier mass change in the Himalayas, Nature, 488, 495–498, doi: 10.1038/nature11324, URL http://www.nature.com/articles/nature11324, 2012.

Lafaysse, M., Hingray, B., Etchevers, P., Martin, E., and Obled, C.: Influence of spatial discretization, underground water storage and glacier melt on a physically-based hydrological model of the Upper Durance River basin, Journal of Hydrology, 403, 116–129, doi: 10.1016/j.jhydrol.2011.03.046, URL http://linkinghub.elsevier.com/retrieve/pii/S0022169411002265, 2011.

Laurent, L., Buoncristiani, J.-F., Pohl, B., Zekollari, H., Farinotti, D., Huss, M., Mugnier, J.-L., and Pergaud, J.: The impact of climate change and glacier mass loss on the hydrology in the Mont-Blanc massif, Scientific Reports, 10, 10 420, doi: 10.1038/s41598-020-67379-7, URL http://www.nature.com/articles/s41598-020-67379-7, 2020.

Lea, J. M.: The Google Earth Engine Digitisation Tool (GEEDiT) and the Margin change Quantification Tool (MaQiT) – simple tools for the rapid mapping and quantification of changing Earth surface margins, Earth Surface Dynamics, 6, 551–561, doi: 10.5194/esurf-6-551-2018, URL https://esurf.copernicus.org/articles/6/551/2018/, 2018.

Lecourt, G.: Physically-based modelisation of the Arve river at Chamonix, application to flood prediction, Theses, Université Paul Sabatier - Toulouse III, URL https://tel.archives-ouvertes.fr/tel-02145983, issue: 2018TOU30134, 2018.

Lencioni, V.: Glacial influence and stream macroinvertebrate biodiversity under climate change: Lessons from the Southern Alps, Science of The Total Environment, 622-623, 563–575, doi: 10.1016/j.scitotenv.2017.11.266, URL https://linkinghub.elsevier.com/retrieve/pii/S0048969717333247, 2018.

Leong, W. J. and Horgan, H. J.: DeepBedMap: Using a deep neural network to better resolve the bed topography of Antarctica, preprint, Ice sheets/Data Assimilation, doi: 10.5194/tc-2020-74, URL https://www.the-cryosphere-discuss.net/tc-2020-74/, 2020.

Lguensat, R., Sun, M., Fablet, R., Tandeo, P., Mason, E., and Chen, G.: EddyNet: A Deep Neural Network For Pixel-Wise Classification of Oceanic Eddies, in: IGARSS 2018 - 2018 IEEE International Geoscience and Remote Sensing Symposium, pp. 1764–1767, IEEE, Valencia, doi: 10.1109/IGARSS.2018.8518411, URL https://ieeexplore.ieee.org/document/8518411/, 2018.

Lguensat, R., Sommer, J. L., Metref, S., Cosme, E., and Fablet, R.: Learning Generalized Quasi-Geostrophic Models Using Deep Neural Numerical Models, arXiv:1911.08856 [physics, stat], URL http://arxiv.org/abs/1911.08856, arXiv: 1911.08856, 2019.

Liu, Y., Racah, E., Prabhat, Correa, J., Khosrowshahi, A., Lavers, D., Kunkel, K., Wehner, M., and Collins, W.: Application of Deep Convolutional Neural Networks for Detecting Extreme Weather in Climate Datasets, arXiv:1605.01156 [cs], URL http://arxiv.org/abs/1605.01156, arXiv: 1605.01156, 2016.

Mackintosh, A. N., Anderson, B. M., and Pierrehumbert, R. T.: Reconstructing Climate from Glaciers, Annual Review of Earth and Planetary Sciences, 45, 649–680, doi: 10.1146/annurev-earth-063016-020643, URL http://www.annualreviews.org/doi/10.1146/annurev-earth-063016-020643, 2017.

Magnin, F., Haeberli, W., Linsbauer, A., Deline, P., and Ravanel, L.: Estimating glacier-bed overdeepenings as possible sites of future lakes in the de-glaciating Mont Blanc massif (Western European Alps), Geomorphology,

350, 106 913, doi: 10.1016/j.geomorph.2019.106913, URL https://linkinghub.elsevier.com/retrieve/pii/S0169555X19304040, 2020.

Martin, S.: Correlation bilans de masse annuels-facteurs météorologiques dans les Grandes Rousses, Zeitschrift für Gletscherkunde und Glazialgeologie, 1974.

Marzeion, B., Jarosch, A. H., and Hofer, M.: Past and future sea-level change from the surface mass balance of glaciers, The Cryosphere, 6, 1295–1322, doi: 10.5194/tc-6-1295-2012, URL https://www.the-cryosphere.net/6/1295/2012/, 2012.

Marzeion, B., Leclercq, P. W., Cogley, J. G., and Jarosch, A. H.: Brief Communication: Global reconstructions of glacier mass change during the 20th century are consistent, The Cryosphere, 9, 2399–2404, doi: 10.5194/tc-9-2399-2015, URL https://www.the-cryosphere.net/9/2399/2015/, 2015.

Marzeion, B., Hock, R., Anderson, B., Bliss, A., Champollion, N., Fujita, K., Huss, M., Immerzeel, W., Kraaijenbrink, P., Malles, J., Maussion, F., Radić, V., Rounce, D. R., Sakai, A., Shannon, S., Wal, R., and Zekollari, H.: Partitioning the Uncertainty of Ensemble Projections of Global Glacier Mass Change, Earth's Future, doi: 10.1029/2019EF001470, URL https://onlinelibrary.wiley.com/doi/abs/10.1029/2019EF001470, 2020.

Marçais, J. and de Dreuzy, J.-R.: Prospective Interest of Deep Learning for Hydrological Inference: J. Marçais and J.-R. de Dreuzy Groundwater xx, no. x: xx-xx, Groundwater, 55, 688–692, doi: 10.1111/gwat.12557, URL http://doi.wiley.com/10.1111/gwat.12557, 2017.

Maussion, F., Gurgiser, W., Großhauser, M., Kaser, G., and Marzeion, B.: ENSO influence on surface energy and mass balance at Shallap Glacier, Cordillera Blanca, Peru, The Cryosphere, 9, 1663–1683, doi: 10.5194/tc-9-1663-2015, URL https://www.the-cryosphere.net/9/1663/2015/, 2015.

Maussion, F., Butenko, A., Champollion, N., Dusch, M., Eis, J., Fourteau, K., Gregor, P., Jarosch, A. H., Landmann, J., Oesterle, F., Recinos, B., Rothenpieler, T., Vlug, A., Wild, C. T., and Marzeion, B.: The Open Global Glacier Model (OGGM) v1.1, Geoscientific Model Development, 12, 909–931, doi: 10.5194/gmd-12-909-2019, URL https://www.geosci-model-dev.net/12/909/2019/, 2019.

Mjolsness, E.: Machine Learning for Science: State of the Art and Future Prospects, Science, 293, 2051–2055, doi: 10.1126/science.293.5537.2051, URL https://www.sciencemag.org/lookup/doi/10.1126/science.293.5537.2051, 2001.

Mohajerani, Y., Wood, M., Velicogna, I., and Rignot, E.: Detection of Glacier Calving Margins with Convolutional Neural Networks: A Case Study, Remote Sensing, 11, 74, doi: 10.3390/rs11010074, URL https://www.mdpi.com/2072-4292/11/1/74, 2019.

Moser, S. C.: Communicating climate change: history, challenges, process and future directions: Communicating climate change, Wiley Interdisciplinary Reviews: Climate Change, 1, 31–53, doi: 10.1002/wcc.11, URL http://doi.wiley.com/10.1002/wcc.11, 2010.

Mourey, J. and Ravanel, L.: Evolution of Access Routes to High Mountain Refuges of the Mer de Glace Basin (Mont Blanc Massif, France): An Example of Adapting to Climate Change Effects in the Alpine High Mountains, Revue de géographie alpine, doi: 10.4000/rga.3790, URL http://journals.openedition.org/rga/3790, 2017.

Nanni, U., Gimbert, F., Vincent, C., Gräff, D., Walter, F., Piard, L., and Moreau, L.: Quantification of seasonal and diurnal dynamics of subglacial channels using seismic observations on an Alpine glacier, The Cryosphere, 14, 1475–1496, doi: 10.5194/tc-14-1475-2020, URL https://tc.copernicus.org/articles/14/1475/2020/, 2020.

Nepal, S., Krause, P., Flügel, W.-A., Fink, M., and Fischer, C.: Understanding the hydrological system dynamics of a glaciated alpine catchment in the Himalayan region using the J2000 hydrological model: HYDROLOGICAL SYSTEM DYNAMICS OF HIMALAYA RIVERS, Hydrological Processes, 28, 1329–1344, doi: 10.1002/hyp.9627, URL http://doi.wiley.com/10.1002/hyp.9627, 2014.

Nepal, S., Pradhananga, S., Shrestha, N. K., Kralisch, S., Shrestha, J., and Fink, M.: Space-time variability of soil moisture droughts in the Himalayan region, preprint, Catchment hydrology/Modelling approaches, doi: 10.5194/hess-2020-337, URL https://hess.copernicus.org/preprints/hess-2020-337/, 2020.

NSIDC, G. a.: Global Land Ice Measurements from Space glacier database. Compiled and made available by the international GLIMS community and the National Snow and Ice Data Center, 2005.

Nussbaumer, S., Steiner, D., and Zumbühl, H.: Réseau neuronal et fluctuations des glaciers dans les Alpes occidentales, 2012.

Oerlemans, J. and Reichert, B. K.: Relating glacier mass balance to meteorological data by using a seasonal sensitivity characteristic, Journal of Glaciology, 46, 1–6, doi: 10.3189/172756500781833269, URL https://www.cambridge.org/core/product/identifier/S0022143000213786/type/journal_article, 2000.

Oliveira, M., Torgo, L., and Santos Costa, V.: Evaluation Procedures for Forecasting with Spatio-Temporal Data, in: Machine Learning and Knowledge Discovery in Databases, edited by Berlingerio, M., Bonchi, F., Gärtner, T., Hurley, N., and Ifrim, G., vol. 11051, pp. 703–718, Springer International Publishing, Cham, doi: 10.1007/978-3-030-10925-7_43, URL http://link.springer.com/10.1007/978-3-030-10925-7_43, 2019.

Olson, M., Wyner, A. J., and Berk, R.: Modern Neural Networks Generalize on Small Data Sets, in: NeurIPS, 2018.

Paquet, E.: Evolution du modèle hydrologique MORDOR : modélisation du stock nival à différentes altitudes, La Houille Blanche, pp. 75–82, doi: 10.1051/lhb:200402008, URL http://www.shf-lhb.org/10.1051/lhb:200402008, 2004.

Paul, F., Kääb, A., Maisch, M., Kellenberger, T., and Haeberli, W.: Rapid disintegration of Alpine glaciers observed with satellite data: DISINTEGRATION OF ALPINE GLACIERS, Geophysical Research Letters, 31, n/a–n/a, doi: 10.1029/2004GL020816, URL http://doi.wiley.com/10.1029/2004GL020816, 2004.

Pedregosa, F., Varoquaux, G., Gramfort, A., Michel, V., Thirion, B., Grisel, O., Blondel, M., Prettenhofer, P., Weiss, R., Dubourg, V., Vanderplas, J., Passos, A., Cournapeau, D., Brucher, M., Perrot, M., Duchesnay, E., and Louppe, G.: Scikit-learn: Machine Learning in Python, vol. 12, 2012.

Ponchaud, A., Avrillon, M., Bondaz, G., Borrel, Y., Gourreau, J.-M., Hosdey, F., Pajeot, E., Peltier, F., Siffointe, R., and Vodinh, J.: Nature et patrimoine en pays de Savoie, CAUE de Haute-Savoie/Maryse Avrillon CNM/Eric Pajeot, 2012.

Rabatel, A., Dedieu, J.-P., and Vincent, C.: Using remote-sensing data to determine equilibrium-line altitude and mass-balance time series: validation on three French glaciers, 1994–2002, Journal of Glaciology, 51, 539–546, doi: 10.3189/172756505781829106, URL https://www.cambridge.org/core/product/identifier/S0022143000210733/type/journal_article, 2005.

Rabatel, A., Letréguilly, A., Dedieu, J.-P., and Eckert, N.: Changes in glacier equilibrium-line altitude in the western Alps from 1984 to 2010: evaluation by remote sensing and modeling of the morpho-topographic and climate controls, The Cryosphere, 7, 1455–1471, doi: 10.5194/tc-7-1455-2013, URL https://www.the-cryosphere.net/7/1455/2013/, 2013.

Rabatel, A., Dedieu, J. P., and Vincent, C.: Spatio-temporal changes in glacier-wide mass balance quantified by optical remote sensing on 30 glaciers in the French Alps for the period 1983–2014, Journal of Glaciology, 62, 1153–1166, doi: 10.1017/jog.2016.113, URL https://www.cambridge.org/core/product/identifier/S0022143016001131/type/journal_article, 2016.

Rabatel, A., Sanchez, O., Vincent, C., and Six, D.: Estimation of Glacier Thickness From Surface Mass Balance and Ice Flow Velocities: A Case Study on Argentière Glacier, France, Frontiers in Earth Science, 6, doi: 10.3389/feart.2018.00112, URL https://www.frontiersin.org/article/10.3389/feart.2018.00112/full, 2018.

Rackauckas, C., Ma, Y., Martensen, J., Warner, C., Zubov, K., Supekar, R., Skinner, D., and Ramadhan, A.: Universal Differential Equations for Scientific Machine Learning, arXiv:2001.04385 [cs, math, q-bio, stat], URL http://arxiv.org/abs/2001.04385, arXiv: 2001.04385, 2020.

Radić, V., Bliss, A., Beedlow, A. C., Hock, R., Miles, E., and Cogley, J. G.: Regional and global projections of twenty-first century glacier mass changes in response to climate scenarios from global climate models, Climate Dynamics, 42, 37–58, doi: 10.1007/s00382-013-1719-7, URL http://link.springer.com/10.1007/s00382-013-1719-7, 2014.

Raissi, M., Perdikaris, P., and Karniadakis, G. E.: Physics Informed Deep Learning (Part I): Data-driven Solutions of Nonlinear Partial Differential Equations, arXiv:1711.10561 [cs, math, stat], URL http://arxiv.org/abs/1711.10561, arXiv: 1711.10561, 2017.

Rasp, S., Pritchard, M. S., and Gentine, P.: Deep learning to represent subgrid processes in climate models, Proceedings of the National Academy of Sciences, 115, 9684–9689, doi: 10.1073/pnas.1810286115, URL http://www.pnas.org/lookup/doi/10.1073/pnas.1810286115, 2018.

Rastner, P., Prinz, R., Notarnicola, C., Nicholson, L., Sailer, R., Schwaizer, G., and Paul, F.: On the Automated Mapping of Snow Cover on Glaciers and Calculation of Snow Line Altitudes from Multi-Temporal Landsat Data, Remote Sensing, 11, 1410, doi: 10.3390/rs11121410, URL https://www.mdpi.com/2072-4292/11/12/1410, 2019.

Rendu, L. and Bischof, G.: Théorie des glaciers de la Savoie, Puthod, 1840.

Richalet, J.-P.: The Scientific Observatories on Mont Blanc, High Altitude Medicine & Biology, 2, 57–68, doi: 10.1089/152702901750067936, URL http://www.liebertpub.com/doi/10.1089/152702901750067936, 2001.

Roberts, D. R., Bahn, V., Ciuti, S., Boyce, M. S., Elith, J., Guillera-Arroita, G., Hauenstein, S., Lahoz-Monfort, J. J., Schröder, B., Thuiller, W., Warton, D. I., Wintle, B. A., Hartig, F., and Dormann, C. F.: Cross-validation strategies for data with temporal, spatial, hierarchical, or phylogenetic structure, Ecography, 40, 913–929, doi: 10.1111/ecog.02881, URL http://doi.wiley.com/10.1111/ecog.02881, 2017.

Robinson, C. T., Thompson, C., and Freestone, M.: Ecosystem development of streams lengthened by rapid glacial recession, Fundamental and Applied Limnology / Archiv für Hydrobiologie, 185, 235–246, doi: 10.1127/fal/2014/0667, URL http://www.ingentaconnect.com/content/10.1127/fal/2014/0667, 2014.

Roe, G. H.: Orographic precipitation, Annual Review of Earth and Planetary Sciences, 33, 645–671, doi: 10.1146/annurev.earth.33.092203.122541, URL http://www.annualreviews.org/doi/10.1146/annurev.earth.33.092203.122541, 2005.

Rounce, D. R., Khurana, T., Short, M. B., Hock, R., Shean, D. E., and Brinkerhoff, D. J.: Quantifying parameter uncertainty in a large-scale glacier evolution model using Bayesian inference: application to High Mountain Asia, Journal of Glaciology, pp. 1–13, doi: 10.1017/jog.2019.91, URL https://www.cambridge.org/core/product/identifier/S0022143019000911/type/journal_article, 2020.

Réveillet, M., Rabatel, A., Gillet-Chaulet, F., and Soruco, A.: Simulations of changes to Glaciar Zongo, Bolivia (16° S), over the 21st century using a 3-D full-Stokes model and CMIP5 climate projections, Annals of Glaciology, 56, 89–97, doi: 10.3189/2015AoG70A113, URL https://www.cambridge.org/core/product/identifier/S0260305500250362/type/journal_article, 2015.

Réveillet, M., Vincent, C., Six, D., and Rabatel, A.: Which empirical model is best suited to simulate glacier mass balances?, Journal of Glaciology, 63, 39–54, doi: 10.1017/jog.2016.110, URL https://www.cambridge.org/core/product/identifier/S0022143016001106/type/journal_article, 2017.

Réveillet, M., Six, D., Vincent, C., Rabatel, A., Dumont, M., Lafaysse, M., Morin, S., Vionnet, V., and Litt, M.: Relative performance of empirical and physical models in assessing the seasonal and annual glacier surface mass balance of Saint-Sorlin Glacier (French Alps), The Cryosphere, 12, 1367–1386, doi: 10.5194/tc-12-1367-2018, URL https://www.the-cryosphere.net/12/1367/2018/, 2018.

Sauquet, E., Arama, Y., Bouscasse, H., Krowicki, F., Rossi, A., Strosser, P., Blanc-Coutagne, E., Brun, J.-F., Cherel, J., Le Goff, I., and others: Risk, water Resources and sustainable Development within the Durance river basin in 2050. R 2 D 2 2050 project, 2014.

Schaefli, B. and Huss, M.: Integrating point glacier mass balance observations into hydrologic model identification, Hydrology and Earth System Sciences, 15, 1227–1241, 2011.

Schaefli, B., Hingray, B., Niggli, M., and Musy, A.: A conceptual glacio-hydrological model for high mountainous catchments, Hydrology and Earth System Sciences, 9, 95–109, doi: 10.5194/hess-9-95-2005, URL https://hess.copernicus.org/articles/9/95/2005/, 2005.

Schaefli, B., Manso, P., Fischer, M., Huss, M., and Farinotti, D.: The role of glacier retreat for Swiss hydropower production, Renewable Energy, 132, 615–627, doi: 10.1016/j.renene.2018.07.104, URL https://linkinghub.elsevier.com/retrieve/pii/S0960148118309017, 2019.

Schut, P.-O.: Sport as a Major Player in the Development of Tourism: The History of Mountaineering in the Pelvoux Massif, France, from 1861 to 1914, The International Journal of the History of Sport, 30, 1329–1350, doi: 10.1080/09523367.2013.784272, URL http://www.tandfonline.com/doi/abs/10.1080/09523367.2013.784272, 2013.

Seabold, S. and Perktold, J.: Statsmodels: Econometric and Statistical Modelingwith Python, PROC. OF THE 9th PYTHON IN SCIENCE CONF., 2010.

Shen, C.: A Transdisciplinary Review of Deep Learning Research and Its Relevance for Water Resources Scientists, Water Resources Research, 54, 8558–8593, doi: 10.1029/2018WR022643, URL https://onlinelibrary.wiley.com/doi/abs/10.1029/2018WR022643, 2018.

Sicart, J. E., Hock, R., and Six, D.: Glacier melt, air temperature, and energy balance in different climates: The Bolivian Tropics, the French Alps, and northern Sweden, Journal of Geophysical Research, 113, D24113, doi: 10.1029/2008JD010406, URL http://doi.wiley.com/10.1029/2008JD010406, 2008.

Six, D. and Vincent, C.: Sensitivity of mass balance and equilibrium-line altitude to climate change in the French Alps, Journal of Glaciology, 60, 867–878, doi: 10.3189/2014JoG14J014, URL https://www.cambridge.org/core/product/identifier/S0022143000202128/type/journal_article, 2014.

Smiatek, G., Kunstmann, H., and Senatore, A.: EURO-CORDEX regional climate model analysis for the Greater Alpine Region: Performance and expected future change: CLIMATE CHANGE IN THE GAR AREA, Journal of Geophysical Research: Atmospheres, 121, 7710–7728, doi: 10.1002/2015JD024727, URL http://doi.wiley.com/10.1002/2015JD024727, 2016.

Smit, M., Amelung, S. B., and Meijering, J. J.: Exploring intergenerational attitudes toward glacier retreat in the Chamonix Mont-Blanc Valley, France, 2019.

Spandre, P., François, H., Verfaillie, D., Pons, M., Vernay, M., Lafaysse, M., George, E., and Morin, S.: Winter tourism under climate change in the Pyrenees and the French Alps: relevance of snowmaking as a technical adaptation, The Cryosphere, 13, 1325–1347, doi: 10.5194/tc-13-1325-2019, URL https://www.the-cryosphere.net/13/1325/2019/, 2019.

Srivastava, N., Hinton, G., Krizhevsky, A., Sutskever, I., and Salakhutdinov, R.: Dropout: a simple way to prevent neural networks from overfitting, J. Mach. Learn. Res., 15, 1929–1958, 2014.

Stahl, K., Moore, R., Shea, J., Hutchinson, D., and Cannon, A.: Coupled modelling of glacier and streamflow response to future climate scenarios, Water Resources Research, 44, 2008.

Steiner, D., Walter, A., and Zumbühl, H.: The application of a non-linear back-propagation neural network to study the mass balance of Grosse Aletschgletscher, Switzerland, Journal of Glaciology, 51, 313–323, doi: 10.3189/172756505781829421, URL https://www.cambridge.org/core/product/identifier/S0022143000214949/type/journal_article, 2005.

Steiner, D., Pauling, A., Nussbaumer, S. U., Nesje, A., Luterbacher, J., Wanner, H., and Zumbühl, H. J.: Sensitivity of European glaciers to precipitation and temperature – two case studies, Climatic Change, 90, 413–441, doi: 10.1007/s10584-008-9393-1, URL http://link.springer.com/10.1007/s10584-008-9393-1, 2008.

Thibert, E., Eckert, N., and Vincent, C.: Climatic drivers of seasonal glacier mass balances: an analysis of 6 decades at Glacier de Sarennes (French Alps), The Cryosphere, 7, 47–66, doi: 10.5194/tc-7-47-2013, URL http://www.the-cryosphere.net/7/47/2013/, 2013.

Thibert, E., Dkengne Sielenou, P., Vionnet, V., Eckert, N., and Vincent, C.: Causes of Glacier Melt Extremes in the Alps Since 1949, Geophysical Research Letters, 45, 817–825, doi: 10.1002/2017GL076333, URL http://doi.wiley.com/10.1002/2017GL076333, 2018.

Tibshirani, R.: Regression Shrinkage and Selection via the Lasso, Journal of the Royal Statistical Society. Series B (Methodological), 58, 267–288, URL http://www.jstor.org/stable/2346178, 1996.

Tibshirani, R., Johnstone, I., Hastie, T., and Efron, B.: Least angle regression, The Annals of Statistics, 32, 407–499, doi: 10.1214/009053604000000067, URL http://projecteuclid.org/euclid.aos/1083178935, 2004.

Verfaillie, D., Déqué, M., Morin, S., and Lafaysse, M.: The method ADAMONT v1.0 for statistical adjustment of climate projections applicable to energy balance land surface models, Geoscientific Model Development, 10, 4257–4283, doi: 10.5194/gmd-10-4257-2017, URL https://www.geosci-model-dev.net/10/4257/2017/, 2017.

Vincent, C., Harter, M., Gilbert, A., Berthier, E., and Six, D.: Future fluctuations of Mer de Glace, French Alps, assessed using a parameterized model calibrated with past thickness changes, Annals of Glaciology, 55, 15–24, doi: 10.3189/2014AoG66A050, URL https://www.cambridge.org/core/product/identifier/S0260305500258096/type/journal_article, 2014.

Vincent, C., Fischer, A., Mayer, C., Bauder, A., Galos, S. P., Funk, M., Thibert, E., Six, D., Braun, L., and Huss, M.: Common climatic signal from glaciers in the European Alps over the last 50 years: Common Climatic Signal in the Alps, Geophysical Research Letters, 44, 1376–1383, doi: 10.1002/2016GL072094, URL http://doi.wiley.com/10.1002/2016GL072094, 2017.

Vincent, C., Soruco, A., Azam, M. F., Basantes-Serrano, R., Jackson, M., Kjøllmoen, B., Thibert, E., Wagnon, P., Six, D., Rabatel, A., Ramanathan, A., Berthier, E., Cusicanqui, D., Vincent, P., and Mandal, A.: A Nonlinear Statistical Model for Extracting a Climatic Signal From Glacier Mass Balance Measurements, Journal of Geophysical Research: Earth Surface, 123, 2228–2242, doi: 10.1029/2018JF004702, URL https://onlinelibrary.wiley.com/doi/abs/10.1029/2018JF004702, 2018.

Vincent, C., Peyaud, V., Laarman, O., Six, D., Gilbert, A., Gillet-Chaulet, F., Berthier, , Morin, S., Verfaillie, D., Rabatel, A., Jourdain, B., and Bolibar, J.: Déclin des deux plus grands glaciers des Alpes françaises au cours du XXIe siècle : Argentière et Mer de Glace, La Météorologie, p. 49, doi: 10.4267/2042/70369, URL http://hdl.handle.net/2042/70369, 2019.

Vionnet, V., Dombrowski-Etchevers, I., Lafaysse, M., Quéno, L., Seity, Y., and Bazile, E.: Numerical Weather Forecasts at Kilometer Scale in the French Alps: Evaluation and Application for Snowpack Modeling, Journal of Hydrometeorology, 17, 2591–2614, doi: 10.1175/JHM-D-15-0241.1, URL http://journals.ametsoc.org/doi/10.1175/JHM-D-15-0241.1, 2016.

Vionnet, V., Six, D., Auger, L., Dumont, M., Lafaysse, M., Quéno, L., Réveillet, M., Dombrowski-Etchevers, I., Thibert, E., and Vincent, C.: Sub-kilometer Precipitation Datasets for Snowpack and Glacier Modeling in Alpine Terrain, Frontiers in Earth Science, 7, 182, doi: 10.3389/feart.2019.00182, URL https://www.frontiersin.org/article/10.3389/feart.2019.00182/full, 2019.

Vuille, M., Carey, M., Huggel, C., Buytaert, W., Rabatel, A., Jacobsen, D., Soruco, A., Villacis, M., Yarleque, C., Elison Timm, O., Condom, T., Salzmann, N., and Sicart, J.-E.: Rapid decline of snow and ice in the tropical Andes – Impacts, uncertainties and challenges ahead, Earth-Science Reviews, 176, 195–213, doi: 10.1016/j.earscirev.2017.09.019, URL https://linkinghub.elsevier.com/retrieve/pii/S0012825216304512, 2018.

Wang, H. and Raj, B.: On the Origin of Deep Learning, arXiv:1702.07800 [cs, stat], URL http://arxiv.org/abs/1702.07800, arXiv: 1702.07800, 2017.

Weisberg, S.: Applied linear regression, Wiley series in probability and statistics, Wiley, Hoboken, NJ, fourth edition edn., 2014.

Werder, M. A., Huss, M., Paul, F., Dehecq, A., and Farinotti, D.: A Bayesian ice thickness estimation model for large-scale applications, Journal of Glaciology, pp. 1–16, doi: 10.1017/jog.2019.93, URL https://www.cambridge.org/core/product/identifier/S0022143019000935/type/journal_article, 2019.

Whittingham, M. J., Stephens, P. A., Bradbury, R. B., and Freckleton, R. P.: Why do we still use stepwise modelling in ecology and behaviour?: Stepwise modelling in ecology and behaviour, Journal of Animal Ecology, 75, 1182–1189, doi: 10.1111/j.1365-2656.2006.01141.x, URL http://doi.wiley.com/10.1111/j.1365-2656.2006.01141.x, 2006.

Winkler, D. A. and Le, T. C.: Performance of Deep and Shallow Neural Networks, the Universal Approximation Theorem, Activity Cliffs, and QSAR, Molecular Informatics, 36, 1600118, doi: 10.1002/minf.201600118, URL http://doi.wiley.com/10.1002/minf.201600118, 2017.

Xu, B., Wang, N., Chen, T., and Li, M.: Empirical Evaluation of Rectified Activations in Convolutional Network, CoRR, abs/1505.00853, URL http://arxiv.org/abs/1505.00853, 2015.

Yuan, J., Chi, Z., Cheng, X., Zhang, T., Li, T., and Chen, Z.: Automatic Extraction of Supraglacial Lakes in Southwest Greenland during the 2014–2018 Melt Seasons Based on Convolutional Neural Network, Water, 12, 891, doi: 10.3390/w12030891, URL https://www.mdpi.com/2073-4441/12/3/891, 2020.

Zekollari, H. and Huybrechts, P.: Statistical modelling of the surface mass-balance variability of the Morteratsch glacier, Switzerland: strong control of early melting season meteorological conditions, Journal of Glaciology, 64, 275–288, doi: 10.1017/jog.2018.18, URL https://www.cambridge.org/core/product/identifier/S0022143018000187/type/journal_article, 2018.

Zekollari, H., Huss, M., and Farinotti, D.: Modelling the future evolution of glaciers in the European Alps under the EURO-CORDEX RCM ensemble, The Cryosphere, 13, 1125–1146, doi: 10.5194/tc-13-1125-2019, URL https://www.the-cryosphere.net/13/1125/2019/, 2019.

Zekollari, H., Huss, M., and Farinotti, D.: On the Imbalance and Response Time of Glaciers in the European Alps, Geophysical Research Letters, 47, doi: 10.1029/2019GL085578, URL https://onlinelibrary.wiley.com/doi/abs/10.1029/2019GL085578, 2020.

Zemp, M., Haeberli, W., Hoelzle, M., and Paul, F.: Alpine glaciers to disappear within decades?, Geophysical Research Letters, 33, doi: 10.1029/2006GL026319, URL http://doi.wiley.com/10.1029/2006GL026319, 2006.

Zemp, M., Huss, M., Thibert, E., Eckert, N., McNabb, R., Huber, J., Barandun, M., Machguth, H., Nussbaumer, S. U., Gärtner-Roer, I., Thomson, L., Paul, F., Maussion, F., Kutuzov, S., and Cogley, J. G.: Global glacier mass changes and their contributions to sea-level rise from 1961 to 2016, Nature, 568, 382–386, doi: 10.1038/s41586-019-1071-0, URL http://www.nature.com/articles/s41586-019-1071-0, 2019.

Zhang, E., Liu, L., and Huang, L.: Automatically delineating the calving front of Jakobshavn Isbræ from multitemporal TerraSAR-X images: a deep learning approach, The Cryosphere, 13, 1729–1741, doi: 10.5194/tc-13-1729-2019, URL https://www.the-cryosphere.net/13/1729/2019/, 2019.

Zhang, Q., Wu, Y. N., and Zhu, S.-C.: Interpretable Convolutional Neural Networks, arXiv:1710.00935 [cs], URL http://arxiv.org/abs/1710.00935, arXiv: 1710.00935, 2018.

Zryd, A.: Les glaciers en mouvement: la population des Alpes face au changement climatique, Presses polytechniques et universitaires romandes, Lausanne, oCLC: 605265269, 2008.